ANTARCTIC CLIMATE & ECOSYSTEMS CRC

climate futures for tasmania

TECHNICAL REPORT

Climate Modelling

Corney SP, Katzfey JJ, McGregor JL, Grose MR, Bennett JC, White CJ, Holz GK, Gaynor SM & Bindoff NL

December 2010

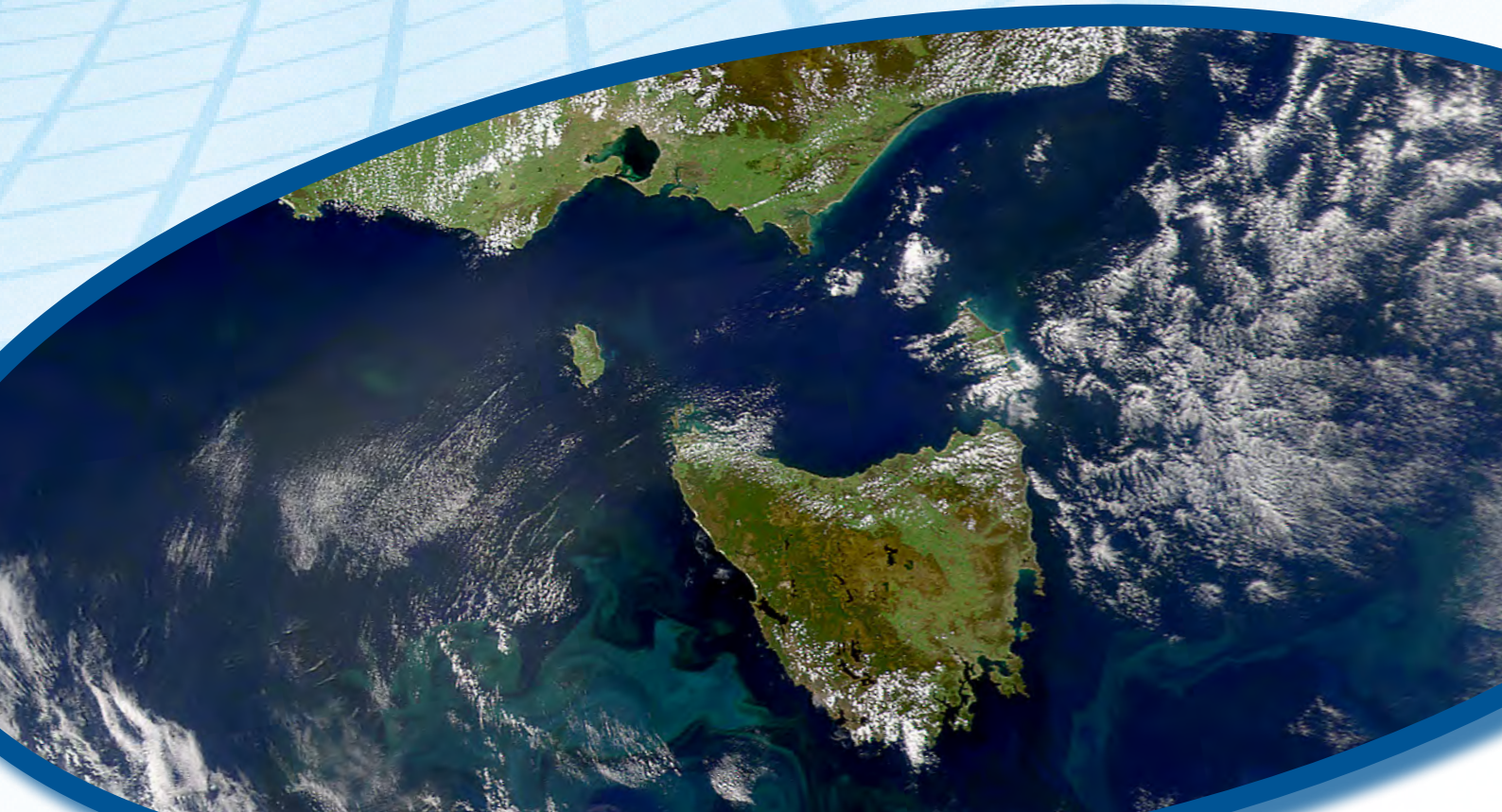

Climate Futures for Tasmania
Climate Modelling Technical Report

ISBN 978-1-921197-06-2

The Manager
Communications
Antarctic Climate & Ecosystems Cooperative Research Centre

Private Bag 80
Hobart Tasmania 7001
Tel: +61 3 6226 7888, Fax: +61 3 6226 2440
Email: climatefutures@acecrc.org.au

Disclaimer

The material in this report is based on computer modelling projections for climate change scenarios and, as such, there are inherent uncertainties in the data. While every effort has been made to ensure the material in this report is accurate, Antarctic Climate & Ecosystems Cooperative Research Centre (ACE) provides no warranty, guarantee or representation that material is accurate, complete, up to date, non-infringing or fit for a particular purpose. The use of the material is entirely at the risk of a user. The user must independently verify the suitability of the material for its own use.

To the maximum extent permitted by law, ACE, its participating organisations and their officers, employees, contractors and agents exclude liability for any loss, damage, costs or expenses whether direct, indirect, consequential including loss of profits, opportunity and third party claims that may be caused through the use of, reliance upon, or interpretation of the material in this report.

Science Reviewers

Professor William Gutowski (Iowa State University), Professor Bruce Hewitson (University of Cape Town) and Dr James Risbey (CSIRO-CAWCR)

The reviewers listed in this report have offered all comments and recommendations in good faith and in an unbiased and professional manner. At no time was the reviewer asked to verify or endorse the project conclusions and recommendations nor was the reviewer privy to the final draft of the report before its release.

The reviewers' role was solely advisory and should not be construed as an endorsement of the project findings by the reviewer or his /her employing organisation. Neither the reviewer nor his/her employing organisation provides any representation or warranty as to the accuracy or suitability of any project findings. Responsibility for all work done in connection with the project remains with the project team.

Photo Credits: Celena Tan (pages 2, 5), Stuart Corney (pp 69, 79), Ian Barnes-Keoghan (p 48)
Suzie Gaynor (pp 10/11, 13, 23, 26/27, 45, 46/47, 52/53, 60, 75, 76, 82)

Graphic Design: Suzie Gaynor

Graphic Layout: Epiphany Public Relations

Citation

Corney SP, Katzfey JJ, McGregor JL, Grose MR, Bennett JC, White CJ, Holz GK, Gaynor SM and Bindoff NL 2010, *Climate Futures for Tasmania: climate modelling technical report*, Antarctic Climate & Ecosystems Cooperative Research Centre, Hobart, Tasmania.

TECHNICAL REPORT

Climate Futures for Tasmania: climate modelling

Corney SP, Katzfey JJ, McGregor JL, Grose MR, Bennett JC, White CJ, Holz GK, Gaynor SM & Bindoff NL

December 2010

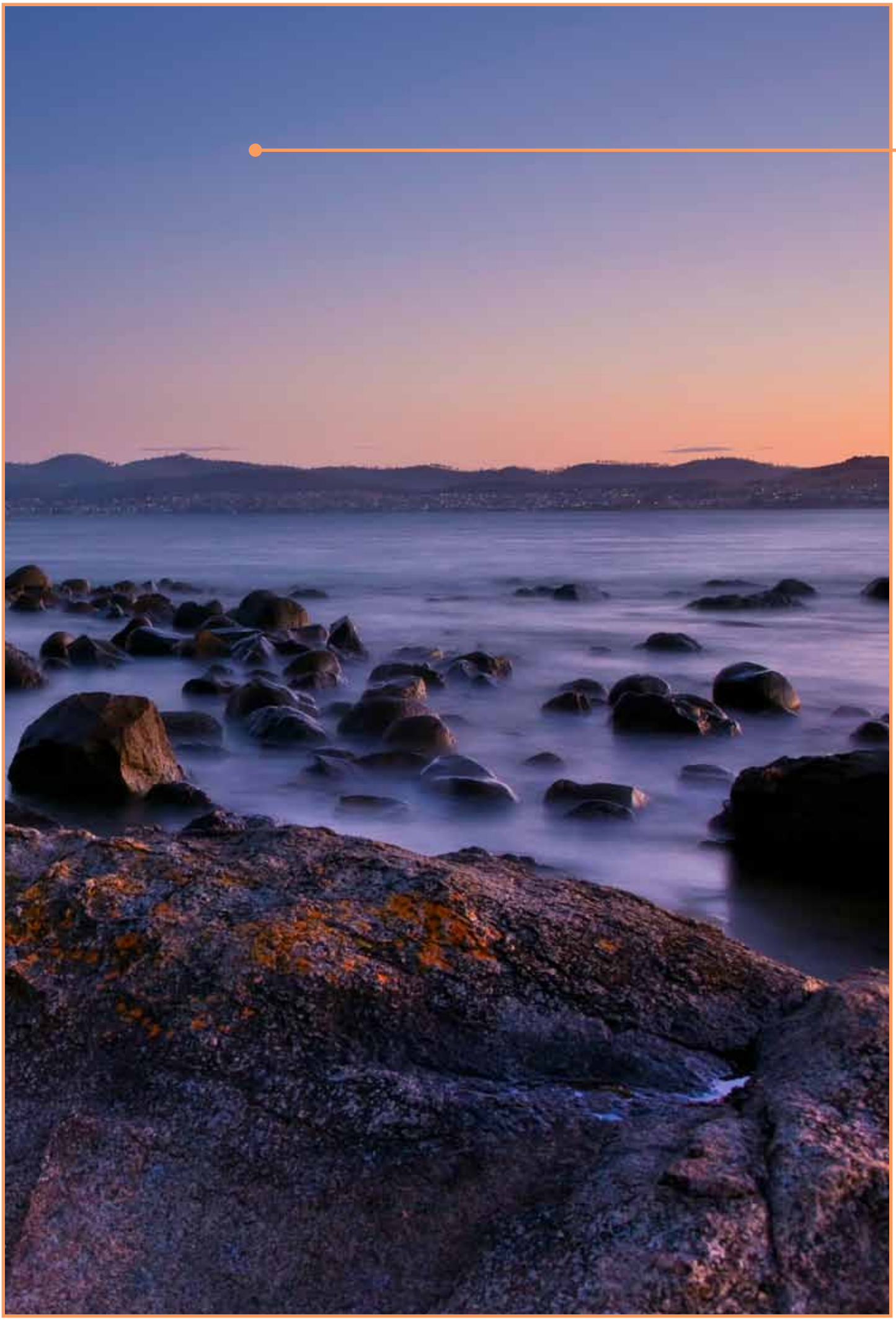

Foreword

The Climate Futures for Tasmania research project is Tasmania's most important source of climate change information tailored specifically for the local climate and conditions of Tasmania. In a first for Australia, and possibly the southern hemisphere, Climate Futures for Tasmania generated local climate information at a scale and level of detail not previously available. The project continues to be invaluable in informing evidence-based decision making in all sectors of government, industry, business and communities in Tasmania.

This collaborative research project, led by Professor Nathan Bindoff, has demonstrated innovative leadership by involving and engaging external stakeholders on all levels. From the beginning of the project, interested end-users were invited to provide input and direction. This has meant that the results and outcomes from the science are directly useable in business systems, applied models and decision-making processes.

The report has passed the rigours of an external scientific review process and I appreciate the efforts of the respected scientists who gave their time and expertise to review the research outcomes. Thank you to Professor William Gutowski (Iowa State University), Professor Bruce Hewitson (University of Cape Town) and Dr James Risbey (CSIRO-CAWCR).

The Climate Futures for Tasmania research project is partly funded through the Commonwealth Environment Research Facilities (CERF) program. Over the last four years, the CERF program has facilitated strong ongoing collaborations across Australia's research institutions and world-class, public good biodiversity research.

On behalf of the Department of Sustainability, Environment, Water, Population and Communities, I thank all those who have contributed to this successful and valuable project.

Alex Rankin
First Assistant Secretary
Information Management Division
Department of Sustainability, Environment, Water, Population and Communities

Executive Summary

Climate Futures for Tasmania is the most complete regional climate change study undertaken in Australia.

Climate Futures for Tasmania is a unique, jointly funded, collaborative research project that generated improved climate change information for Tasmania. In a first for Australia, and the southern hemisphere, Climate Futures for Tasmania generated ensemble climate simulations of future climate with direct applications to the impacts on water and catchments, agriculture and climate extremes for local communities, for businesses and decision making in Tasmania.

Climate Futures for Tasmania generated the most detailed simulations of Tasmania's future climate.

Climate Futures for Tasmania used a dynamical downscaling method to generate climate projections over Tasmania at a finer scale than ever before. We have simulated the complex processes that influence Tasmania's weather and climate, thus providing a detailed view of Tasmania's possible future climates. The dynamical downscaling used in this project is an established technique that uses inputs from global climate models to generate fine-resolution climate simulations.

Climate Futures for Tasmania used several global climate models to provide a range of likely 21st century climates.

We have used six global climate models of the kind that were reported in the IPCC Fourth Assessment Report. By using an ensemble of global climate models we have increased confidence in our projections (where the simulations agree) and can use the differences in the simulations to estimate the range of future climates. Two emissions scenarios were chosen, a high and a low scenario, bracketing plausible future climate change without mitigation policies.

The new climate modelling shows a high level skill in simulating the current temperature and rainfall distributions over Tasmania.

The simulations contain more than 140 individual climate variables recorded every six hours, and provide estimates of the Tasmanian climate for both the recent past (1961-2007) and the future (2010-2100). The downscaled models have a high level of skill in reproducing the recent climate of Tasmania for temperature and rainfall. For the period 1961-1990, the model-mean statewide daily maximum temperature is within 0.1 °C of the Bureau of Meteorology observed value of 10.4 °C; the annual total rainfall of 1385 mm is very close to the observed value of 1390 mm. The pattern of mean temperature over Tasmania for the recent past has a spatial correlation of 0.93 with gridded observations. For mean rainfall, the spatial correlation is 0.63. Spatial correlations for rainfall for some models across all seasons exceeds 0.80. Successful validation of climate models gives confidence in projections of future temperature and rainfall.

Climate models inform us of the long-term trends and statistics of the climate. They are not predictions of the weather for a particular day, month or year.

Climate simulations are not weather forecasts, and cannot tell us what will happen on any given day, month, or year. Climate simulations project long-term changes to climate. That is, the modelled daily variables (or even weekly, monthly or annual) do not match between the simulations and observations. The simulations are intended to give an indication of projected climate over decadal time scales. It is the long-term trends that inform us of the likely changes.

Climate Futures for Tasmania generated a comprehensive dataset, more than twice the size of that used to inform the IPCC's Fourth Assessment Report.

There are 17 simulations of the climate of Tasmania at a resolution of 0.1-degree (about 10 km) or better. These simulations were all downscaled from global climate models of the kind used in the IPCC Fourth Assessment Report. The quantity of modelling output was in excess of 75 terabytes of data and took approximately 1200 days of continuous computer time on a 0.82 teraflop machine. This is more than twice the climate modelling output considered by the IPCC in compiling their Fourth Assessment Report.

Bias-adjusted simulations were created for use in biophysical and hydrological models.

Climate Futures for Tasmania produced bias-adjusted simulations designed specifically to be used with biophysical and hydrological models. Bias-adjusted simulations were calculated for each downscaled simulation using gridded observations from the Australian Water Availability Project (AWAP). The bias-adjustment process was applied to five variables and the bias-adjusted simulations contain 11 commonly used climate variables. These simulations were used directly in biophysical and hydrological models.

Climate Futures for Tasmania produced datasets that are relevant and usable for Tasmanian businesses and communities.

Climate Futures for Tasmania was strongly end-user driven, with the information needs of community, industry and government central in the research analyses. This technical report deals specifically with the climate modelling program undertaken, and an assessment of the simulations against current climate. The general climate impacts report investigated the general climate trends evident in the simulations, along with further analysis of the present climate (against observations) and, importantly, how the climate of Tasmania is projected to change in the 21st century. The remaining reports assess specific aspects of the future climate, notably impacts to agriculture, extreme events, and water and catchments.

FREQUENTLY USED ACRONYMS

Australian Water Availability Project	AWAP
Conformal Cubic Atmospheric Model	CCAM
Intergovernmental Panel on Climate Change	IPCC
IPCC Fourth Assessment Report	AR4
Global Climate Model	GCM
Intergovernmental Panel on Climate Change	IPCC
National Centers for Environmental Prediction	NCEP
Special Report on Emissions Scenarios	SRES
Sea Surface Temperature	SST

ABBREVIATIONS USED FOR GLOBAL CLIMATE MODELS

CSIRO (Australia) GCM	CSIRO-Mk3.5
Max Planck Institute (Germany) GCM	ECHAM5/MPI-OM
Geophysical Fluid Dynamics Laboratory (USA) GCM	GFDL-CM2.0
Geophysical Fluid Dynamics Laboratory (USA) GCM	GFDL-CM2.1
University of Tokyo (Japan) GCM	MIROC3.2(medres)
The Met Office (UK) GCM	UKMO-HadCM3

Table of Contents

1 Introduction

Evidence for the warming of the climate system is now unequivocal (IPCC 2007). There is an increasing body of evidence that most of the observed increase in global average temperatures since the mid-20th century is very likely due to the observed increase in anthropogenic greenhouse gas concentrations (IPCC 2007). This observed warming is consistent with our knowledge of the physical climate system (the atmosphere, oceans, land and sea ice) and with projections of the earth's climate over the 21st century (Meehl et al 2007a). The entire climate system is affected by this warming, including changes to rainfall, wind, evaporation and the hydrological cycle.

Climate change is a global phenomenon whose impacts will be most keenly felt at a local level. The projected effects of global climate change are not evenly distributed over the globe (see Figure 1.1). It is because of this spatial variation that local or regional studies are required to understand the local effects of climate change.

Tasmania is unique in its global perspective with regard to climate change. It lies on the border between a region where most global climate models show a drying trend and a region that will undergo a wetting trend (Meehl et al 2007b). These factors make Tasmania a difficult region to project climate change for variables like precipitation using just global climate models. Tasmania is an Australian state in the south-east of the continent. It consists of a main island (up to 300 km across) and a number of smaller islands. Tasmania's topography is highly variable causing a varied climate on island scales, ranging from an annual rainfall of more than 3000 mm on the mountainous west coast, to about 500 mm on the drier east coast.

Dynamical downscaling of global climate models is a way of incorporating Tasmania's complex topography and maritime influenced climate to provide a greater realism of regional variations in key climate variables such as rainfall, winds and temperature. However, the models are not perfect; they do not simulate every aspect of the climate system. Downscaled climate models can reproduce many aspects of the patterns of variability and weather systems that describe the overall climate and as such, they are our best, and often the only, tool for assessing potential changes in the future climate (Randall et al 2007).

For Tasmania, regional dynamical downscaling of global climate models was first undertaken in a joint project involving the Tasmanian Partnership for Advanced Computing and CSIRO Marine and Atmospheric Research, commissioned by Hydro Tasmania (McIntosh et al 2005). The initial project used CSIRO's Conformal Cubic Atmospheric Model (CCAM) to create local-scale projections, tuned to the complexities of the Tasmanian climate.

This initial study identified a range of limitations. Using a single scenario of future emissions did not provide any insight into the potential range, or uncertainty estimates of the possible future climates. It used a relatively short projection period (to 2040) and provided only a single projection for one greenhouse gas emissions scenario. The initial study provided a better understanding of what is a reasonable time period to assess climate change, the potential problems that occur when downscaling a global climate model, the potential value of the downscaling approach, and the availability and accuracy of observed data. Valuable lessons were learned on how to manage a multi-disciplinary research project. The recommendations for future climate modelling included longer simulations into the future, updated and improved models, multiple IPCC emissions scenarios and an ensemble of models to refine the projections and give a more complete assessment of likely climate futures in Tasmania (McIntosh et al 2005). All of these recommendations were incorporated into the Climate Futures for Tasmania project.

Project research components

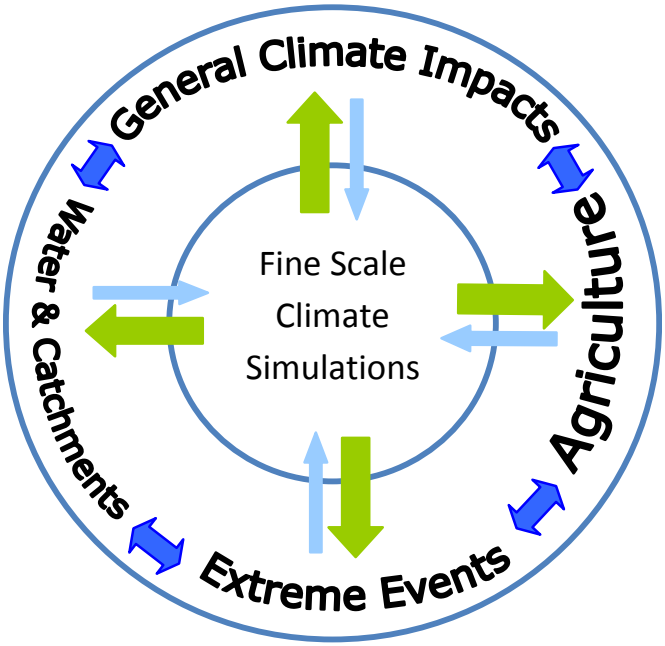

The pilot study also identified the value of a prior understanding of the climate change information needs of end-users. Extensive consultation with diverse potential end-users confirmed widespread demand for climate change research and, more importantly, identified many specific outputs from the research that would be useful to each end-user group.

Climate Futures for Tasmania built on the 2004 pilot study by expanding the IPCC emissions scenarios to two (a high (A2) and a low (B1) emissions scenario), increasing the number of GCMs used to six, extending the time period of simulations to 2100, using ensembles in the analyses and significantly expanding the involvement of end-users.

This collaborative research project is unique in its involvement of state and federal governments, universities, research organisations and Tasmanian stakeholders. In a first for Australia, Climate Futures for Tasmania generated local climate information at a scale and level of detail not previously available.

The climate modelling program described in this report is one of the five areas, or components, of research undertaken in the project. The remaining areas of research are general climate impacts, water and catchments, impacts on agriculture and extreme events. This report focuses on the performance of the simulations in reproducing Tasmanian climate and assesses the likelihood that they can accurately project future climate change for the Tasmanian region. The results of the other areas of research are in separate technical reports (Bennett et al 2010; Grose et al 2010; Holz et al 2010; White et al 2010).

About the project

Climate Futures for Tasmania is the Tasmanian Government's most important source of climate change data at a local scale. It is a key part of Tasmania's climate change strategy as stated in the Tasmanian Framework for Action on Climate Change and is supported by the Commonwealth Environment Research Facilities as a significant project.

The project used a group of global climate models to simulate the Tasmanian climate. The project is unique in Australia: it was designed from conception to understand and integrate the impacts of climate change on Tasmania's weather, water catchments, agriculture and climate extremes, including aspects of sea level, floods and wind damage. In addition, through complementary research projects supported by the project, new assessments were made of the impacts of climate change on coastal erosion, biosecurity and energy production, and the development of tools to deliver climate change information to infrastructure asset managers and local government.

As a consequence of this wide scope, Climate Futures for Tasmania is an interdisciplinary and multi-institutional collaboration of twelve core participating partners (both state and national organisations). The project was driven by the information requirements of end users and local communities.

The Climate Futures for Tasmania project complements climate analysis and projections done at the continental scale for the Fourth Assessment Report from the Intergovernmental Panel on Climate Change, at the national scale in the *Climate Change in Australia* Report and data tool, as well as work done in the south-east Australia region in the *South Eastern Australia Climate Initiative*. The work also complements projections done specifically on water availability and irrigation in Tasmania by the *Tasmania Sustainable Yields Project*.

IPCC Projections of Temperature Change

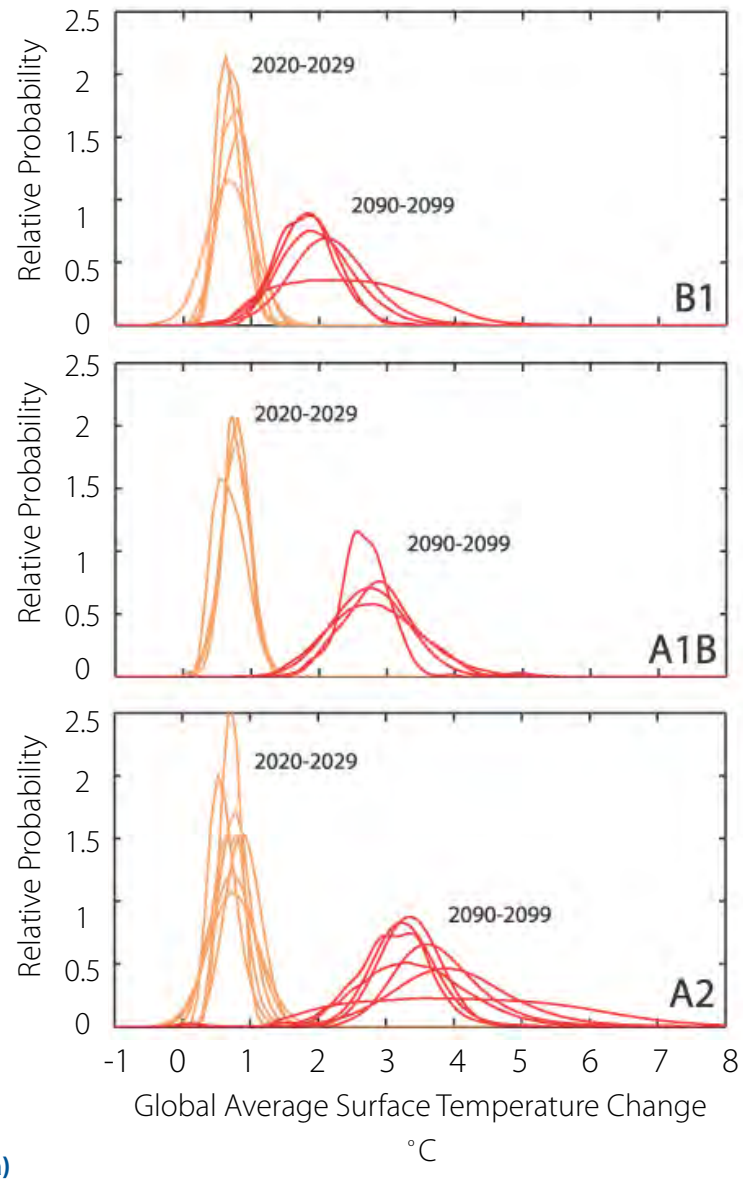

(a)

Figure 1.1 Model mean of projected change in global surface temperature from the early and late 21st century, relative to the period 1980-1999 (from IPCC 2007). The central and right panels (b) show the multi-model mean projections for the 23 GCMs reported in the IPCC AR4 for the B1 (top), A1B (middle) and A2 (bottom) SRES scenarios. The left panels (a) show the corresponding spread in the models used to create the mean picture.

IPCC Projections of Temperature Change

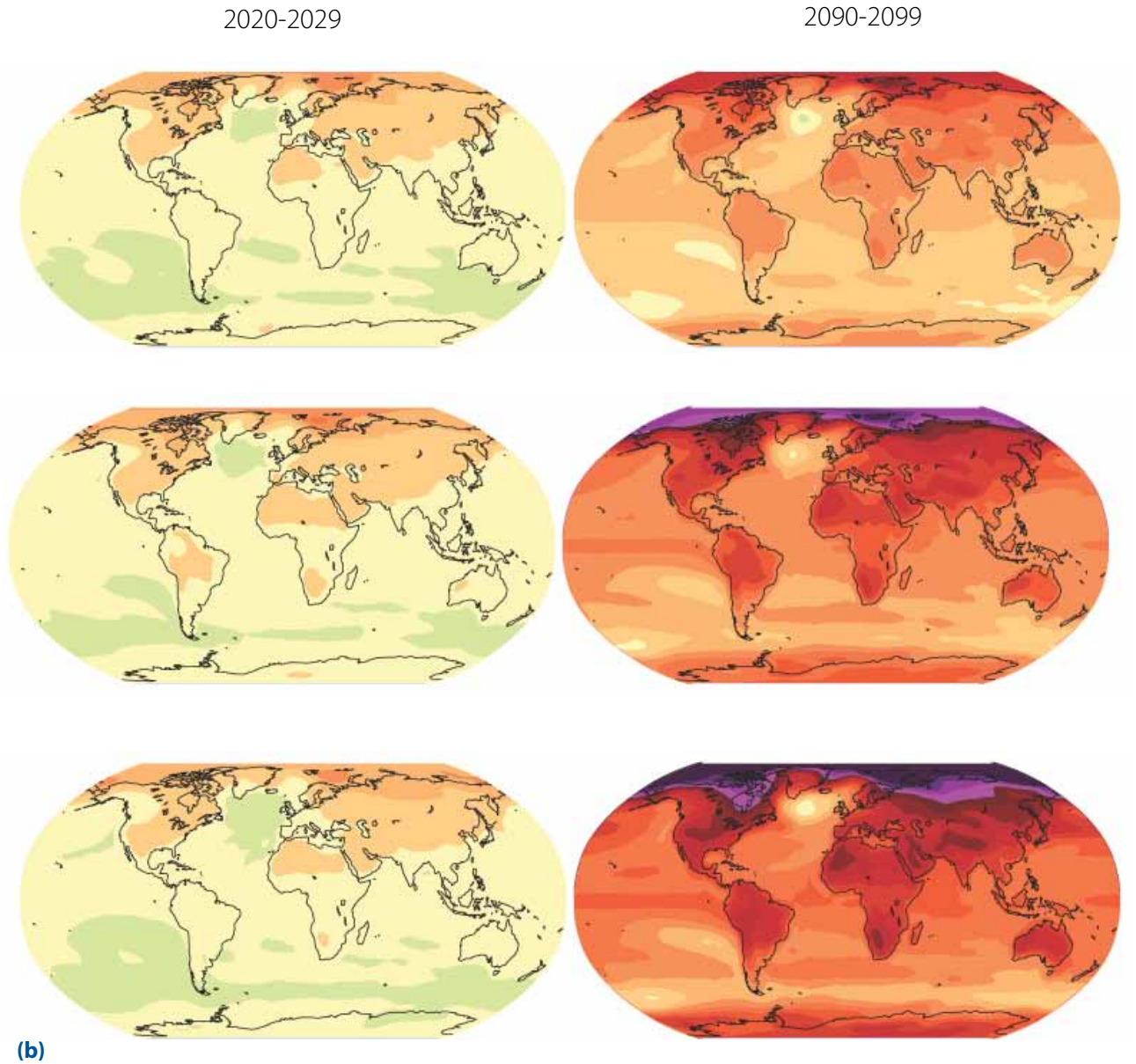

2 Background

Coupled Ocean-Atmosphere General Climate Models (GCMs) provide the best estimates of change to our climate on a global scale to the end of this century. The Intergovernmental Panel on Climate Change's (IPCC) Fourth Assessment Report (2007) used climate modelling output from 23 different GCMs as the basis of their global assessment of climate change (Meehl et al 2007b). Because GCMs are global in scale, with a limited resolution, they cannot provide a detailed picture of climate variables at regional scales. Tasmania's diverse geography and varied climate make assessing the regional impacts of climate change on temperature, rain and other climate variables in Tasmania particularly difficult when relying solely on low resolution GCMs.

The foundation of Climate Futures for Tasmania was to take the simulations produced by six global climate models, using two IPCC SRES emissions scenarios, and use these projections as inputs into a high-resolution climate model that is focused on Tasmania. By modelling the atmosphere and local environment at a much finer scale than is possible using a standard GCM, we expected to better simulate the specific processes that drive Tasmania's weather and climate. The Climate Futures for Tasmania downscaled simulations add value to the global-scale information provided in the IPCC Fourth Assessment Report, and are tied to the accuracy of the global projections made by the host GCMs. The aim was to produce projections of climate change for the Tasmanian region that were sufficiently detailed to allow the resolution of changes in the projected climate at finer temporal and spatial scales across Tasmania.

2.1 Choice of IPCC SRES emissions scenarios

Given that it is very likely that rising greenhouse gases and aerosols are responsible for recent global warming (IPCC 2007), it follows that the extent of climate change is dependent on the amount of future greenhouse gas emissions. Therefore, the choice of a gas emissions scenario to use in the climate simulations is of utmost importance. The most commonly used and accepted set of greenhouse gas emissions scenarios, known as the SRES emissions scenarios, comes from the IPCC. These were first presented in a 1992 IPCC Second Assessment Report (IPCC 1996) and were termed the IS92 emissions scenarios (Leggett et al 1992). The emissions scenarios were then updated in 2001, reported in the Special Report on Emissions Scenarios (SRES). They are now named the SRES emissions scenarios (Nakicenovic & Swart (eds) 2000). The SRES emissions scenarios were used in the IPCC Third Assessment Report in 2001 (IPCC 2001) and in the IPCC Fourth Assessment Report (AR4) in 2007 (IPCC 2007). The SRES emissions scenarios are divided into six families: A1FI, A2, A1B, B2, A1T and B1. The families are based on future technological and societal changes, such as population growth, and not just on a 'high, medium and low' scale of carbon emissions. Figure 2.1 shows carbon dioxide emissions levels for these six families from the year 2000 projected to the year 2100, as well as the range of likely emissions scenarios (post SRES). Note that the six families do not follow the same profile over the coming century, with some showing a constant increase and others levelling and decreasing by 2100.

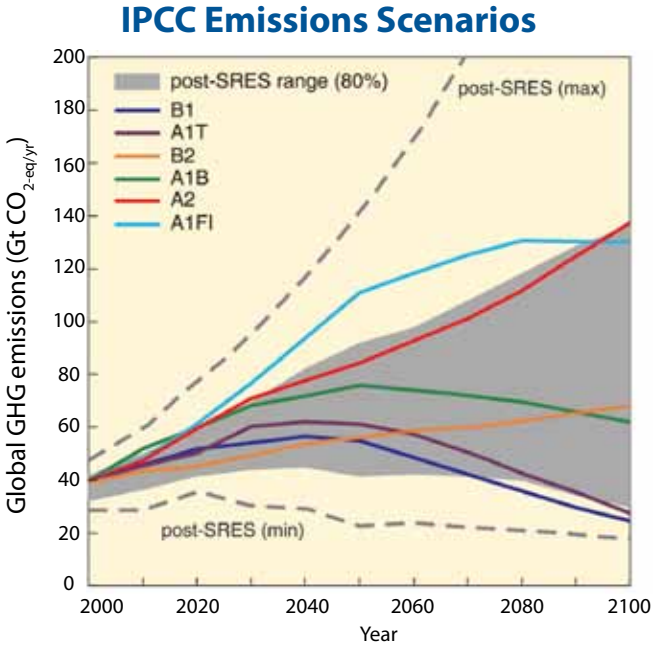

Figure 2.1 Global greenhouse gas emissions scenarios for the 21st century. Greenhouse gases include carbon dioxide, but also other gases such as methane and nitrous oxides. Also shown is the updated likely range of greenhouse gas emissions presented in the Fourth Assessment Report (post-SRES) (from IPCC, 2007).

The IPCC recommends that more than one of the SRES emissions scenario families be used in any analysis. As such, we chose to downscale GCM modelling output from two climate scenarios, one categorised as a high (A2) and one categorised as a low (B1) emissions pathway. By considering differing emissions scenarios, we have an indication of the range of possible climate change.

Since 2001, the observed global greenhouse gas emissions have been tracking above A1FI, the highest SRES emissions scenario. This may suggest that a higher emissions scenario such as A1FI would be the most realistic choice for the study, at least in the short-term, but this emissions scenario was rejected for two main reasons. The A1FI emissions scenario, the most fossil fuel intensive scenario, starts with high levels of carbon dioxide emissions, but involves a rapid change in technology around the middle of this century. In contrast, the A2 emissions scenario features less rapid technological change, and a more heterogeneous world, with emissions that outstrip the A1FI emissions scenario by the end of the century. Second, and more importantly for this project, the IPCC AR4 did not feature any GCM simulations for the A1FI emissions scenario. Instead, likely changes under the A1FI emissions scenario in temperature and sea level rise variables were scaled up from results under a lower emissions scenario (A1B). This scaling approach disqualifies the A1FI emissions scenario from being used in the project, as unscaled GCM modelling outputs are required for our downscaling method.

For a low emissions future, we chose the B1 emissions scenario. The B1 family of emissions scenarios describes a world with a focus on rapid changes in economic structures towards a service and information economy, and the introduction of new technology. The B1 emissions scenario assumes coordinated global effort on economic, social and environmental sustainability, but no additional climate initiatives, such as mitigation of carbon dioxide emissions.

Choosing the A2 and B1 emissions scenarios covers the range of plausible emissions scenarios for unmitigated climate change and thus provides a good range of climate change projections. It is worth noting that the change in global mean near-surface temperature is roughly the same across all emissions scenarios until the mid-21st century, and so the choice of SRES emissions scenario does not become important until the latter half of the century. More details on the changes produced by these emissions scenarios can be seen in Figure 10.4 and Figure 10.5 of Meehl et al (2007b). We will show in the General Climate Impacts Technical Report (Grose et al 2010) that the intra-scenario variability, produced by multiple models, each with slightly different internal mechanisms, is at least as great as the inter-scenario variability. This leads us to believe that diversity of GCMs (discussed in Section 2.2) is of more importance than the spread of emissions scenarios, and so we have chosen to concentrate on more models and only two emissions scenarios.

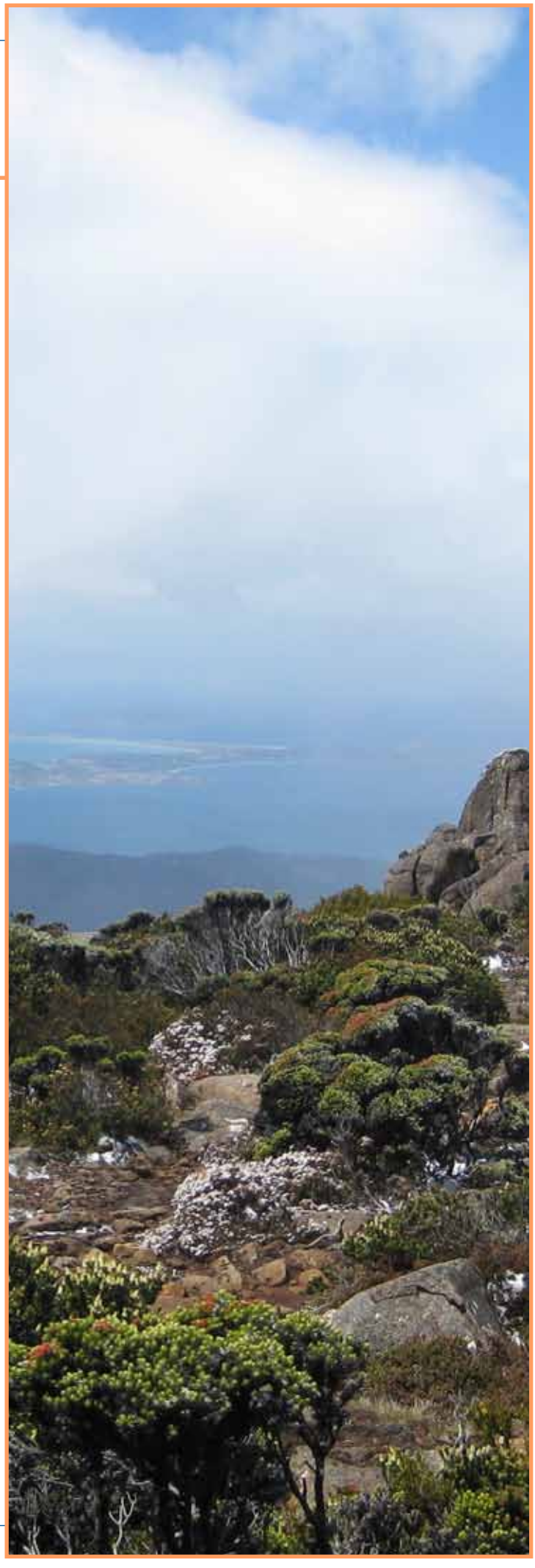

2.2 Choice of coupled global climate models

The IPCC considered 23 GCMs when compiling its Fourth Assessment Report (AR4). The output from these GCMs (along with two more that were submitted after AR4 was written) are all publically available through the World Climate Research Programme's Coupled Model Intercomparison Project Phase 3 (CMIP3) (Meehl et al 2007a) (www-pcmdi.llnl.gov/ipcc/about_ipcc.php). The use of an ensemble of GCMs by the IPCC allowed for a more robust estimate of the climate change signature by examining the ensemble mean of key variables (such as temperature and rainfall), as well as an estimate of the uncertainty in these climate variables through the spread of the models. Climate Futures for Tasmania has employed the same multi-model approach.

Due to the relatively modest scale of the project compared to the IPCC AR4, we have chosen to use six of the 25 GCMs available from the CMIP3 archive to produce fine-scale climate projections over Tasmania. There are many ways to decide on the "best" six GCMS to use. The ability to reproduce hemispheric-scale modes of the atmosphere (such as El Niño, the Antarctic Oscillation et cetera) and sensitivities to climate change, are all important. The decision on the best models to use is also tied to the specific use of the results generated and this choice can be an entire study in itself. We have decided to base our choice of models on the work of Smith and Chandler (2009) who argue that some models can be shown to perform relatively poorly when assessed by their ability to simulate present day means and variability. The ability to accurately simulate present climate is a necessary, but not wholly sufficient, condition for a good projection of climate change. In particular, regional projections of rainfall are characterised by a high level of uncertainty. Smith and Chandler argue that discounting models that have been shown to perform poorly over south-east Australia can reduce uncertainty in model projections.

The eight criteria, in order of importance, that Smith and Chandler developed to assess the performance of GCMs in reproducing present-day climate variability in the Australian region are in Table 2.1. They then assessed each of the 23 GCMs reported in the IPCC AR4 against these criteria and determined that only five models (ECHAM5/MPI-OM, GFDL-CM2.0, GFDL-CM2.1, MIROC3.2(hires) and UKMO-HadCM3) were able to provide good spatial distribution of Australian rainfall and credible representations of ENSO. These five models became the basis of our choice of models for the downscaling project. Note that GFDL-CM2.0 and GFDL-CM2.1 can be considered as independent GCMs. These two models have different dynamical cores, ocean time-stepping scheme and lateral viscosity. The final model chosen was CSIRO-Mk3.5. CSIRO-Mk3.5 has been developed since the release of the IPCC Fourth Assessment Report and has since been included in the CMIP3 archive. Mk3.5 is an updated version of CSIRO-Mk3.0. CSIRO-Mk3.0 was ranked in the top half of the 23 GCMs considered by Smith and Chandler. The relative improvement of CSIRO-Mk3.5 over CSIRO-Mk3.0 has been discussed in a number of papers. Gordon et al (2010) showed that CSIRO-Mk3.5 performed better than CSIRO-Mk3.0 in a number of metrics, such as improved replication of the El Niño Southern Oscillation (ENSO). Watterson (2008) ranked the CSIRO-Mk3.5 GCM slightly higher than CSIRO-Mk3.0 GCM on model skill, and gave CSIRO-Mk3.5 a similar skill score to the UKMO-HadCM3 and MIROC3.2(medres) GCMs. Finally, Rotstayn et al (2010) compared the performance of CSIRO-Mk3.0, CSIRO-Mk3.5 and

Table 2.1 The eight tests used to assess the performance of the 23 IPCC models in their ability to reproduce present day climate in the Australian region (Smith & Chandler 2009).

	Test	Citation
1	Number of rainfall criteria failed	(Smith & Chandler 2009)
2	Satisfied ENSO criteria	(Min et al 2005; van Oldenborgh et al 2005)
3	Satisfied criteria for rainfall, temperature and MSLP	(Suppiah et al 2007)
4	M-statistic representing goodness of fit at simulating rainfall, temperature and MSLP over Australia	(Watterson 2008)
5	Satisfied criteria for daily rainfall over Australia	(Perkins & Pitman 2009)
6	Satisfied criteria for daily rainfall over MDB region	(Maximo et al 2008)
7	Satisfied criteria for MSLP over MDB region	(Charles et al 2007)
8	Below median errors for 14 variables	(Reichler & Kim 2008)

Table 2.2 The six global climate models chosen for use in Climate Futures for Tasmania, along with their country of origin and approximate horizontal resolution over Australia.

Global Climate Model	Country of origin	Approximate horizontal resolution (km)
CSIRO-Mk3.5	Australia	200
GFDL-CM2.0	USA	300
GFDL-CM2.1	USA	300
ECHAM5/MPI-OM	Germany	200
MIROC3.2(medres)	Japan	300
UKMO-HadCM3	United Kingdom	300

(the recently developed) CSIRO-Mk3.6 and showed that CSIRO-Mk3.5 was significantly improved over a number of metrics compared to CSIRO-Mk3.0.

Finally, CSIRO is a major partner in the project and thus the use of CSIRO-Mk3.5 as one of the models was desirable (CSIRO-Mk3.6 had not been developed at the start the project). None of the six models chosen has a mean global warming at the extreme ends of the range of warmings projected by the simulations reported by the IPCC for either of the emissions scenarios.

Another practical consideration when choosing the six GCMs, was to ensure that each of the selected models simulated by the IPCC for the chosen emissions scenarios was available, since the downscaling technique requires input from GCM simulations. Smith and Chandler (2009) assessed the MIROC3.2(hires) model as one of the most suitable models for use in this study. However, modelling output did not exist for the primary emissions scenario chosen for use in the project (A2) and thus was excluded from our study. MIROC3.2(medres) was subsequently chosen as it performs well in all tests except for the number of rainfall criteria it failed (Smith & Chandler 2009). Smith & Chiew (2009), using a combined measure, ranked MIROC3.2(medres) as the fifth best GCM for generating inputs to hydrological models across south-east Australia. The fact that it is the same model as MIROC3.2(hires) with the same implementation of the physics, but at a different resolution, was also considered to be advantageous. The final list of six GCMs chosen for the project is in Table 2.2.

By concentrating our efforts on these six models, we limited the size of the computational task associated with downscaling, while also understanding the inter-model difference and uncertainty.

A detailed report on the performance and climate sensitivity of each of the chosen GCMs is not included in this report. Five of the six models (the exception is CSIRO-Mk3.5) are described in detail and assessed in Chapter 8 (Randall et al 2007) and Chapter 10 (Meehl et al 2007b) of the IPCC Fourth Assessment Report (along with 17 other GCMs). CSIRO-Mk3.5 is described by Gordon et al (2010). The performance of four of the six GCMs in the Tasmanian context has been partly assessed in the *Tasmanian Sustainable Yields: Production of climate scenarios technical report* (CSIRO 2009). The *Climate Futures for Tasmania: general climate impacts technical report* (Grose et al 2010) assesses the trends of the chosen GCMs in the context of the model mean reported by the IPCC in Chapter 10.

The six GCMs used in the project have been chosen because of their ability to model current south-east Australian climate means and variability. Aside from this crucial metric, the six GCMs span a broad range of the metrics used to assess GCM performance and climate sensitivity considered in the above reports. Finally, it should be noted that the simulations archived by CMIP3 (and thus reported by the IPCC) represent only a subset of the possible future climate scenarios. As such, the results presented in this report necessarily under-represent the full envelope of future climates.

The decision to use six GCMs and the metrics employed for choosing these six models is an area of study that could benefit from future work. The exact effect on the ensemble spread for the current climate and the climate response of choosing these six GCMs has not been fully investigated. Such an investigation was beyond the scope of the current project but would form an interesting aspect of future work in the area of dynamical downscaling of GCMs for climate change studies.

3 Methods used in climate projections

This section outlines the method used to downscale from global climate models (GCMs) with a resolution of 200 km to 300 km to the fine-scale 0.1-degree (about 10 km) simulations.

Two established methods exist for downscaling climate information from the coarse spatial scales of GCMs to a finer scale suitable for regional studies: dynamical and statistical downscaling. Dynamical downscaling feeds output from a host GCM into either a limited-area model or a stretched grid global climate model. The result is a fine-scale dynamical model over the area of interest, often called a regional climate model. Regional climate models are based on the same physics as GCMs, and can be just as complex. However, because a regional climate model focuses on a small area, it can provide more detail over that area than is possible with a GCM alone. Statistical downscaling assumes that local climate is conditioned by large-scale climate along with local features such as topography, distance to coast and vegetation. By assuming these relationships, statistical downscaling identifies empirical links between large-scale patterns of climate elements and local climate, in order to arrive at fine-scale projections of climate based on coarse GCM simulations.

Several studies have compared the results from statistical and dynamical downscaling (Cubasch et al 1996). The general conclusion from these studies is that the two downscaling methods perform similarly for present-day climate. However, the two methods frequently differ when examining future climate projections.

One of the limitations of statistical downscaling is the assumption that observed links between large-scale climate variables (from the GCM) and local climate will persist in a changed climate regime. A second limitation, when using this method to project a changing climate, is that the observational dataset being used for the downscaling must span the range of projected future climate responses. In practice, this necessitates having available a long, reliable observational series of both the large and fine-scale climate. Finally, it is difficult to resolve changes in timing and frequency (seasonality) of weather events using statistical downscaling. Some more complex methods of statistical downscaling do allow for changes in seasonality of events but most statistical approaches do not.

The main constraints of dynamical downscaling include the technical complexity and computational cost involved in generating the projections of current

Conformal Cubic Grid

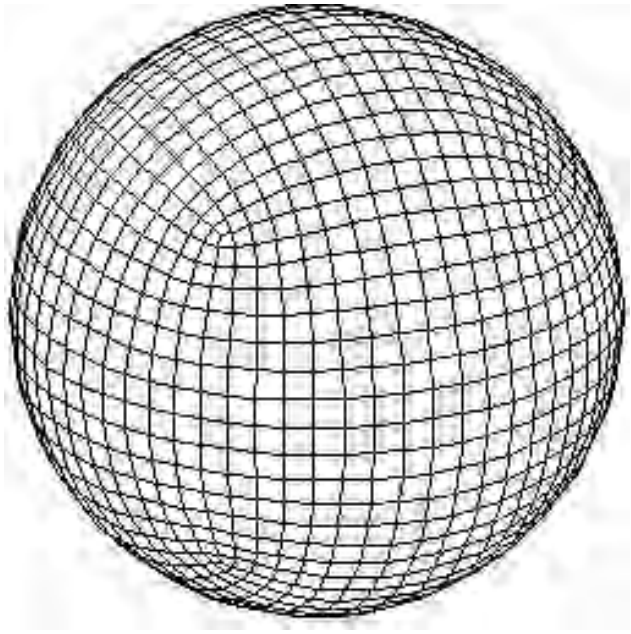

Figure 3.1 An example of a conformal cubic grid projected on to a sphere.

and future climate. Just as important is demonstrating that the model can simulate the current climate and atmospheric processes. Successfully reproducing the current climate indicates that the downscaled model is correctly simulating the processes that influence and control the Tasmanian climate and weather. Reproducing the current climate gives confidence that the downscaling model will be able to simulate the future (changed) climate. However, the future climate may be strongly influenced by processes that are not as significant in the current climate (for example, increased amount of convective rainfall in the atmosphere).

The use of dynamical downscaling allows us to demonstrate changes in the local climate of Tasmania, such as changes to seasonality, changes to the frequency and intensity of weather events and the relationships between different climate variables. Dynamical downscaling also maintains the relationships between different climate variables (for example, rainy days are also cloudy, or when a cold front passes over Tasmania the temperature drops). Because of these capabilities of downscaling, Climate Futures for Tasmania made the technical and financial commitment to undertake an extensive dynamical downscaling process involving multiple GCMs and SRES emissions scenarios, as detailed in the following sections of the report. This commitment has led to the provision of the most detailed projections

of Tasmania's future climate. Significantly for this project, dynamical downscaling not only accounts for the dynamical relationship between local features (such as orography) and synoptic patterns in the present climate, but also allows these relationships to evolve into the future.

3.1 Introduction to CCAM

CSIRO Marine and Atmospheric Research has been undertaking regional climate modelling for well over a decade. For much of this time, the Conformal Cubic Atmospheric Model (CCAM) has been the mainstay of the dynamical downscaling undertaken at CSIRO (McGregor 2005; McGregor & Dix 2001; McGregor & Dix 2008). CCAM is a full atmospheric global climate model, based on using a conformal-cubic grid, (Figure 3.1). To allow for downscaling experiments, CCAM can be configured to use a stretched grid by utilising the Schmidt transformation (Schmidt 1977) of the coordinates and dynamical equations. A stretched grid allows for higher resolution in areas of interest (see Figure 3.2) and lower resolution elsewhere.

CCAM uses a semi-Lagrangian advection scheme and semi-implicit time step with an extensive set of physical parameterisations: the GFDL parameterisation for long-wave and short-wave radiation (Lacis & Hansen 1974; Schwarzkopf & Fels 1991) is used, with interactive cloud distributions determined by the liquid and ice-water scheme of Rotstayn (1997); the model uses a stability-dependent boundary layer scheme based on Monin-Obukhov similarity theory (McGregor et al 1993); the canopy scheme described by Kowalczyk et al (1994) is employed with six layers for soil temperature, six for soil moisture and three layers for snow; and the cumulus convection scheme with both downdrafts and detrainment, as well mass-flux closure, as described by McGregor (2003). A current limitation of CCAM is that it uses fixed vegetation and soil type. Changes in distribution of vegetation and soil can be important for local changes, and future versions of CCAM are planned that will allow these fields to evolve in response to climate change.

CCAM Grid Projected on Earth

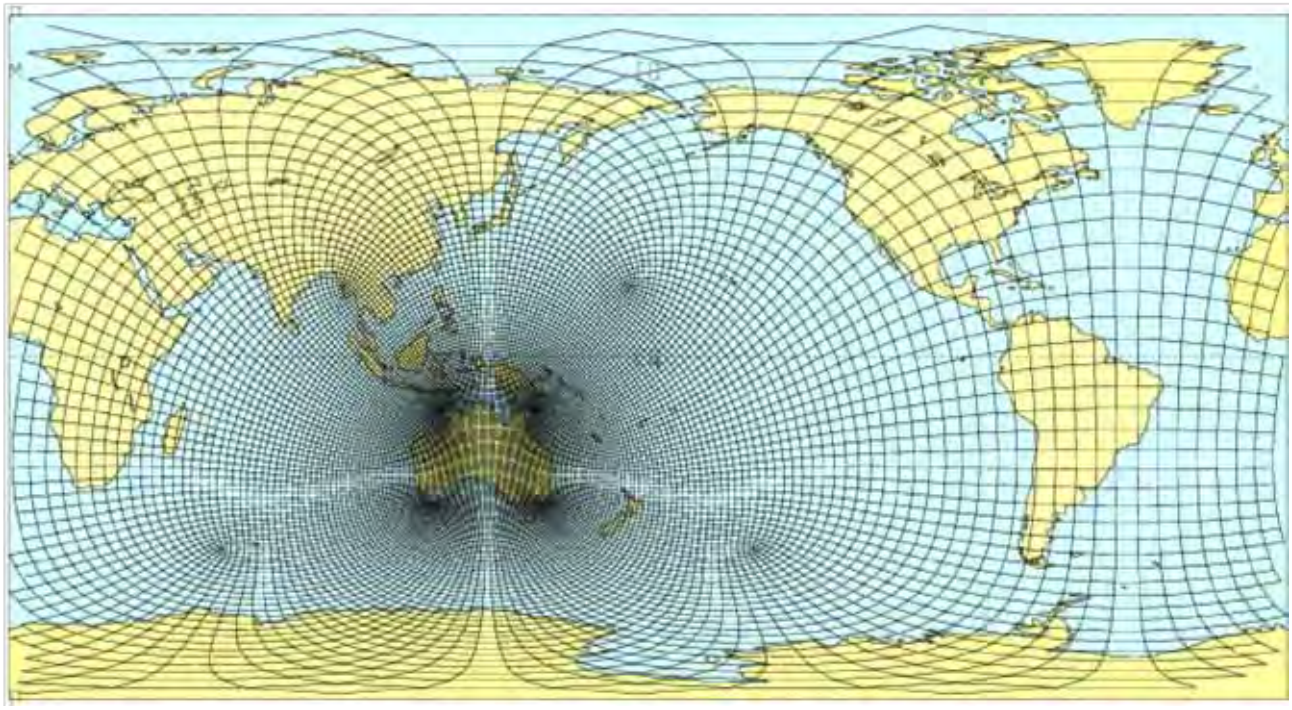

Figure 3.2 The CCAM grid projected on to the Earth. The grid has been stretched to provide higher resolution (approximately 60 km grid cells) over Australia. This is the grid used in the first step of the downscaling process.

CCAM's predecessor, DARLAM, took part in many regional and stretched-grid inter-comparisons with models from other climate institutions including COMPARE 1 (short-term regional modelling of cyclogenesis over Canada) and COMPARE 2 (modelling flow over the Pyrenees, (Georgelin et al 2000)) as well as the PIRCS regional climate modelling inter-comparison over the USA (Anderson et al 2003; Takle et al 1999).

The physical parameterisations of DARLAM, and to a lesser extent its numerics, were carried over into CCAM. Numerous improvements have since been implemented in CCAM. International CCAM inter-comparisons include COMPARE 3 (tropical cyclone genesis (Nagata et al 2001; Nagata et al 2000)) and the two RMIP regional climate model inter-comparisons over Asia for one and ten years (Fu et al 2005), as well as SGMIP, an inter-comparison of the four existing stretched grid global climate models (Fox-Rabinovitz et al 2006; Fox-Rabinovitz et al 2008). In all the inter-comparisons, both models performed as well, or better than, the other downscaling models.

Other investigators for regional climate studies have also used DARLAM and CCAM over other parts of the world. DARLAM has been used to generate simulations over South Africa (Joubert et al 1999) and New Zealand (Renwick et al 1999). Simulations using CCAM have also been successfully undertaken over South Africa (Engelbrecht et al 2009), Fiji (Lal et al 2008) and Indonesia.

The exact choice of downscaling method affected the detail of the results generated in this report. Using a different dynamical downscaling model, such as WRF (the Weather and Research Forecast Model), or using statistical downscaling, may impact the fine detail of the results, such as the spatial correlation between the modelling output for temperature and the observed value, but the broad picture will be consistent across different methodologies. An important element of this difference is how the model resolves topography within each cell. The differences that come with improved topography will be discussed in Section 5.8. The exact nature, or size, of these differences is beyond the scope of this study. Any downscaling method that does not model the current climate accurately should be rejected. A further discussion on the differences that can arise from using different downscaling methods can be seen in the ENSEMBLES Final Report (van der Linden & Mitchell (eds) 2009).

Even when choosing between dynamical downscaling models differences can arise. A major driver of these differences is the exact boundary conditions required for different downscaling models. As CCAM is a stretched grid global model it does not require lateral boundary conditions and thus can be forced using only SST from the host GCM. A limited area model such as WRF must use atmospheric variables from the host GCM in order to provide the lateral boundary conditions necessary in such a model. This issue will be explored further in Section 3.4.

CCAM Grid Centred on Tasmania

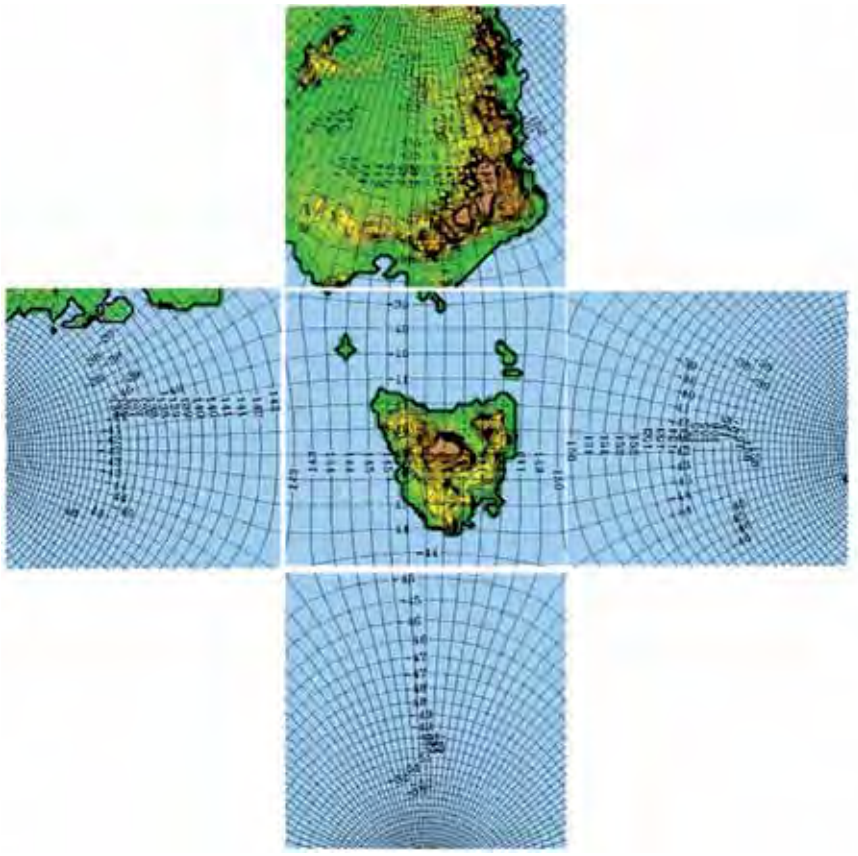

Figure 3.3
A flat representation of the CCAM grid with 48 by 48 (C48) cells on each face, stretched to an average of 10 km per grid cell over Tasmania. Tasmania appears largely as one would expect, but the surrounding areas are increasingly distorted and compressed the further they lie from the high-resolution centre panel. The "back" face of the conformal cubic grid, which contains most of the world, is not shown in this picture.

3.2 Downscaling process

A basic principle of weather forecasting is that processes at even the finest of scales can influence large-scale weather (the butterfly flapping its wings in Australia causing a hurricane in South America is a popularisation of this principle). The implications of this principle on climate modelling is that the finer the resolution of a model, the more capable that model is of simulating the small scale processes that influence weather. As one increases resolution, one more realistically simulates the surface forcings, especially orographic effects. In addition, as with weather prediction, in general the model will more realistically capture the dynamics (and hopefully physics) of weather systems.

Unfortunately, increasing model resolution is expensive; doubling the resolution typically equates to an eightfold increase in computation and storage requirements. Appropriate parameterisation schemes can also go a long way to negating the effects of limited resolution. Furthermore, when choosing an appropriate model resolution, some thought must be given to the intended purpose of the simulation: GCMs are broad-scale models, but give a perfectly acceptable indication of the changes to climate on a continental scale. In contrast, if one wants to model wind hazards at the household scale, then a model with far greater detail is required, perhaps with a spatial resolution approximating the size of the households.

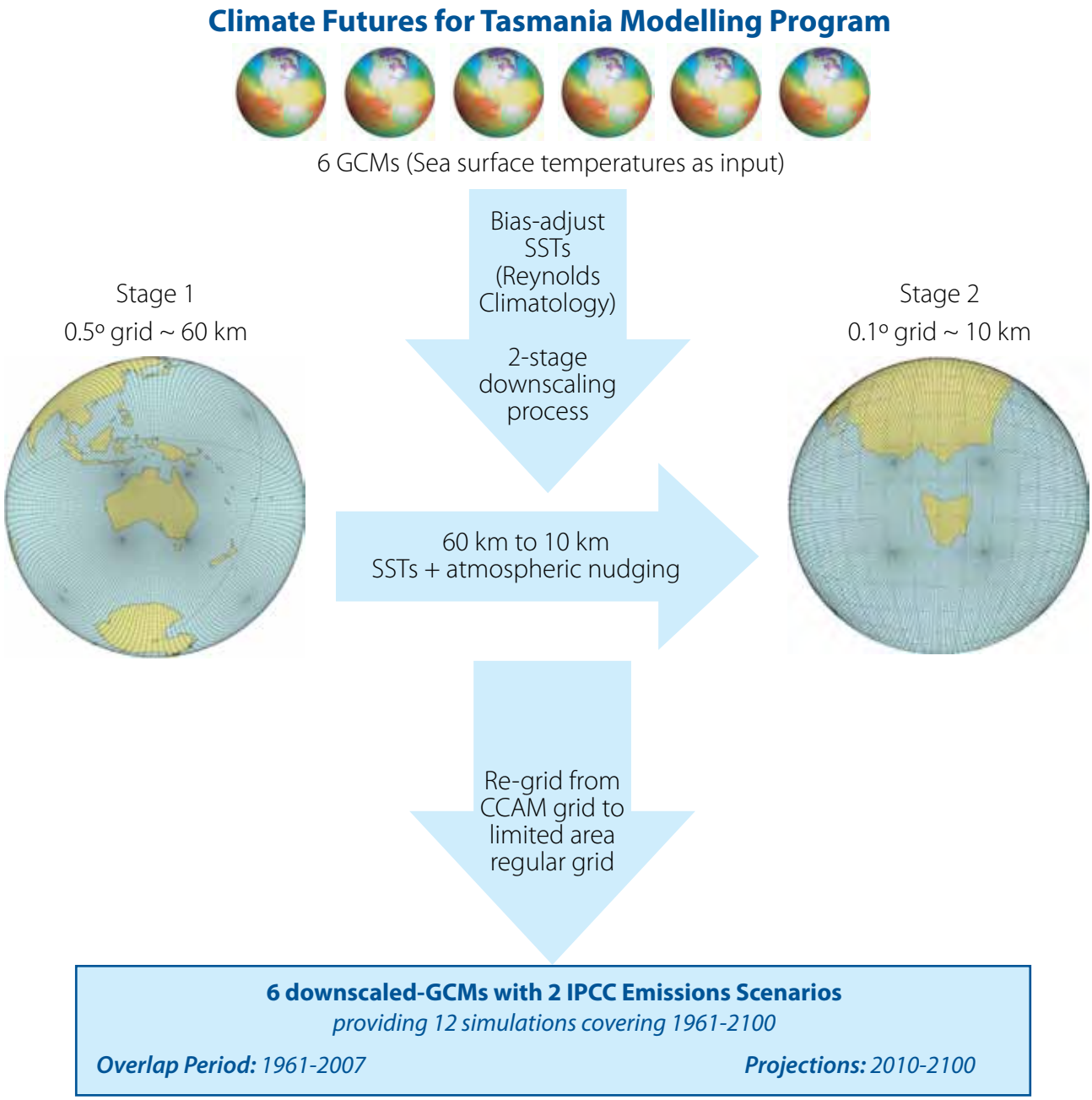

Figure 3.4 Schematic of the dynamical downscaling process used in Climate Futures for Tasmania, from the low resolution coupled GCM boundary conditions (Sea Surface Temperatures) through the intermediate resolution (0.5-degree) to the high resolution CCAM 0.1-degree grid.

Tasmania is roughly 350 km by 300 km, the size of a few of GCM grid cells. After carefully weighing up the costs and benefits involved with downscaling to different grid-scales, a decision was reached to achieve a final resolution of 0.1-degree for Tasmania, corresponding to a grid where each individual cell has side lengths of approximately 10 km. CCAM uses a stretched grid with continuously varying resolution; by centring the high-resolution panel over Tasmania and choosing a grid with 48 by 48 cells on each face, we were able to achieve an average resolution over Tasmania of approximately 10 km for the fine-scale simulations. Figure 3.3 shows how 10 km CCAM views Tasmania and surroundings (that is the rest of the world). Note that the further points lie from the high-resolution panel the more they become compressed in this image.

The downscaling process undertaken in the project is outlined in Figure 3.4. The process starts with input from a coarse resolution GCM simulation (hereafter referred to as the host GCM) into one of the chosen SRES emissions scenarios.

Previous studies using CCAM have shown that the downscaling process can produce less accurate advection of synoptic systems if the ratio of grid size between the parent and downscaled model is too large (see for example Denis et al 2002; Denis et al 2003). The GCMs in Section 1 all have a resolution between 200 km and 300 km and thus in order to achieve a final resolution of 10 km, it was desirable to undertake a two-step downscaling process, using an intermediate resolution model to ensure modest ratios between the host and downscaled simulations. We chose an intermediate model configuration of CCAM that has 64 by 64 (C64) cells on the primary face and covers the Australian continent. This gave an average resolution of 60 km on the primary face. Figure 2.2 shows the stretching of the grid from the 60 km primary face out to the North Atlantic, where the resolution degrades to around 400 km. Even at this coarse resolution, the model is still fine enough to simulate the broad features of the climate system and so will not degrade the performance of the simulation over Australia.

3.3 Boundary conditions and forcing in the downscaling process

Nested, limited-area regional models require boundary conditions for both the bottom and the sides of the domain. As CCAM is a global, stretched grid model it can be configured to only require bottom boundary conditions from the host GCM. The C64 (60 km) intermediate model takes interpolated monthly sea surface temperature (SST) and ice-cover from the host GCM as the bottom boundary condition. It does not use any forcing of the atmospheric fields between the GCM and CCAM, and so is said to be operating in unforced mode. CCAM does however, use the same radiative forcing and atmospheric composition as the host GCM. Katzfey et al (2009) have shown that atmospheric forcing of fields from the GCM into CCAM is not needed, and in fact may degrade the performance of the model, especially when a bias-correction is applied to the SSTs (this will be discussed in the next subsection). Further, this paper shows that just the bottom boundary conditions are sufficient to produce a downscaled model of the host GCM that reflects the climatic changes seen in the host model. This point is explored further in Section 5, and in the General Climate Impacts Technical Report (Grose et al 2010).

The C48 (10 km) model is forced using output from the corresponding intermediate C64 model. Like the C64 model, the C48 model uses the SST from the host GCM (that has come, via interpolation, from the intermediate C64 model) as a bottom boundary condition, and the radiative forcing and atmospheric composition used in both the host GCM and the intermediate C64 model. However, unlike the intermediate C64 model the atmosphere of the C48 model is forced using several model variables from the C64 model.

Fine resolution models add value to GCMs by taking into account the influence of local orography, land use and fine-scale climate. However, regional models such as the 10 km configuration of CCAM also need to account for the influence of atmospheric conditions outside their region of focus, that is outside the primary panel of the grid. For this reason, nudging techniques are essential to ensure the relevant large-scale atmospheric phenomena from the intermediate C64 model are assimilated into the fine-scale C48 model.

Two options are available in CCAM atmospheric forcing of the pressure and velocity fields: far-field forcing or spectral nudging. Far-field forcing forces the far-field atmosphere of the fine-scale model using the atmosphere of the intermediate model. We define the far-field as the back panel and half of each side panel. Spectral nudging applies a spectral filter that ensures the broad features (of a length scale similar to the high-resolution panel or longer) of the intermediate model are passed through to the fine-scale model.

We performed short simulations using both far-field forcing and spectral nudging (results not shown) and chose to implement spectral nudging (also known as a scale-selective filter) (Thatcher & McGregor 2009) in our configuration of the C48 model. Preliminary experiments with the 10 km model prior to starting the main simulations showed that the low resolution of the far-field (the area away from Tasmania) of the C48 model precluded resolution of realistic features such as cyclones and fronts, and thus this configuration of the model was unable to

develop large-scale atmospheric phenomena that are a feature of a real atmosphere. Spectral nudging, where forcing is used at larger scales but smaller scales are allowed to develop independently, ensures that these large-scale features in the C64 model are passed into the fine-scale C48 configuration.

For the C48 model simulations, we implemented a scale-selective filter to spectrally nudge the surface pressure, wind fields, temperature and atmospheric moisture above 850 hPa. Thatcher and McGregor (2009) have shown that nudging surface pressure, temperature and winds resulted in consistent improvements in pattern correlation and root-mean squared (RMS) errors, both at the surface and at the 500 hPa level. That is, it is beneficial for reproducing patterns of the host model above the specified length scale.

Other variables are not nudged (forced) but are free to evolve within the model; however the model will attempt to maintain dynamical balance so all variables will be affected by this nudging process.

Spectral nudging replaces the lateral boundaries that effectively exist in far-field forcing, with a cutoff in the spectral domain at a specific length-scale. This allows the model to evolve freely at small length-scales, with the regional atmosphere at large length scales specified by the intermediate model. Typically, spectral nudging is significantly more computationally expensive than far-field forcing ($O(N^2 log^2 N)$, where O = the order of magnitude and N = the number of grid points) for N^2 grid points as compared with $O(N)$). Thatcher and McGregor (2009) have shown that a one dimensional scale-selective filter can be used effectively in CCAM when downscaling for a regional area and at significant computational savings.

3.4 Bias-adjustment of sea surface temperatures

Analysis of the GCMs reported in Chapter 8 of the IPCC AR4 (Randall et al 2007) show that they tend to have biases in the sea surface temperatures (SST) generated relative to the observed climate (Reynolds 1988). Katzfey et al (2009) have shown that correcting the SSTs for this bias, rather than using the raw SSTs from the GCMs, produces more realistic precipitation in the C64 (60 km) simulations. To achieve this, monthly average GCM SSTs for 40 years (1961-2000) were averaged to produce one mean for January, one for February and all other months over the entire period. The differences between these values and the calculated monthly Reynolds' SST (Reynolds 1988) values over the same period were then determined, and these differences (the bias for each month) were subtracted from the GCM SSTs for the corresponding month, for each year over the length of the simulation, where SSTs were available (1961-2100). The corrected SST values were then input for the C64 downscaled simulations. Note that there is no need for a similar bias-adjustment to be applied to the SSTs generated by the C64 simulations before they are put into the C48 simulations. This technique preserves the decadal and intra-annual variability of the host GCM, but ensures that the monthly climatology of the SSTs in the downscaled model is the same as the observed Reynolds' dataset (Reynolds 1988). Because the bias-adjustment is determined, by comparison of the observed and simulated SSTs and this cannot be computed for future climates, the monthly biases are assumed invariant over time. As a consequence, the bias of the GCM SSTs is unaltered in the C64 downscaled model in the simulation to 2100.

In this study, the choice was made not to attempt atmospheric forcing, or adjustment, of other atmospheric fields generated in the GCMs such as surface pressure, wind fields, temperature and moisture fields, since they are influenced by the unadjusted SSTs and there is no technical approach to make the forcing consistent with the bias-adjusted SSTs.

Katzfey et al (2009) have shown that using bias-adjusted SSTs with no atmospheric forcing produces a better current climatology of rainfall than unadjusted SSTs with atmospheric forcing. We also use the raw sea-ice distribution directly from the host GCM. This can lead to an inconsistency as the SST is adjusted, but not the sea-ice boundary. However, as CCAM is an atmosphere only model there was no easy way of correcting the sea-ice boundary in line with the bias-adjusted SST. This issue was investigated prior to starting the climate modelling program and the inconsistencies that arose do not appear to affect the simulations in the region of interest. It should also be noted that there are often large temperature gradients at the sea-ice boundary even without bias-adjustment of SST, and that the adjustments did not noticeably change these gradients. It is believed that these findings also hold true for the climate change signal, and thus we have chosen to force the 60 km model only with the bias-corrected SSTs and the raw sea-ice distribution from the host GCM.

The ability to adjust the SSTs from the host GCMs before using them as input into the downscaled C64 model is a significant advantage of using a stretched grid global model over a limited area regional model. As stated above, this adjustment allows us to better simulate the current climate, while preserving the climate change signature from the host GCM. Limited area models require lateral boundary conditions and thus must use atmospheric variables from the host GCM. As such it is difficult, if not impossible, to adjust the SST while maintaining consistency between the atmospheric and sea-surface forcing.

3.5 Post-processing of modelling output

Although both the C64 and C48 configurations of CCAM are global atmospheric models, only the modelling output from the region of interest was post-processed to a number of limited-area regular grids for ease of access (Figure 3.5). The post-processed modelling output is available for download from the data portal of the Tasmanian Partnership for Advanced Computing (TPAC). For more specialised uses, the raw modelling output has been stored and can be accessed by directly contacting TPAC at www.tpac.org.au.

The C48 model is processed to a regular 0.1-degree grid that covers Tasmania and the Bass Strait islands (Figure 3.5a). The processed area covers the region between 143.5 degrees east to 149 degrees east and 44 degrees south to 39 degrees south. It has only one vertical level and contains all the variables that exist in the C48 configuration of the model, with a six-hour time step.

The C64 model is post-processed to two grids, each containing different variables. The first, and major output product, is a 0.5-degree grid covering the region from 125 degrees east to 170 degrees east and 50 degrees south to 25 degrees south (Figure 3.5b). It has only one vertical level, the bottom level of the model, along with all the surface variables that exist in the model (more than 140). Modelling output is written at least once every six hours (with several variables, such as temperature and rainfall written out every three hours).

The second product from the C64 model is a pressure level product. The modelling output is regridded to regular 0.5-degree cells, ranging from 100 degrees east to 180 degrees east and 65 degrees south to 5 degrees south (Figure 3.5c). This product has three vertical levels, at 1000 hPa, 850 hPa and 500 hPa and a six-hour time step. At each level, we have included the temperature, geopotential height, meridional and zonal wind, as well as the mean sea level pressure (MSLP), surface temperature and 10 m wind speed. This product is designed to allow us to study the large-scale pressure fields over the Australian region, both now and into the future, and to examine how they affect Tasmanian weather and climate.

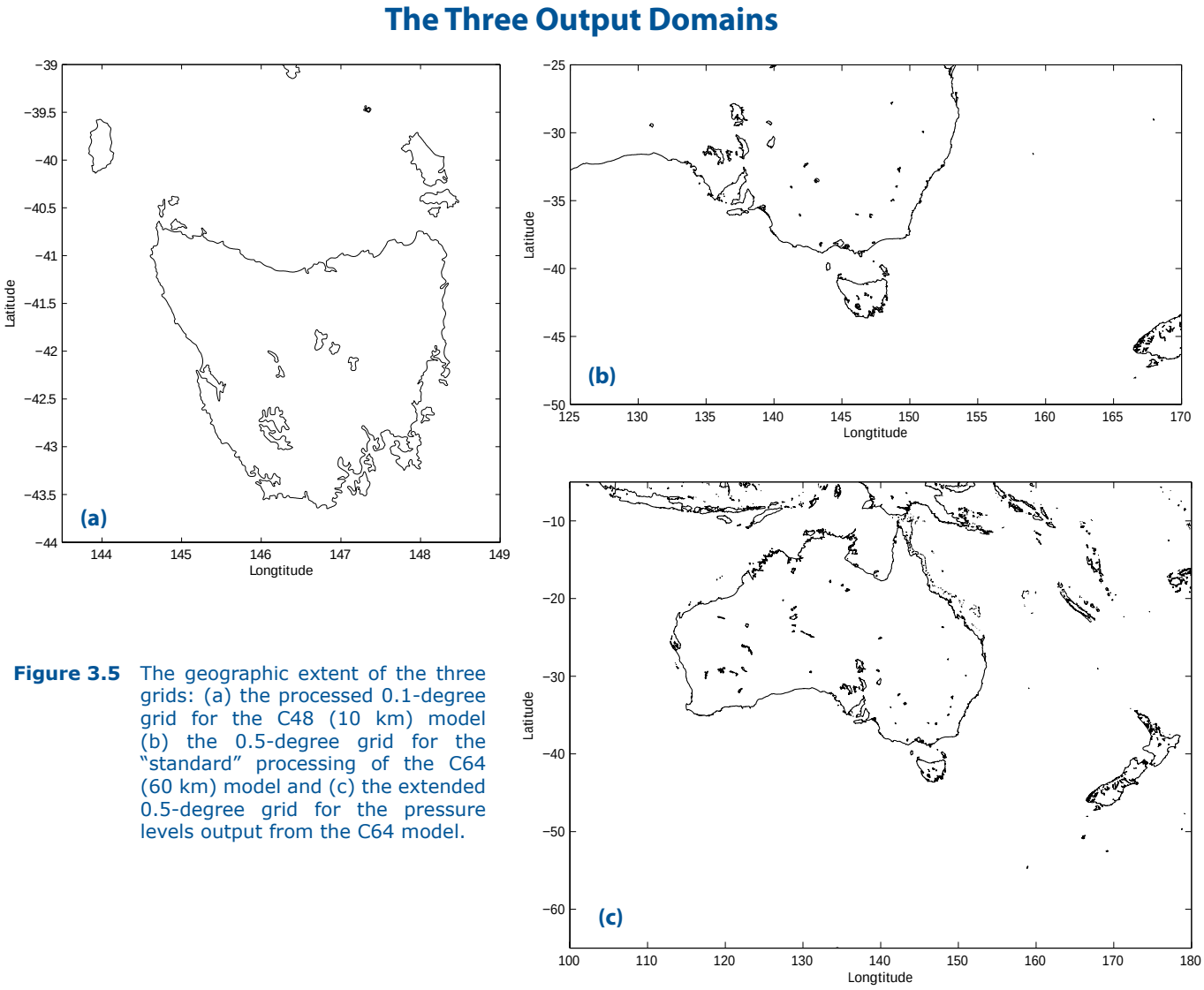

Figure 3.5 The geographic extent of the three grids: (a) the processed 0.1-degree grid for the C48 (10 km) model (b) the 0.5-degree grid for the "standard" processing of the C64 (60 km) model and (c) the extended 0.5-degree grid for the pressure levels output from the C64 model.

4 Modelling program

The Climate Futures for Tasmania climate modelling program has created a unique and valuable dataset that provides daily modelling output for more than 140 climate variables for more than 720 grid cells over Tasmania and the Bass Strait islands. In line with the approach taken by the IPCC, we have undertaken an approach using an ensemble of models and SRES emissions scenarios. The ensemble approach allows for greater confidence in the projections through the use of the ensemble mean, as well as giving an indication of the uncertainty through the spread of the models. Using the spread across the simulations as a measure of confidence in the projections is especially valuable when the modelling output is used as input to, for example, biophysical or hydrological models.

4.1 Phase 1

The majority of the climate modelling program was undertaken in the first phase. This phase (shown in Table 4.1) involved carrying out the two-stage downscaling process for each of the six global climate models (GCM) across the two chosen SRES emissions scenarios; a total of 24 simulations.

For Phase 1, the downscaling process from GCM through the 0.5-degree model to the 0.1-degree model was identical for each of the 12 downscaling simulations. Accordingly, the only difference between the six 0.1-degree model simulations for each SRES emissions scenario was caused by the host GCM (through the sea surface temperature (SST) as the bottom boundary conditions).

4.2 Phase 2

The second phase of the climate modelling program (Table 4.2) comprised a number of simulations that complemented or added to the modelling from the Phase 1. We also corrected any errors that had been identified during the first phase. Each of the simulations carried out during Phase 2 is discussed separately below.

4.2.1 Evaluation against downscaled NCEP reanalysis

The NCEP/NCAR Reanalysis 1 is a project undertaken by NOAA/NCEP (National Oceanic and Atmospheric Administration/National Centers for Environmental Prediction) in the US, to produce global analyses of atmospheric fields such as pressure, temperature, winds and humidity, through the data assimilation of a range of quality-controlled observations (Kalnay et al 1996). The reanalysis is not an observational dataset, it is a model that is strongly forced by available observations, and thus will be similar to observations where they occur. Nonetheless it has its own errors and biases. The NCEP Reanalysis does not have the capacity to project future climate, but functions as an observational dataset that can be used to assess both the behaviour of downscaled GCM simulations and the downscaling process itself. The NCEP Reanalysis data was provided by the NOAA/OAR/ESRL PSD, Boulder, Colorado, USA, from www.esrl.noaa.gov/psd/.

Table 4.1 Summary of Phase 1 of the climate modelling program, detailing the 24 simulations undertaken in this stage.

	SRES Emissions Scenarios			
GCM	**A2**	**A2**	**B1**	**B1**
	0.5°	0.1°	0.5°	0.1°
CSIRO–Mk3.5	✓	✓	✓	✓
GFDL–CM2.0	✓	✓	✓	✓
GFDL-CM2.1	✓	✓	✓	✓
MIROC3.2(medres)	✓	✓	✓	✓
UKMO-HadCM3	✓	✓	✓	✓
ECHAM5/MPI-OM	✓	✓	✓	✓

Table 4.2 Summary of Phase 2 of the climate modelling program. Note that the B35 initialisation of CSIRO-Mk3.5 GCM was used in Phase 1

Host Model	0.5°	0.1°	0.05°
NCEP Reanalysis 1 (forced by SST and atmosphere)	✓	✓	
NCEP Reanalysis 1 (forced by SST only)	✓	✓	
CSIRO-Mk3.5 A2 emissions scenario (with spectral nudging of atmospheric moisture)	✓	✓	
CSIRO-Mk3.5 A2 emissions scenario (F35 initialisation)	✓	✓	
CSIRO-Mk3.5 A2 emissions scenario (G35 initialisation)	✓	✓	
CSIRO-Mk3.5 A2 emissions scenario (high resolution)			✓
AWAP data regridded (0.1° over Tasmania)		✓	

The NCEP Reanalysis is a global model with an output resolution of 2.5-degrees (approximately 250 km over Australia). This is similar in resolution to the six GCMs we chose for downscaling, and allows us to treat the NCEP Reanalysis as another (the seventh) host GCM. For our project, we have performed our downscaling process on NCEP Reanalysis 1 from 01/01/1961 to 31/12/2006.

Changes in large-scale pressure fields, such as movement of the subtropical ridge, are expected to play a key role in future changes to the climate (Grose et al 2010). The motivation behind a downscaled NCEP Reanalysis simulation was to establish confidence in the ability of the downscaled simulations to reproduce these large-scale patterns in the current climate. Like all other downscaling simulations for the project, we force the 0.5-degree CCAM model with the sea surface temperatures (SST) from the host (the NCEP Reanalysis data). In this case the bottom boundary conditions are observed SSTs and not bias-adjusted GCM SSTs used in the downscaling process. But unlike the other downscaling simulations, we also forced this 0.5-degree model with the surface pressure, temperature, wind and atmospheric moisture above 850 hPa from the NCEP Reanalysis data. Forcing the atmospheric components between the GCM and 0.5-degree model ensures that the large-scale pressure fields from the GCM are preserved through to the 0.5-degree model (see results in Section 5.5). This process gives us a 0.5-degree dataset that reproduces NCEP atmospheric pressure (as well as temperature, wind and moisture above 850 hPa) and thus allows comparison between the downscaled GCMs (that are forced only through SST) and the downscaled NCEP. The downscaled NCEP simulation that is created using atmospheric and SST forcing is referred to as the forced NCEP simulation.

As a second experiment, we also downscaled NCEP Reanalysis data using only the SST. This downscaled modelling output can be compared to the (atmospherically) forced NCEP downscaled modelling output to allow an assessment of the change in atmospheric fields produced by downscaling with only SST. The downscaled NCEP simulations that were created using only SST forcing are referred to as the unforced NCEP simulation. The same spectral nudging was applied between the 0.5-degree and 0.1-degree models as in the Phase 1 simulations, to ensure that the large-scale patterns in the atmospheric fields were maintained through the downscaling process.

Because downscaling of the NCEP Reanalysis produces a simulation at the same temporal and spatial resolution as the 0.5-degree and 0.1-degree simulations produced in Phase 1, it is possible to compare pressure and other fields for coincident periods, and thus use the NCEP Reanalysis to validate these simulations.

4.2.2 Testing the spectral nudging of water vapour: the A2s simulation

CCAM has a number of switches controlling how the spectral forcing applies between each 0.1-degree model and its host 0.5-degree model. One of these switches changes how atmospheric moisture (water

vapour) is forced between the two models; either the switch is set so that the global total water vapour loading is constant (called the global fix-up option), with no forcing from the host 0.5-degree model, or the global total water vapour is allowed to vary and the moisture is spectrally nudged from the 0.5-degree model (spectral nudging option). Note that there is the potential for the relative humidity to go above 100% with the spectral nudging of the water vapour. However, for this to occur, the unadjusted relative humidity must be very close to 100% as all changes are small. Also, if the humidity does exceed 100%, then it will be immediately lost as precipitation at the next time step.

While undertaking Phase 1 of the climate modelling program, we observed that changing this switch had a significant effect on the total volume of rain that fell over Tasmania. We chose to use the global fix-up option. A single simulation (called the A2S simulation), using the CSIRO-Mk3.5 CGM and the A2 SRES emissions scenario, was undertaken using the spectral nudging option. This simulation is not reported in detail in this report. A comparison between the two CSIRO-Mk-3.5 A2 simulations showed that only the rainfall differed between them. Further, the temporal pattern of rainfall was identical in the two simulations. The difference between the two simulations was evident in the spatial pattern and total volume of rainfall that fell on Tasmania. The spectral nudging simulation under-estimated the rainfall in the west of Tasmania, resulting in a statewide annual rainfall close to 15% less than the global fix-up simulation. The spatial pattern (and statewide annual total) displayed in the global fix-up simulation is much closer to the observed values, thus the glocal model fix-up switch was chosen for the remainder of the simulations.

4.2.3 Three member ensemble to assess intra-model variability

The six different GCMs chosen for this study have all been shown to perform reasonably well over Australia, that is, they give a good representation of Australian rainfall and temperature, and credible representations of ENSO (Smith & Chandler 2009). However, each model is constructed differently and thus they produce a range of projected values. This range gives us an estimate (albeit it a lower bound) on the uncertainty of future climate change that beyond what can be provided by using a single model and a single simulation. One question that remains is what part of the range of uncertainty is related to inter-model variability (variation between models) and what part is related to intra-model variability (variation between various simulations of the same model. Note that since GCM simulations are not tied to observations, the simulations evolve into independent realisations of the climate through their internal processes (even from the same initialisation), and ensemble members of the same model will not be the same. An ensemble consisting of multiple simulations from the same GCM initialised with different initial conditions can be used to evaluate the intra-model variability over Tasmania due to differences in initial conditions and GCM internal variability.

Climate Futures for Tasmania used a three-member ensemble of simulations based on the CSIRO-Mk3.5 GCM. As part of the CMIP3 Project (Meehl et al 2007a), CSIRO Marine and Atmospheric Research produced three independent GCM simulations using CSIRO-Mk3.5 for the period from 1871 until 2100, labelled B35 (the simulation used in Phase 1), F35 and G35. These simulations had the same external forcing but different initial conditions. Modelling output from this three-member ensemble was downscaled in the manner used in Phase 1. Analysis of results is given in Section 5.7.

4.2.4 Demonstrating the effects of higher resolution: the 0.05-degree simulation

Deficiencies in any model will most likely arise from the discrepancy between the limited complexity and resolution of the model, and the complexity of the physical world. The downscaled models used in the project are no exception, having both finite resolution and complexity. We have chosen a resolution of approximately 10 km for the primary panel of the downscaled simulations (post-processed to a regular grid of 0.1-degree). This resolution strikes a balance between the fine scale of results and manageability of the generated dataset (the complete dataset encompassing all simulations is more than 75 Tb). We could not afford the time nor funds to increase resolution significantly for all SRES emissions scenarios and GCMs; however, the detail contained in the 0.1-degree simulations is adequate for most purposes. Indeed, the project simulations

are of a higher spatial and temporal resolution than any comparable study in Australia.

To examine the effect of increased model resolution, we performed one simulation where the primary face of the CCAM downscaled model has approximately 6 m grid cells, and interpolate the output to a regular 0.05-degree grid. This simulation was done using the CSIRO-Mk3.5 model (B35) as host GCM for the A2 emissions scenario. The downscaling process involved two steps, first generating the 0.5-degree simulation, and then downscaling this directly to a 0.05-degree grid.

The motivation for choosing this resolution was twofold. First, there are two interpolated observational datasets at 0.05-degree resolution: AWAP (Joens et al 2009) and SILO (Jeffrey et al 2001). Both of these datasets have been used in several studies with hydrological and agricultural biophysical models (Bennett et al 2010; Holz et al 2010). Having a simulation at this resolution allowed us to examine the differences between model-generated output at 0.05-degrees and modelling output interpolated from our regular 0.1-degree simulations to a 0.05-degree. Second, preliminary analysis of the simulations indicated that there was a large bias in local rainfall in the upper midlands region of Tasmania. We suspected that this bias was largely caused by the inability of the 0.1-degree model to completely incorporate the effects of the orography on rain across Tasmania (notably the Great Western Tiers). Thus doubling the resolution of the simulation should significantly reduce the rainfall bias in this region. This issue is discussed, along with results from the simulations, in more detail in Section 5.8 of this report.

4.3 The AWAP data as a gridded observational dataset

In order to gain confidence in the projections produced by Climate Futures for Tasmania, it is necessary to show that the simulations can reproduce the current climate accurately. This is done by evaluating the modelling output against observational data. The modelling output for any variable is representative of the smoothed values over a 0.1-degree by 0.1-degree grid cell (roughly 10 km by 10 km), whereas station data are representative of only a single point within that grid. For example, the temperature record for Hobart is taken at Ellerslie Rd, Battery Point. The temperature for other sites within a 10 km by 10 km cell centred at Ellerslie Rd may at times differ by several degrees.

A better approach when evaluating the simulations against observations is using a gridded observational dataset over the whole of Tasmania.

Two such products exist and are in common use for Australia: SILO (Jeffrey et al 2001) and AWAP (Jones et al 2009). Both products are based largely on the same observing-station records. AWAP was chosen because it is freely available and has been shown to have reduced network-derived inhomogeneity in rainfall over Tasmania (Fawcett et al 2010), which is likely to make this dataset more robust for climate research. The AWAP data was supplied by the Bureau of Meteorology in February 2009, and was the most up-to-date revision of the AWAP data at the time. Since that time, further revisions of AWAP have been released (the latest in March 2010). These revisions of AWAP address some minor issues with the first release (February 2009), mostly pertaining to the long-term trends in the data (D Jones 2010 pers comm 03 March).

The remaining Climate Futures for Tasmania technical reports incorporate data from the latest release of AWAP, but it was not possible to include this data in this report. It should be noted that all gridded datasets based on station records are influenced by the location and number of stations. Tasmania has only a limited number of high-quality observing stations (six for temperature) and this may effect the spatial pattern and temporal variability of observational products derived from these sites.

The AWAP data contains a range of observational data including maximum daily temperature, minimum daily temperature, daily rainfall, solar radiation and potential evaporation. The AWAP data does not contain pressure, thus necessitating the use of the forced NCEP Reanalysis simulation for validation of this variable over the Tasmanian region.

The AWAP data is produced on a 0.05-degree grid. In order to allow direct comparison with the Climate Futures for Tasmania simulations, we interpolate the AWAP data for Tasmania on to the same 0.1-degree grid used in the simulations.

5 Skill of the simulations at modelling Tasmanian climate

The previous sections have dealt with the climate modelling program and the configuration of the 0.5-degree and 0.1-degree models. In this section, the capacity of each simulation to reproduce the climate of the recent past (1961-2007) is tested. This capacity is assessed by examining the simulations and comparing them against the observed gridded AWAP data, the global NCEP Reanalysis and the forced downscaled NCEP model discussed in Section 4.2.1. In this section, we concentrate on those variables that are available in gridded datasets, thus allowing for direct comparisons. We also compare the forced and unforced NCEP simulations to examine the effect of the SST-only forcing on the surface pressure and other atmospheric variables.

An important point to consider when undertaking an assessment of the skill of a climate model is that GCM simulations provide an independent time series of the climate that does not correspond to the observational record; there is nothing in the GCM simulation to say that the weather on a particular day (or for a particular week or month) should be the same as the observed weather for that period. However, the models are expected to reproduce the typical range of weather and climate variations that are observed. That is, they reproduce the statistics of the mean climate. That GCMs do produce a global climate that is similar to the observed climate (including changes to temperature due to anthropogenic forcing) is a remarkable example of the skill of the models.

The downscaled simulations that have been produced are no more closely tied to the observed climate than the host GCMs. However, the downscaled simulations produce weather systems that are comparable to the observations and over a long enough period define a climate that closely matches the observations. Throughout the project, we have chosen 10 years, and often use 30 years, as the minimum time period for making valid comparisons between observations and the simulations.

To assess and interpret the general climate variables in the downscaled simulations, the representation of current climate is compared to observed datasets. This comparison gives the context and framework for the interpretation of the modelling outputs for the future period and is included in the General Climate Impacts Technical Report (Grose et al 2010). For models to project future climate conditions reliably, they must as a minimum precondition, simulate the current climate state with some degree of fidelity. Furthermore, poor model skill in simulating present climate could indicate some systematic errors or biases in physical or dynamical processes. However, there are differences between the modelling outputs and observed data. Such differences can be due to a number of factors, for example internal natural variability, evolving unique local scale systems or errors in observational data. The main consideration is whether the model appropriately reflects the synoptic scale events (Denis et al 2002; Denis et al 2003). Differences between the modelling output and observed data do not negate the usefulness of the modelling but it does affect how the modelling outputs are used and interpreted. Models may be used as a tool for understanding processes in certain components of the climate systems, or the outputs may be used quantitatively to examine future trends.

In this section, the ability of the ensemble of simulations to reproduce the observed climate over Tasmania is evaluated. Both mean values and variability are assessed. In this report, we cannot evaluate the performance of every climate variable, and thus we have chosen to concentrate our assessment on five key variables: temperature, precipitation, solar radiation, potential evaporation and pressure. These variables were chosen as they have corresponding observational datasets and are all key fields in the assessments of future climate that are included in the remaining technical reports. In addition, the various simulations in both Phase 1 and Phase 2 are examined. Results from Phase 1 are mostly evaluated using six member means from the six downscaled simulations – called the six-model-mean.

5.1 Temperature

Tasmania's temperature is strongly influenced by the surrounding ocean temperature. As explained in Section 2, the sea surface temperature (SST) for all GCMs were bias-adjusted to match the observed SST between 1961 and 2000. Thus, we expect the mean temperature for Tasmania to closely match the observed temperature for this period, as portrayed by the AWAP data. However, just as important as getting the mean temperature correct is matching the temporal and spatial variability of the simulated temperature. This includes replicating variability at several different time scales, such as daily, seasonal and interannual.

Since station records and gridded AWAP data of temperature are based on temperature within a Stevenson Screen at approximately 1.2 m height, and are recorded as daily maximum and minimum temperature, the equivalent variables from the models are compared (daily maximum screen temperature, daily minimum screen temperature).

The AWAP data is interpolated from the observing station data using a statistical model. As such, the spatial pattern of AWAP data is fixed, given a particular set of observations. This statistical scaling from limited observations may lead to under-estimates in the variability of temperature across Tasmania in the AWAP dataset. There is good agreement between the six-model-mean and AWAP mean annual daily maximum temperature (Figure 5.1a and Figure 5.1c). The statewide mean daily Tmax for the six-model-mean is almost identical to the AWAP statewide mean value of 10.4 °C. The spatial correlation of mean daily Tmax between the AWAP data and the six-model-mean is 0.94. The variances of daily Tmax between the AWAP data and the six-model-mean are not as strongly correlated as the mean values (Figure 5.1b and Figure 5.1d). The standard deviation of the AWAP data is very smooth, showing smaller variance around the coast and rising to a maximum in the centre of the state. Shorter spatial scales are evident in the model mean variance, and there is higher variance on the east coast. The significance of these differences in terms of the model or AWAP data is unclear.

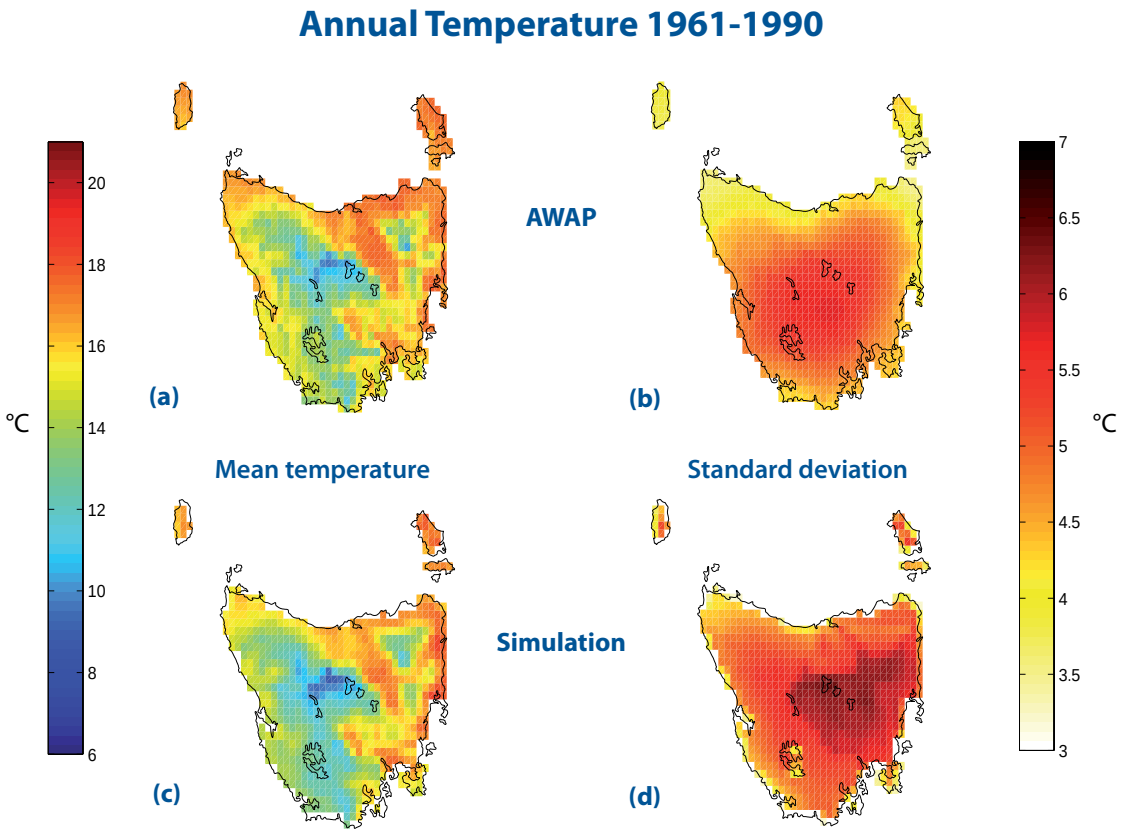

Figure 5.1 Annual mean daily maximum temperature for AWAP (top) and the six-model-mean of the simulations (bottom) for the period 1961-1990. The right hand column shows the corresponding standard deviation. For the six-model-mean, the standard deviation is the mean of the six standard deviation figures.

We compared temperatures in the AWAP data and the models across the entire distribution of the data at two example locations (Figure 5.2).The grid cell covering Hobart is shown as an example of a populated coastal centre, and the grid cell covering Osterley is chosen as an example inland site. There is a high level of agreement between the models for both locations for both maximum and minimum temperature. The largest difference between the models and the AWAP data is seen as a small, but consistent, offset in minimum temperature for the inland site.

We assessed the ability of the models used in the project to reproduce observed seasonality by repeating the analysis of Figure 5.1, with output from the months December-March (Figure 5.3) and May-August (Figure 5.4). These periods are chosen for two reasons: four-month periods (instead of three) allow for more of the year to be included in these calculations and the Tasmanian summer often extends well into March and so the December-March period reflects the local conditions. Similarly, a winter period of May-August also matches with local conditions. The mean temperature for the summer period shows good agreement (spatial correlation of 0.91), while for the winter period the AWAP data appears to be warmer around the coast than the six-model-mean (but with a higher spatial correlation coefficient of 0.97). The variance in both the summer and winter periods is of the right magnitude in the six-model-mean, but the spatial pattern of variance is not closely aligned with the spatial pattern of the variance in the AWAP data.

It is important when comparing the AWAP data and the simulations to consider the limited number of observing stations (especially for temperature) that make up the observational network that forms the basis of the AWAP gridded data. This is particularly relevant on the sparsely populated west coast of Tasmania.

The AWAP data is generally slightly warmer than the six-model-mean (less than 2 °C difference), but in parts of the east coast it is cooler (Figure 5.5a). Each of the six models simulate daily weather patterns and are unphased on a daily basis with each other and with the AWAP data. Thus on each day the difference between any of the six models, the six-model-mean and the AWAP data may be large. However, Figure 5.5b and Figure 5.5c show that over the 30-year period the daily values of the model display the correct seasonal trends and variation with the six-model-mean value within one standard deviation of the AWAP data 67% of the time. In the north of the state, one standard deviation is around 3 °C, while in the south it is up to 6 °C.

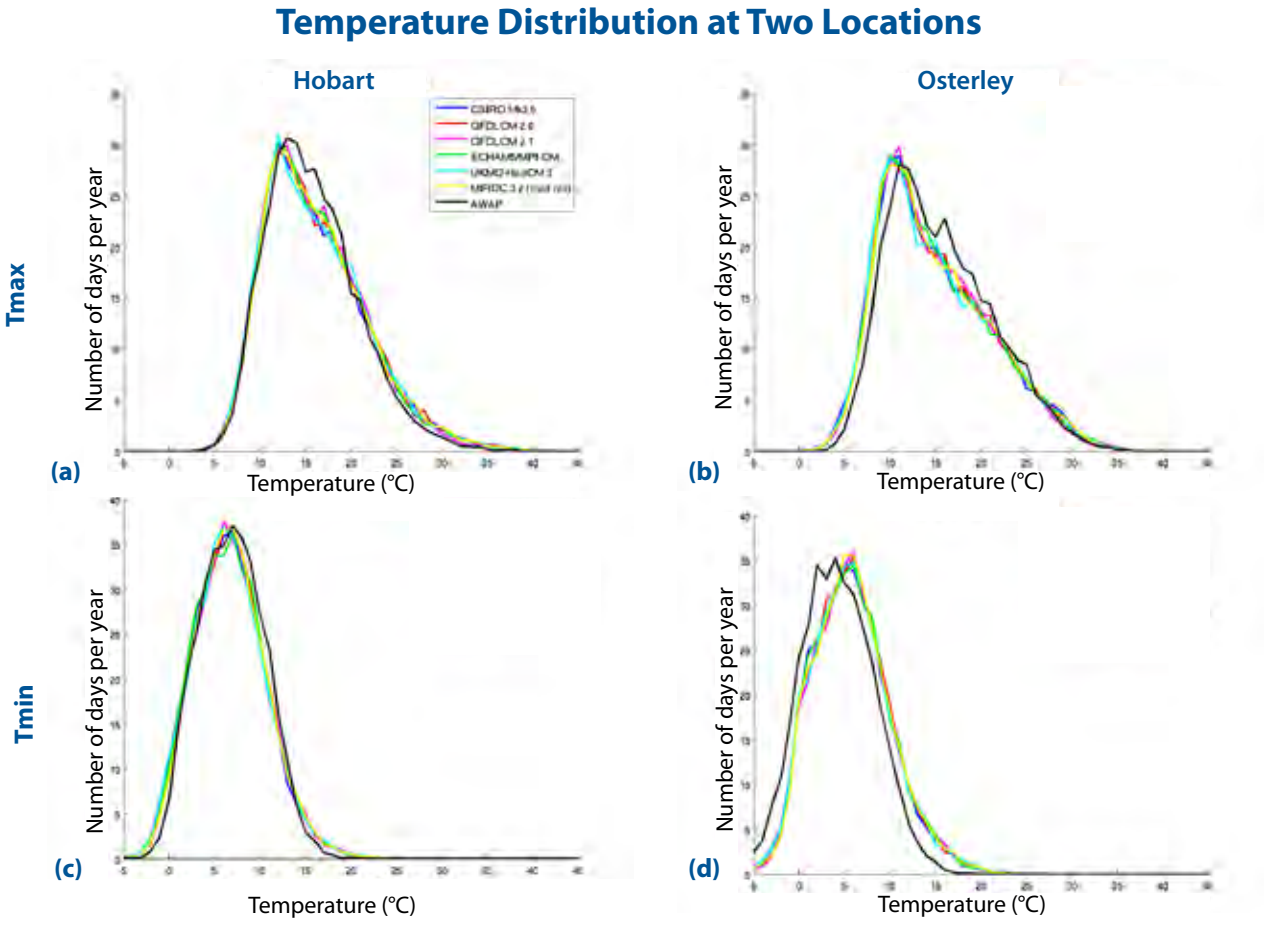

Figure 5.2 Distribution histograms of daily maximum temperature and daily minimum temperature for the period 1961-1990 in the grid cells that cover two Tasmanian locations (Hobart and Osterley) in AWAP and each of the six simulations.

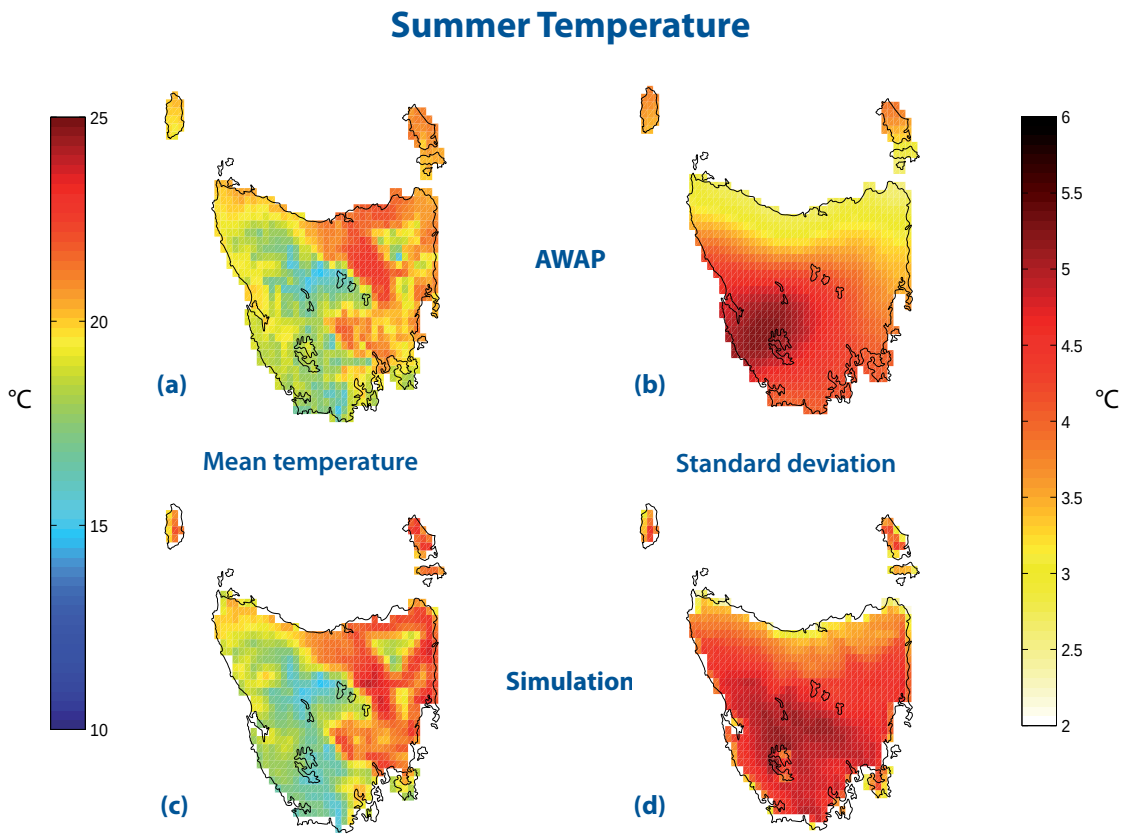

Figure 5.3 Mean daily maximum summer temperature (left column) for the months December-March for the period 1961-1990, along with the standard deviation of the daily mean (right column). The top row is AWAP, with the six-model-mean on the bottom row.

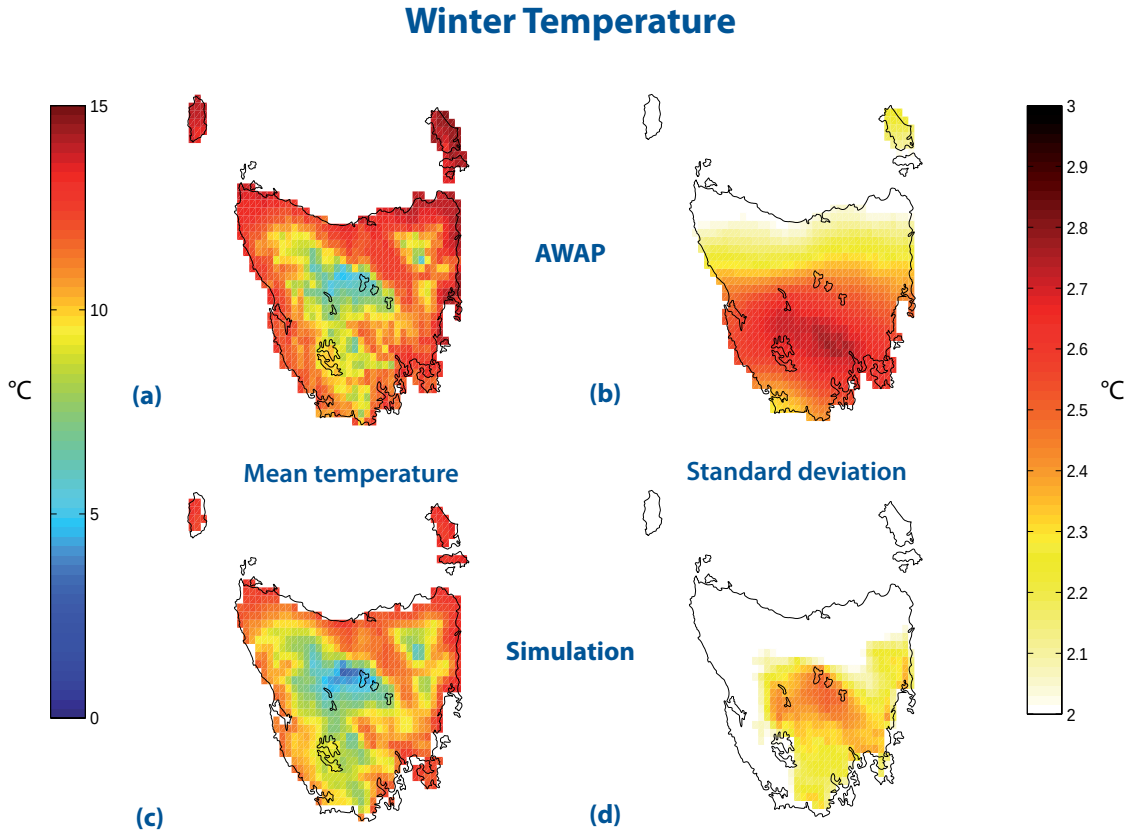

Figure 5.4 Mean daily maximum winter temperature (left column) for the months May-August for the period 1961-1990, along with the standard deviation of the daily mean (right column). AWAP is on the top row, with the six-model-mean on the bottom row.

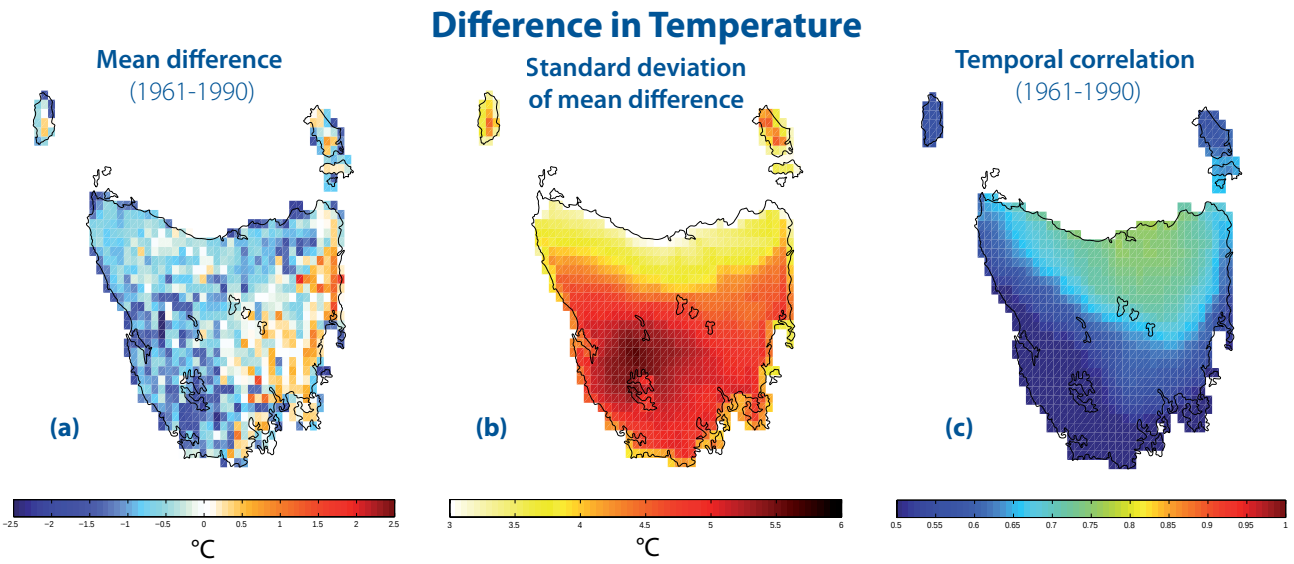

Figure 5.5 Comparison of AWAP and the six-model-mean temperature difference for 1961-1990. The figure on the left shows the mean daily difference, the middle figure shows the standard deviation of this difference, and the figure on the right shows the correlation between the daily value of AWAP and the daily six-model-mean over the 30-year period.

The ability of the simulations to reproduce the seasonal mean and seasonal variance is equally as important as capturing the daily values. Figure 5.6 shows that in summer the model mean is generally slightly too hot, but in autumn and winter this situation is reversed. In spring, the west is too cold but the east is too warm. The spatial correlation between the monthly values of the AWAP data and the monthly mean for the six-model-mean is very high, above 0.9 over the entire state, and generally above 0.95. The standard deviation for the model monthly mean is close to that for the AWAP data in summer, autumn and winter. In spring, the variance of the AWAP data resembles a 'bullseye' target, with highest values in the centre, while the model variance shows more structure and is generally higher on the east coast than the corresponding region in the AWAP data. The bottom graph in Figure 5.6 shows how closely clustered the model values are during the period where the SST has been bias-adjusted to observations. This close agreement between all of the models and the AWAP data is in part the result of the bias-adjustment of the GCM SSTs based on the period from 1961-1990. This bias-adjustment ensures that the mean monthly sea surface temperature of all the GCMs matches the observed SST monthly climate over this period. The mean surface temperature over a relatively small island like Tasmania is strongly dependent on the surrounding sea surface temperature.

The daily minimum temperature (Tmin) performs similarly to the maximum temperature. The daily outputs show the six-model-mean performing well against the AWAP data for the period December to March (Figure 5.7). The standard deviation for AWAP over this period is very uniform over the state. The model mean standard deviation shows more of a dependence on orography and is generally higher than the variability of the AWAP data. Comparison between the six-model-mean standard deviation and that for each model shows that the spatial pattern is consistent across the six models. Over the period May to August, the daily outputs show that the six-model-mean for Tmin is again similar to the AWAP data (Figure 5.8), but the standard deviation again shows more spatial structure in the six-model-mean than the AWAP data.

The seasonal differences between the AWAP data and the model mean are all generally less than 2 °C, and the standard deviations are similar for each season (Figure 5.9). In particular, for Tmin there was no difference between the smooth variance of the AWAP data and the six-model-mean variance.

In order to simulate the observed diurnal temperature range, the seasonality of the daily minimums and maximums of temperature in the model must be correctly aligned (for example, a hot summer day is likely to have a warmer overnight minimum temperature). The ability to reproduce diurnal range is thus more difficult than maximum or minimum temperature alone, and thus gives a second order assessment of the model performance. We show the mean diurnal range and the variance of the diurnal range for the periods December to March (Figure 5.10) and May to August (Figure 5.11). The models do a good job of capturing the broad features of the diurnal range exhibited by the AWAP data, as can be seen in the two figures. Similarly, the comparison of standard deviation between the AWAP data and the six-model-mean shows that the models are in the right temperature range. Once again, the standard deviation of the AWAP data is very smooth, while the six-model-mean displays a dependence on orography.

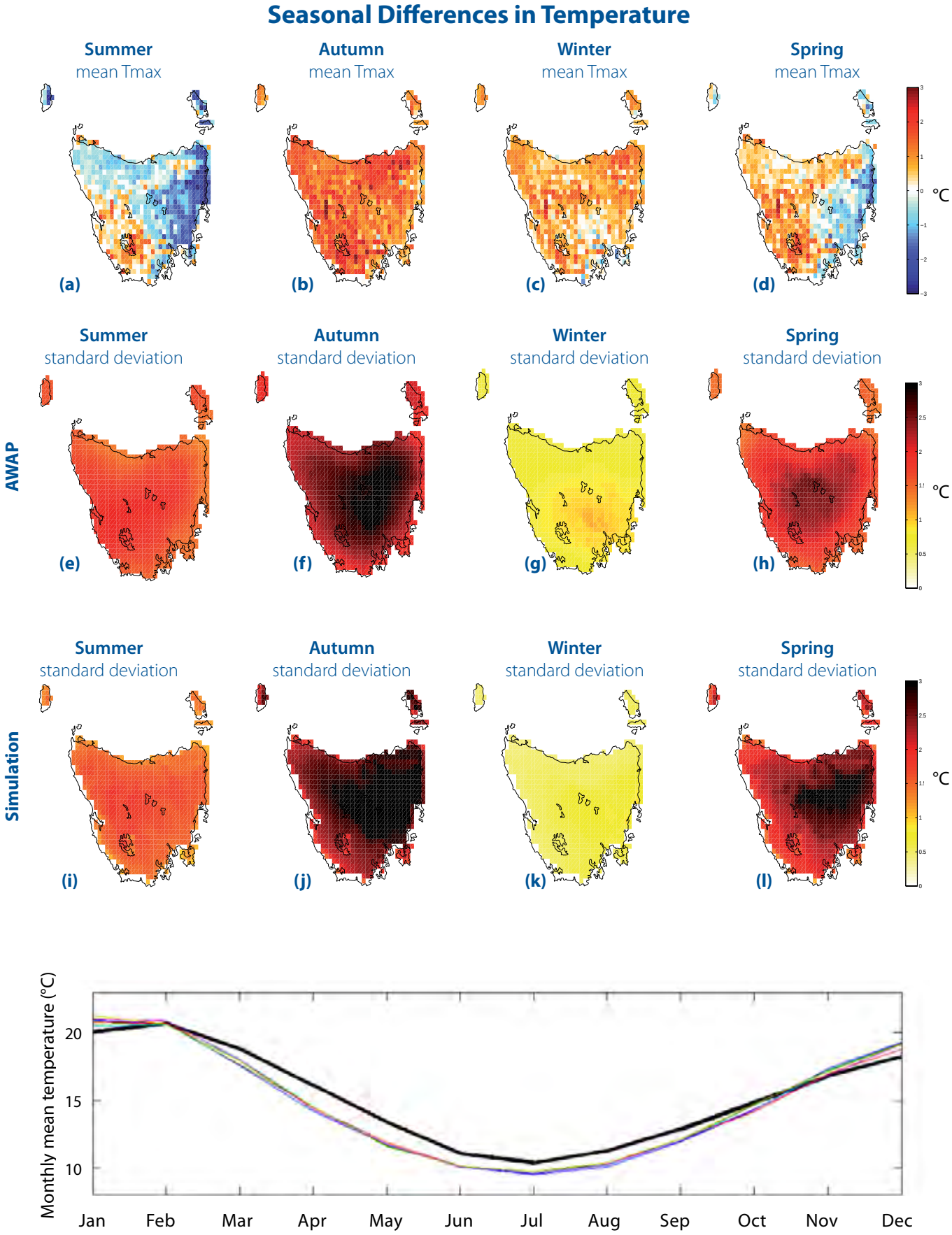

Figure 5.6 Seasonal differences between AWAP and the six-model-mean for daily maximum temperature for the period 1961-1990. The variances are calculated using the monthly mean values of daily maximum temperature for each season. The bottom graph shows the monthly statewide mean daily maximum temperature for each simulation (coloured) and for AWAP (black line). Note the strong alignment of the statewide mean of the simulated temperatures.

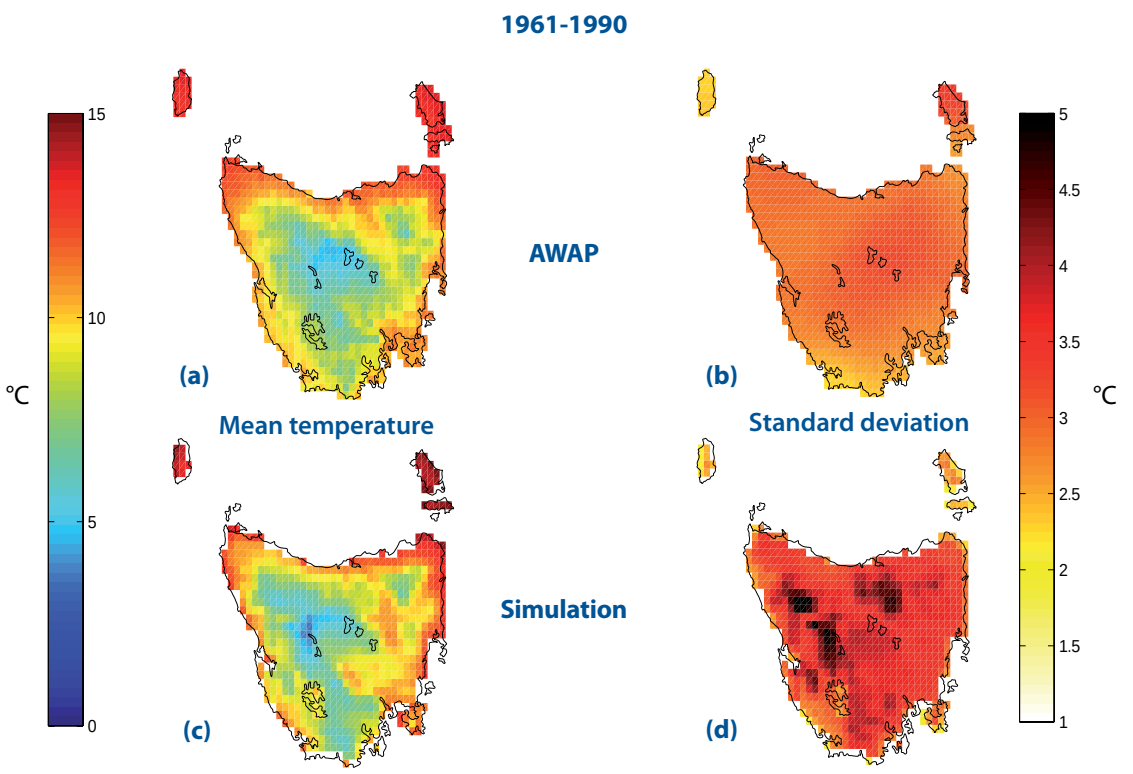

Figure 5.7 Mean daily minimum summer temperature (left column) for the months December-March for the period 1961-1990, along with the standard deviation of the daily mean (right column). AWAP is on the top row, with the six-model-mean on the bottom row.

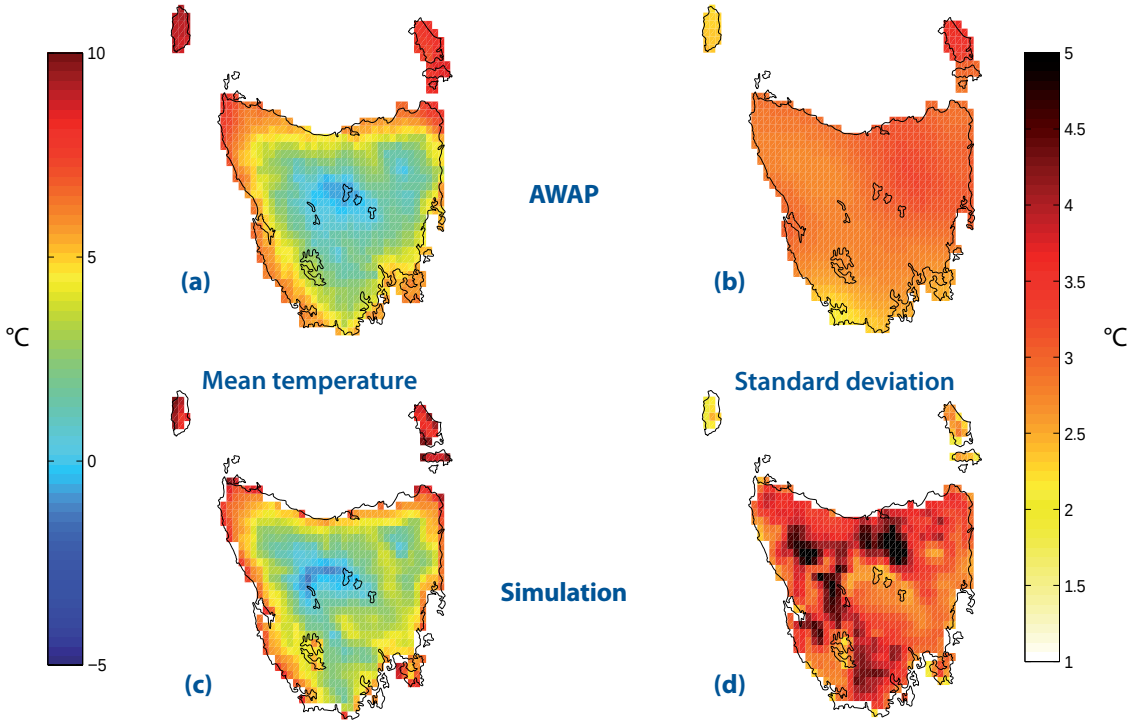

Figure 5.8 Mean daily minimum winter temperature (left column) for the months May-August for the period 1961-1990, along with the standard deviation of the daily mean (right column). AWAP is on the top row, with the six-model-mean on the bottom row.

Seasonal Differences in Minimum Temperature

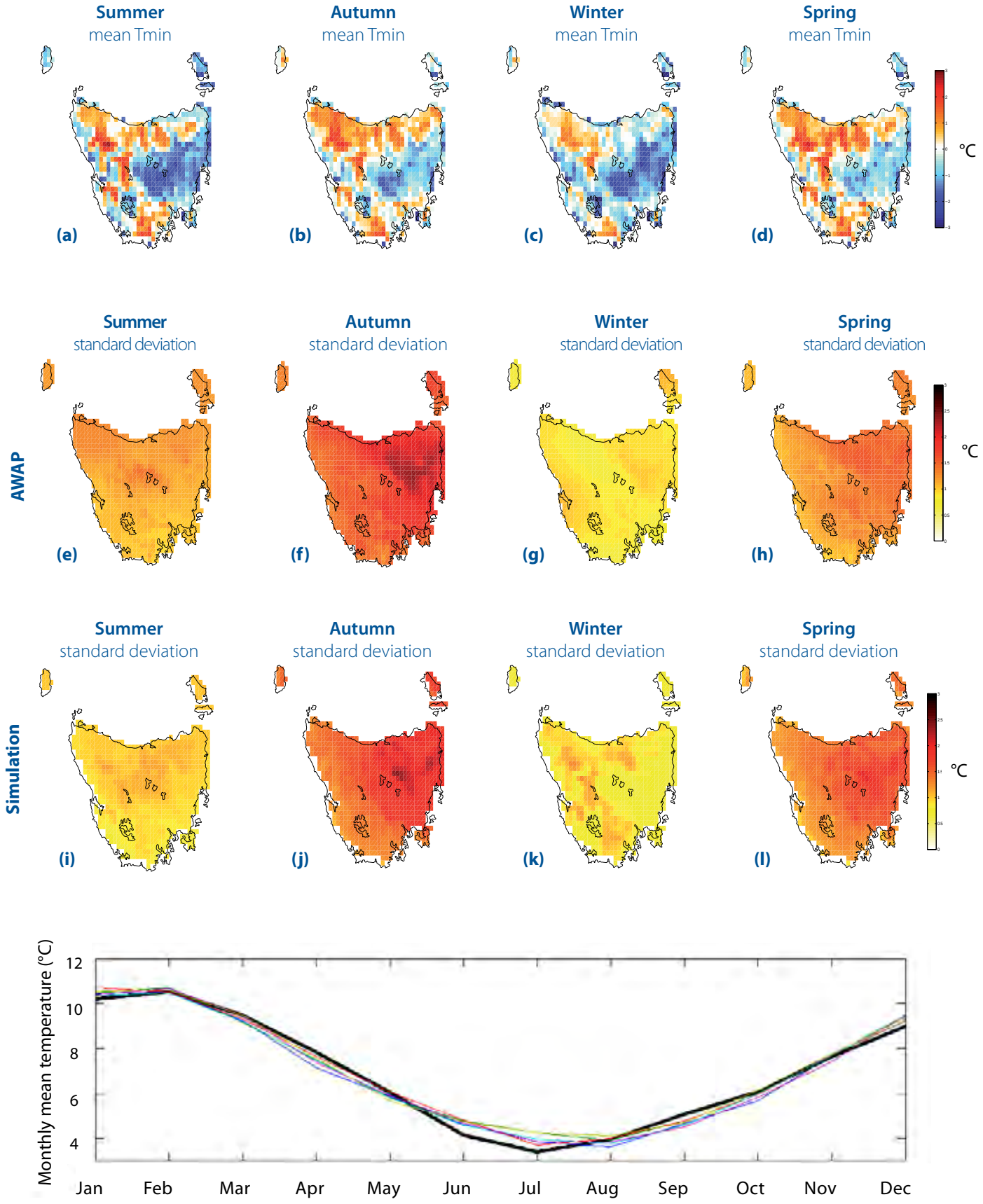

Figure 5.9 Seasonal differences between AWAP and the six-model-mean for daily minimum temperature for the period 1961-1990. The variances are calculated using the monthly mean values of daily minimum temperature for each season. The bottom figure shows the monthly statewide mean daily minimum temperature for each model (coloured) and for AWAP (black line). Note the strong alignment of the statewide mean of the simulated temperatures.

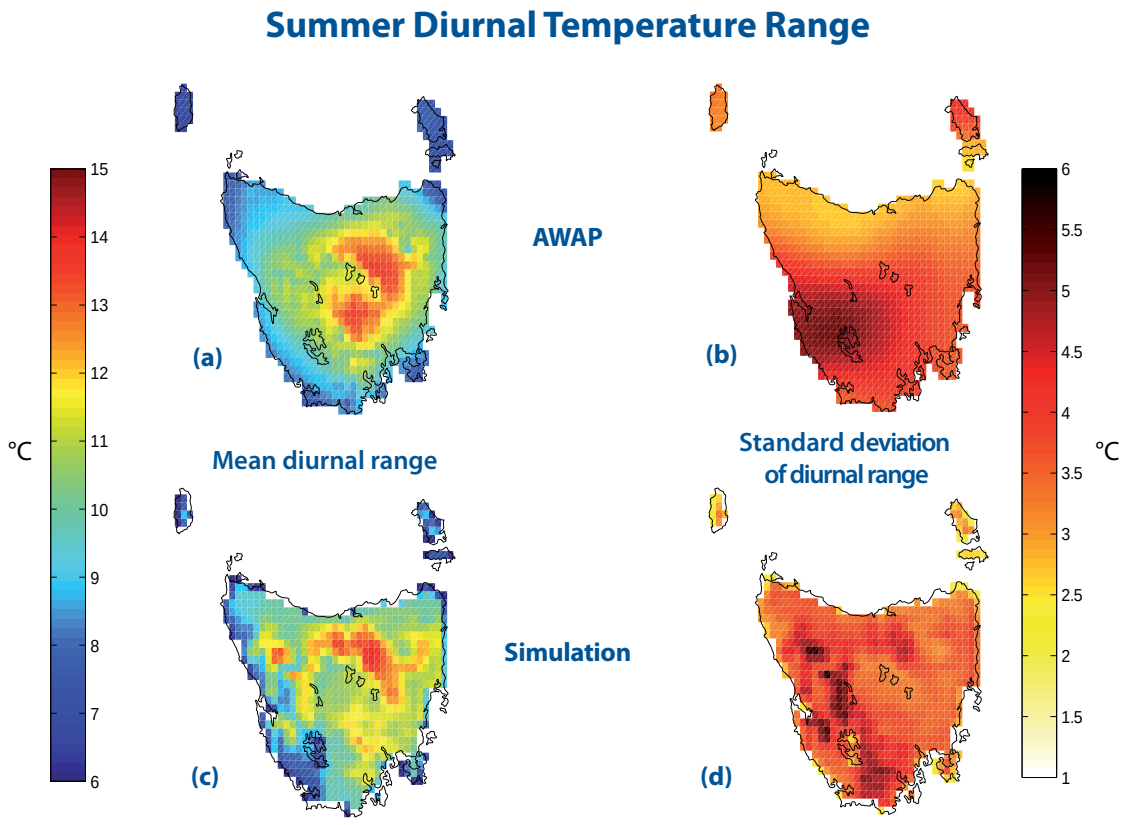

Figure 5.10 The mean diurnal temperature range for AWAP and the six-model-mean for the months December-March for the period 1961-1990 (left column), along with the standard deviation of the diurnal range (on a daily basis) over the thirty year period (right column).

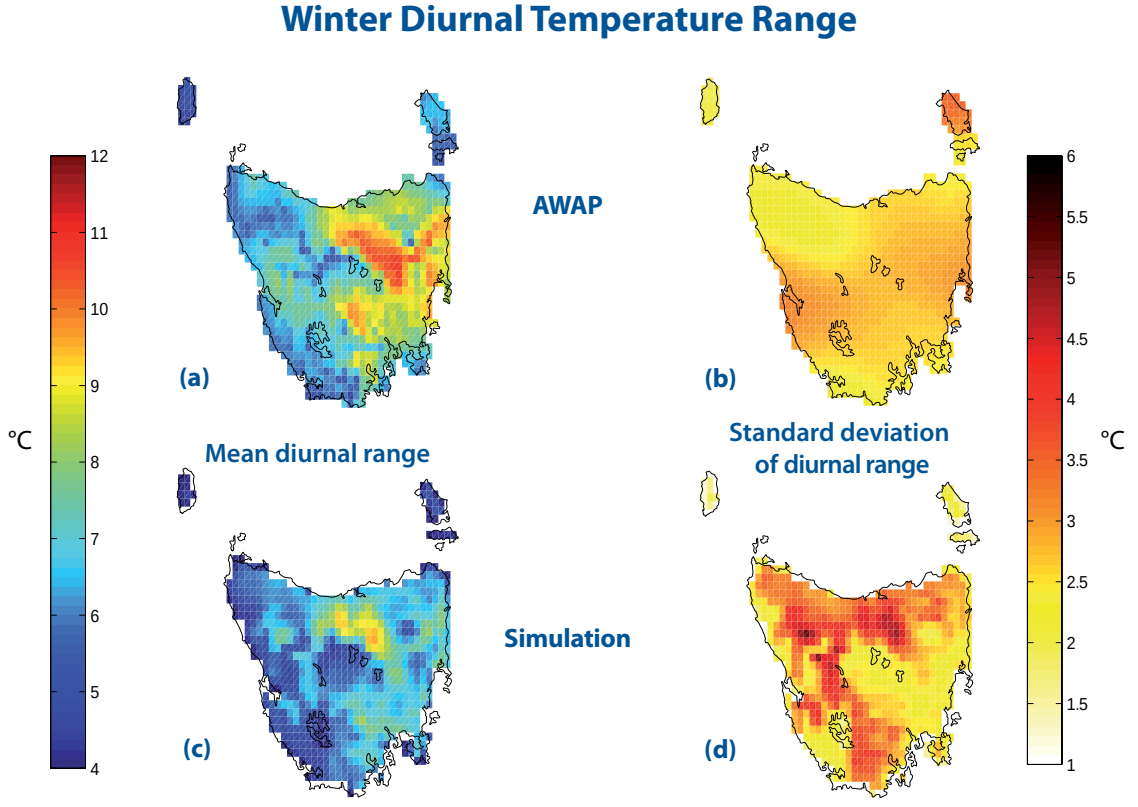

Figure 5.11 The mean diurnal temperature range for AWAP and the six-model-mean for the months May-August for the period 1961-1990 (left column), along with the standard deviation of the diurnal range (on a daily basis) over the thirty year period (right column).

5.2 Precipitation

Precipitation is a result of complex interactions between temperature, moisture and wind, and is therefore more likely to be independent of the bias-adjusted sea surface temperatures (SST). To see if inter-model variability is large for precipitation, annual total rainfall for each of the six downscaled GCMs is compared in Figure 5.12, along with six-model-mean annual rainfall and the AWAP annual rainfall. All of the models show a similar pattern of annual rainfall for the period 1961-1990. The statewide mean annual rainfall for the six-model-mean is 1385 mm. This compares well with the statewide mean annual rainfall calculated from the AWAP data of 1390 mm. The spatial correlation between the six-model-mean and the rainfall from the AWAP data is 0.63.

On a daily basis, rainfall is not normally distributed: the distribution of number of days with a certain volume of rain is closer to a power law (with days of no rain being the most common result). Due to the shape of the distribution of rain, it makes more sense to plot number of days with certain volumes of rain or as percentiles rather than as a mean and variance.

There is strong agreement between the AWAP data and the six-model-mean across the spectrum of rainy days (shown for the summer period December to March in Figure 5.13). The most noticeable features of these figures are the under-estimate of no-rain days in the six-model-mean for the Tamar Valley and upper midlands region, and the under-estimate of heavy rain days in the west. Both of these observations can be explained in part by the lower resolution of the orography across Tasmania in the downscaled simulations. The model does not fully account for the steep mountain ranges inland of the west coast that catch a lot of rain, nor the steep drop from the Western Tiers just west of the upper midlands, that casts a rain-shadow over this region and results in significantly less rain than surrounding areas. This hypothesis is examined using the 0.05-degree simulation discussed below.

There is similarly strong agreement between the AWAP data and the six-model-mean when we consider percentiles of daily rain for the period December to March (Figure 5.14). Once again, the lower rain in the mountainous west and higher rain in the Tamar Valley/upper midlands region is seen in the six-model-mean.

For the winter months May to August, we can see higher rainfall in the six-model-mean relative to the AWAP data in the Tamar Valley/upper midlands and the lower rainfall in the mountainous westerly region (Figure 5.15 and Figure 5.16). Interestingly, the low rainfall is least evident during winter in the 95th-percentile rainfall days. This percentile matches well with the AWAP data.

The errors in rainfall present in the simulations in the Tamar Valley/upper midlands region is clearly visible across all seasons, especially winter and spring (Figure 5.17). The under-estimate across the western ranges is clear in summer, but less so in other seasons. However, statewide monthly mean rainfalls are very close to values calculated from the AWAP data.

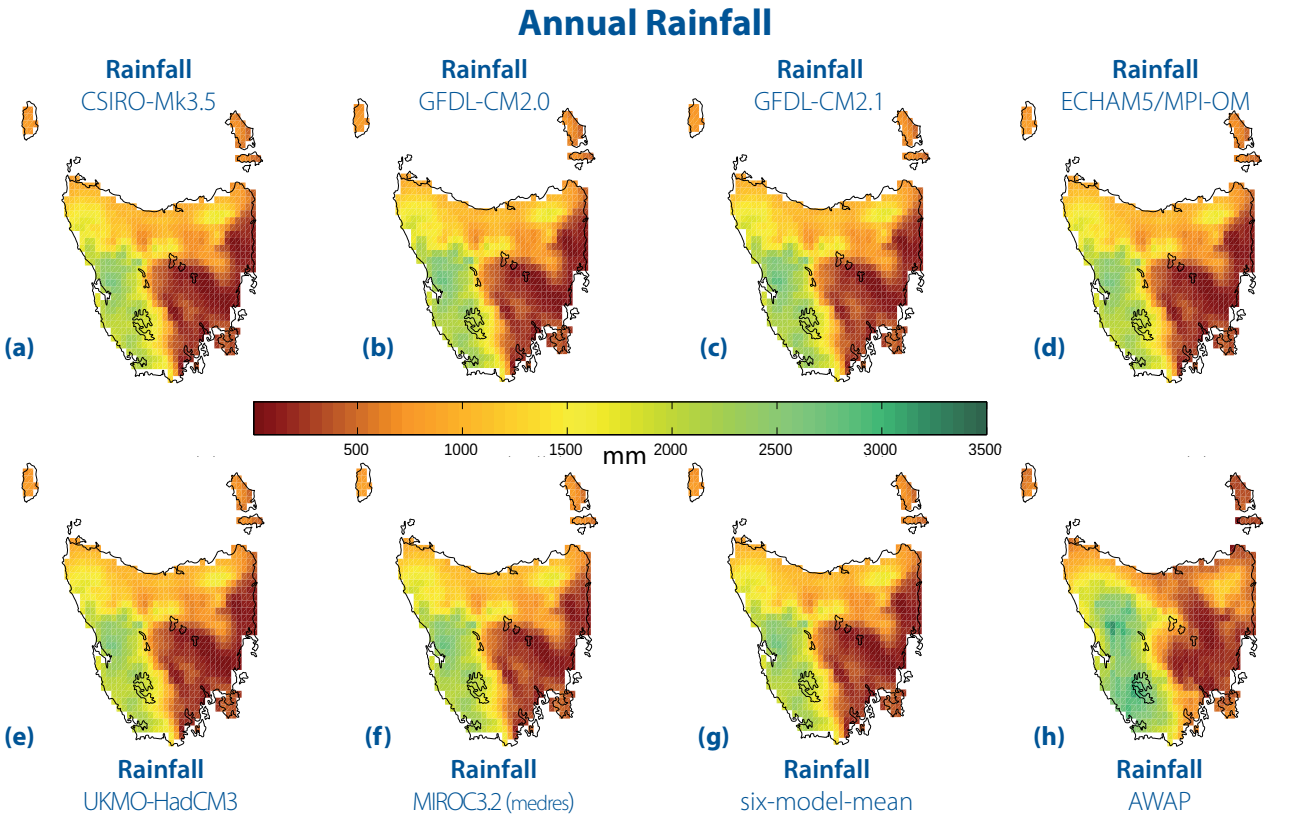

Figure 5.12 The annual total rainfall (mm) for each of the six downscaled GCMs for the period 1961-1990, along with the six-model-mean and AWAP (bottom row, right).

Summer Rain Days

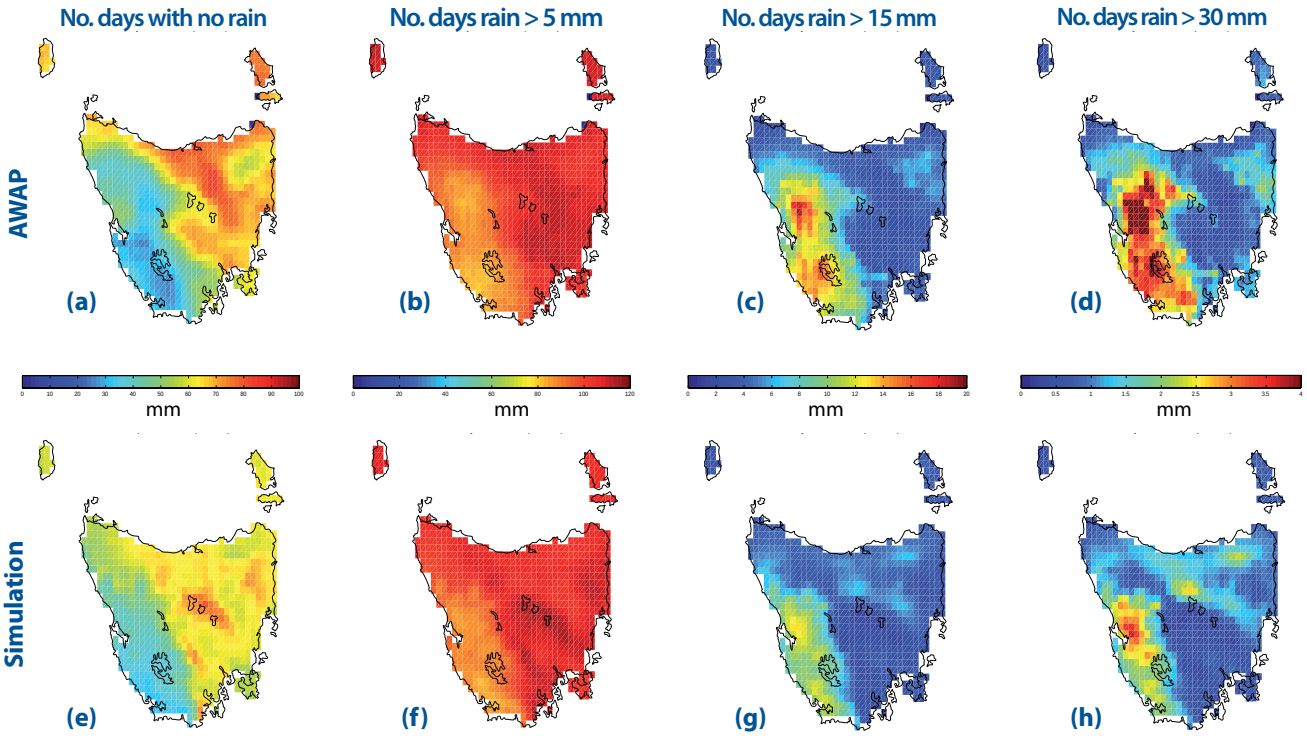

Figure 5.13 Comparison of the distribution of daily rainfall in AWAP (top) and the six-model-mean (bottom) for the months December to March for the period 1961-1990. Displayed is the number of days per year with no rain (far left), less than 5 mm of rain (middle left), greater than 15 mm of rain (middle right) and greater than 30 mm of rain (far right column).

Summer Rainfall

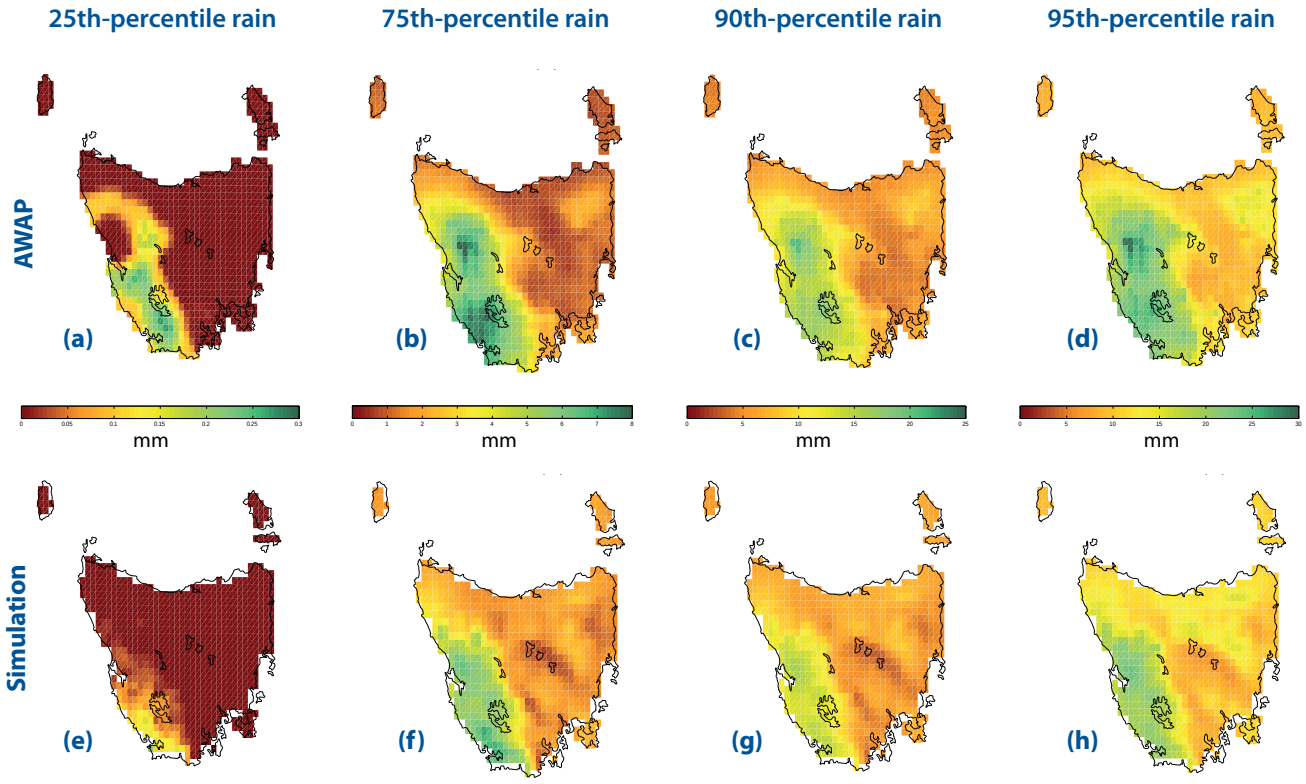

Figure 5.14 Comparison of the distribution of daily rainfall in AWAP and the six-model-mean for the months December to March for the period 1961-1990. Displayed (left to right) are the 25th, 75th, 90th and 95th-percentile rain for AWAP (top) and the six-model-mean (bottom).

Winter Rain Days

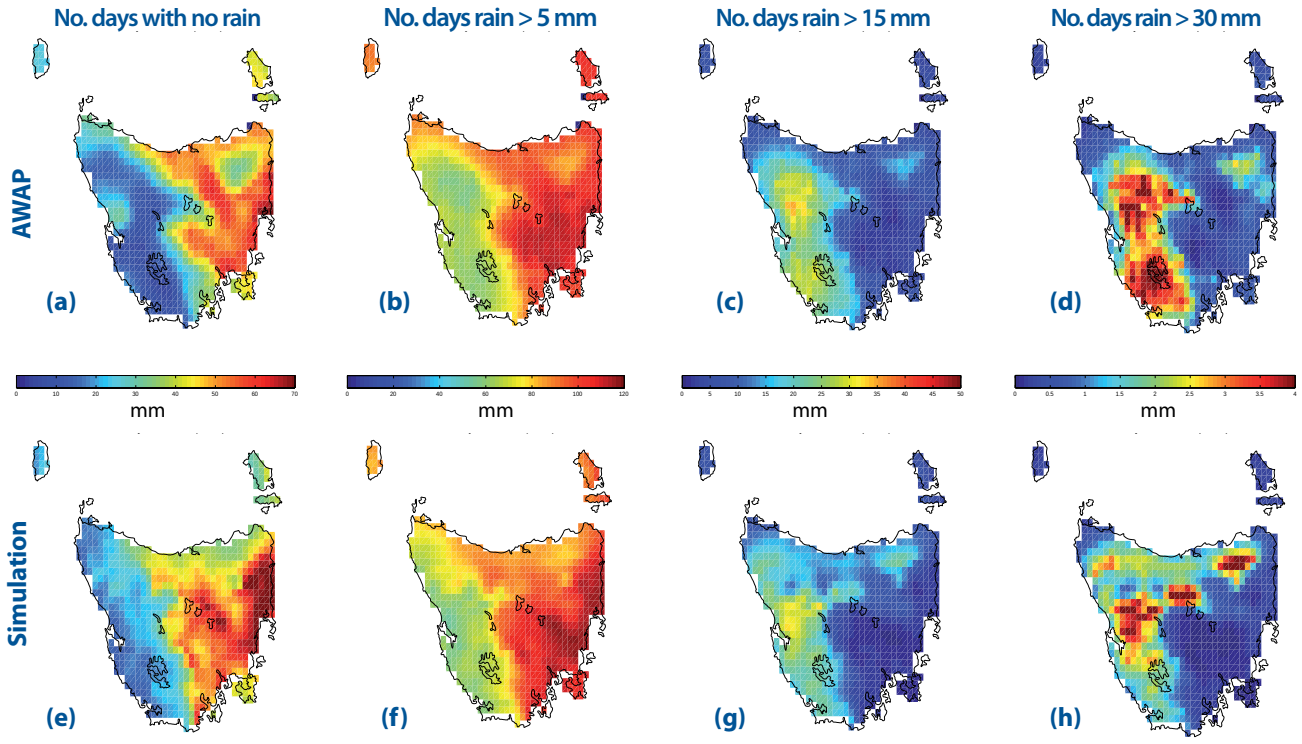

Figure 5.15 Comparison of the distribution of daily rainfall in AWAP (top) and the six-model-mean (bottom) for the months May to August for the period 1961-1990. Displayed is the number of days per year with no rain (far left), less than 5 mm of rain (middle left), greater than 15 mm of rain (middle right) and greater than 30 mm of rain (far right).

Winter Rainfall

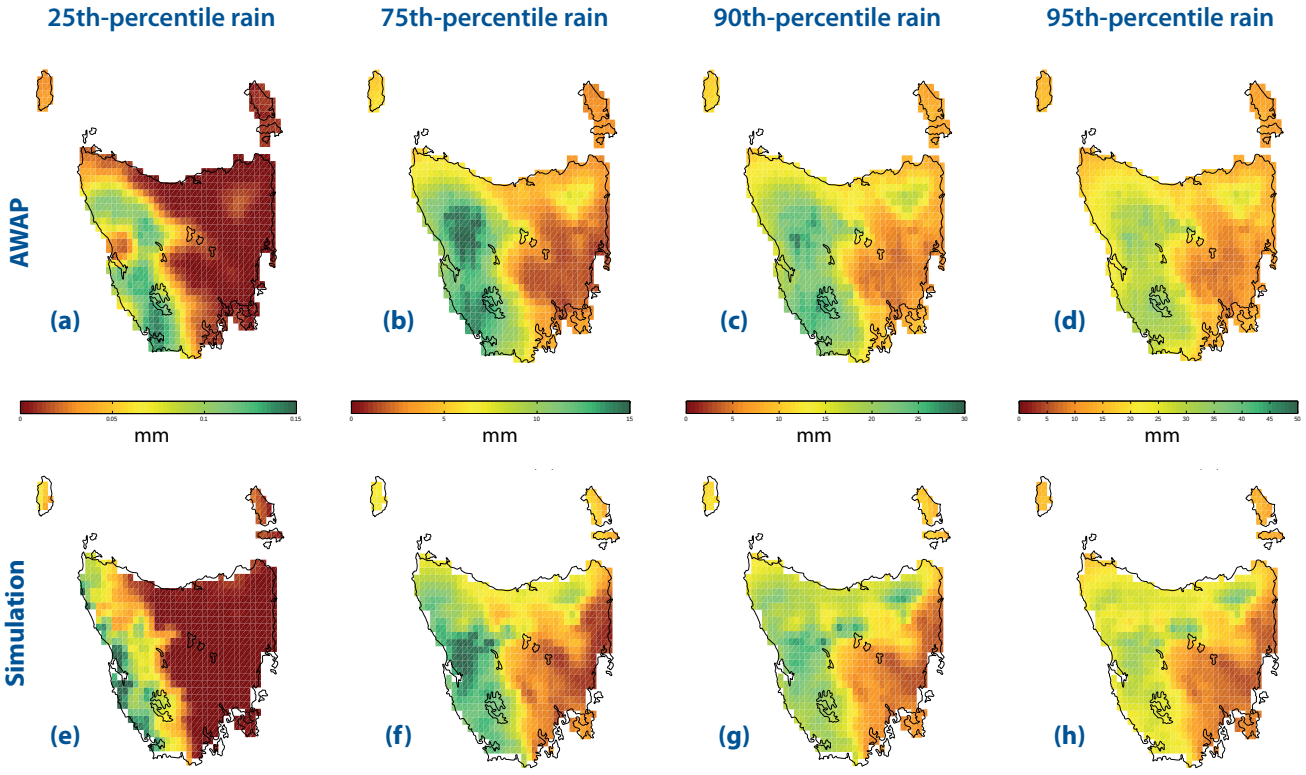

Figure 5.16 Comparison of the distribution of daily rainfall in AWAP and the six-model-mean for the months May to August for the period 1961-1990. Displayed (left to right) is the 25th, 75th, 90th and 95th-percentile rain for AWAP (top) and the six-model-mean (bottom).

Seasonal Differences in Rainfall

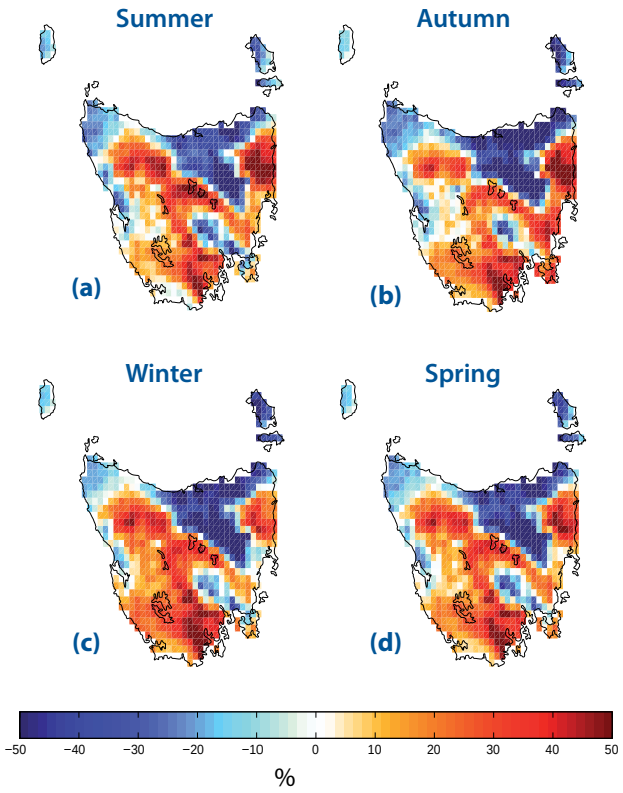

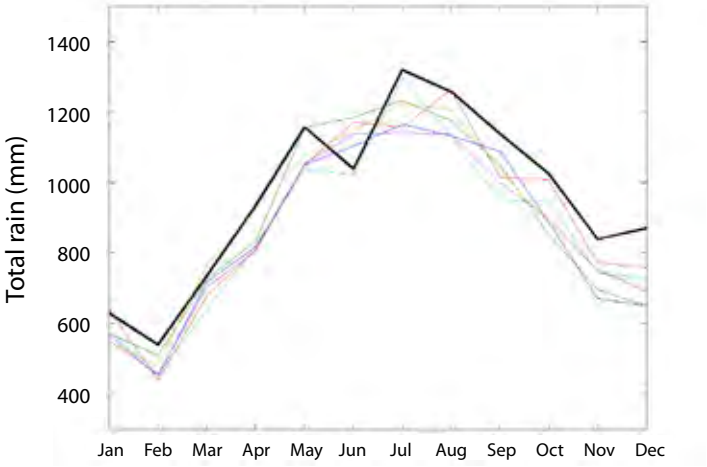

Figure 5.17 The seasonal differences (%) between AWAP and the six-model-mean for annual rainfall. The bottom figure shows the statewide mean rainfall value (mm) by month for each of the six downscaled models (coloured) and AWAP (black).

5.3 Solar Radiation

Estimates of solar radiation at the earth's surface with complete spatial coverage have only been possible since 1990 with the advent of satellite records of cloud cover and albedo. The mean annual solar irradiance from the AWAP data and the mean of the simulations is shown in Figure 5.18. The mean difference is -0.1 MJ m^{-2} d^{-1}, and there is an east-west pattern to the difference, where the models showing higher radiation than the AWAP data on the east coast, and lower on the west coast. There is a strong correlation (correlation coefficient of 0.98), but more spatial detail and stronger gradients in the simulations than in the AWAP data.

It is not possible to quantify the contribution from errors and limitations in the AWAP data and from the model in this difference. The east-west pattern to the difference is not strongly correlated with rainfall, but is plausibly related to cloud cover. The AWAP dataset (or any other available gridded observational dataset) does not include cloud cover and so the relationship to observed cloud is not possible to test.

Solar Radiation

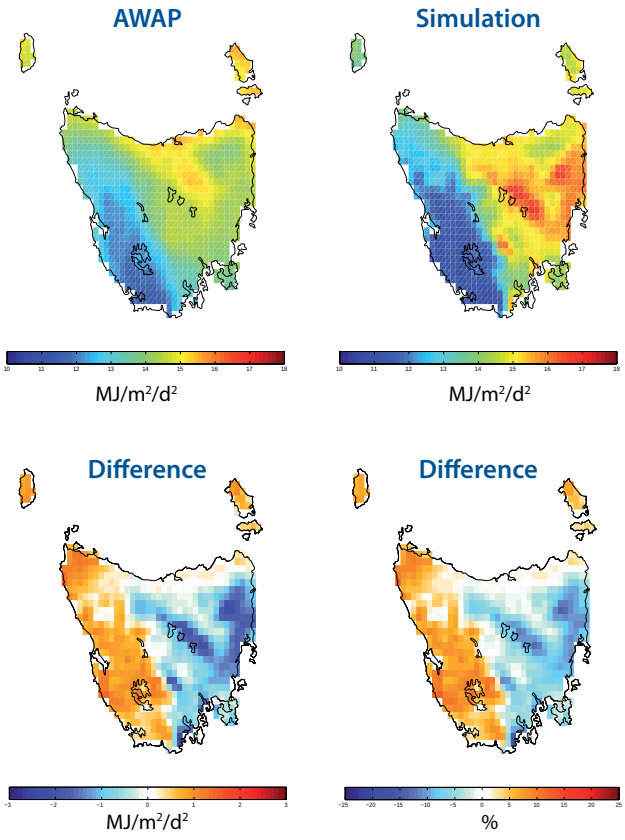

Figure 5.18 Mean downward solar radiation for the period 1961 2007 for AWAP, the six model-mean, and the difference between them.

5.4 Potential evaporation

Contributors to the loss of water from the soil to the atmosphere are physical processes (evaporation) and a term that includes the loss of water through vegetation (evapotranspiration). For each of these there are two possible estimates: total evaporation given the water present and potential evaporation assuming unlimited water. While evaporation terms are highly quantifiable phase transition processes, they are difficult to reliably quantify with complete spatial coverage over heterogeneous land cover under typical environmental conditions. In any estimate of evaporation, there are assumptions or simplifications about the type and proportion of land cover, and then a balance between the comprehensiveness of the equation used to describe evaporation and the quality of the input data. Equations for this estimate use up to four variables as input: radiation, temperature, wind and relative humidity. Some equations replace some of these terms with a constant since the quality of the input data is not considered appropriate (for example wind).

Potential evaporation calculated within the model has the advantage of having complete coverage of input variables to draw from. The downscaled model (CCAM) uses all four input variables listed above within the Penman-Monteith equations (Allen et al. 1998). The AWAP dataset uses the Priestley equations of potential evaporation (Raupach 2000; Raupach 2001), based on net radiation and soil heat flux. The equation replaces the turbulence term of the calculation (incorporating wind speed and relative humidity) with a dimensionless empirical multiplier (the Priestley-Taylor coefficient). This is considered an acceptable compromise for this calculation from observed data since the datasets of wind and relative humidity are less robust than for temperature or rainfall (Jones et al 2009).

Mean annual potential evaporation for the overlap period 1961-2007 for the mean of models and for the AWAP data is shown in Figure 5.19. As with radiation, there is a small mean difference between the simulations and gridded observed data (20 mm) and a high spatial correlation (0.83) with more spatial detail in the simulations compared to the AWAP data.

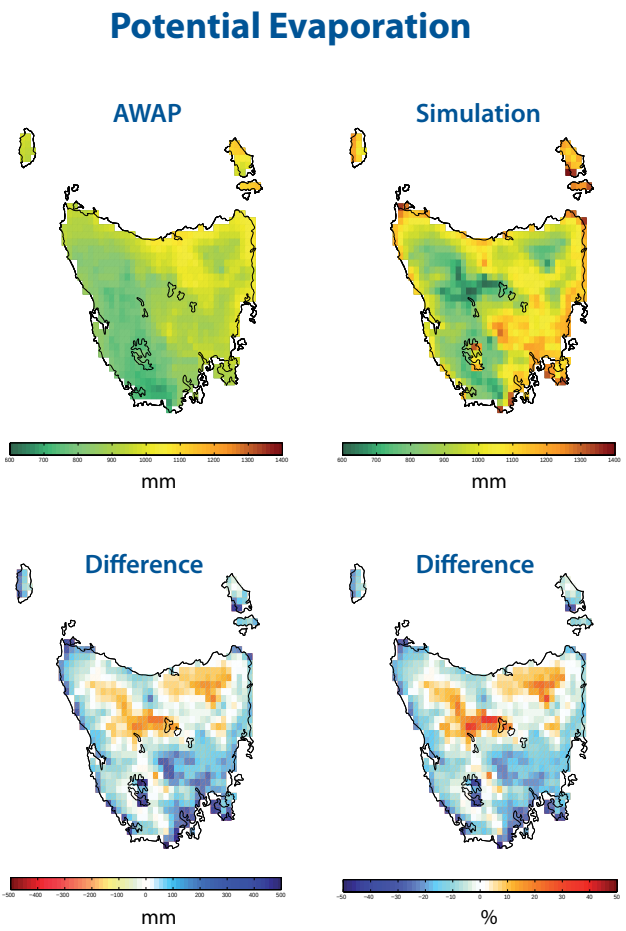

Figure 5.19 Mean annual total potential evaporation (mm) for the period 1961-2007 for AWAP, the six-model-mean, and the difference between them.

5.5 Pressure

The AWAP dataset does not contain an observed pressure field. Thus, this dataset cannot be used to compare pressure from the models with gridded observations. We chose to use the NCEP Reanalysis as a validation dataset. The NCEP Reanalysis features a global suite of assimilated observations on a 2.5-degree grid. At this resolution, the pressure field from NCEP Reanalysis strongly incorporates available observations.

As was discussed in Section 4.2.1, we have undertaken two downscaling simulations from the NCEP Reanalysis. The first simulation is the forced NCEP simulation. This simulation downscales NCEP from the global 2.5-degree dataset to the 0.5-degree model using sea surface temperature (SST) as the bottom boundary condition and spectrally nudges the atmosphere to maintain the same large-scale surface pressure, temperature, wind fields and 850 hPa moisture. By forcing these fields (Figure 5.20 to Figure 5.23), we have ensured that the large-scale patterns in these 0.5-degree simulations of NCEP are similar to the global NCEP reanalysis and thus the pressure field from the downscaled model gives us a good representation of pressure in the Australian region. The downscaling process from the 0.5-degree simulations to the 0.1-degree simulations is identical to that used for the six GCMs.

The 0.5-degree downscaled model accurately reproduced annual and seasonal NCEP mean monthly pressure fields (Figure 5.20). The forcing of surface pressure, temperature, wind fields and atmospheric moisture is sufficient to ensure that the downscaled model is very highly correlated with the global NCEP Reanalysis (above 0.95) throughout the area of interest.

The downscaling process preserves temperature characteristics between the raw NCEP Reanalysis and the forced 0.5-degree downscaled simulation of the same (Figure 5.21 and Figure 5.22). The temperature relationships are discussed further in the General Climate Impacts Technical Report (Grose et al 2010).

Pressure is a large-scale driver of weather, and thus simulating the correct overall pressure fields in our models is important. Equally as important is simulating the correct passage of pressure fields across the Australian region at the correct time of year. An examination of pressure fields as a driver of weather in our models is included in the General

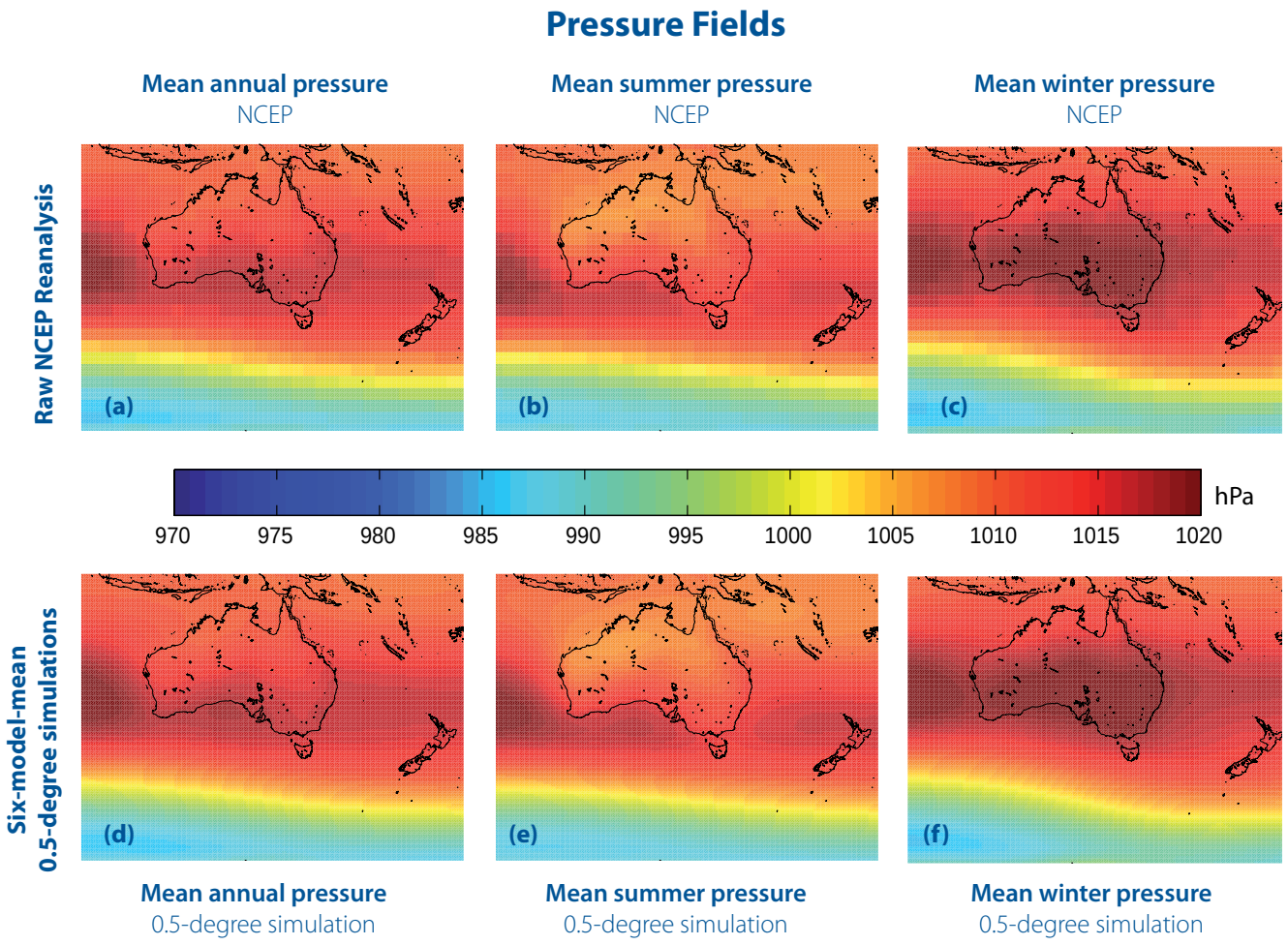

Figure 5.20 Mean pressure fields for raw NCEP Reanalysis (top row) and the six-model-mean of the downscaled 0.5-degree simulations (bottom row) for the period 1961-1990. The left column shows the annual pattern, the middle column shows the pattern for the months December to March and the right column the months May to August.

Climate Impacts Technical Report (Grose et al 2010). In this report, we confine our attention to whether the monthly mean pressure fields produced by the suite of 0.5-degree models are similar in spatial distribution and variance to the downscaled NCEP simulation.

The pressure field of the six-model-mean displays a very similar pattern to the 0.5-degree downscaled NCEP model for each of the four seasons (Figure 5.23). The range of pressures displayed and the longitude of the pressure gradient are closely aligned. One difference between the six-model-mean and downscaled NCEP pressure fields is the orientation of the pressure gradient that passes south of New Zealand. In the downscaled NCEP field (and also the raw NCEP Reanalysis), the longitude of the gradient varies with latitude (this is especially noticeable in winter). In the six-model-mean, the longitudinal variation with latitude is less pronounced. The models correctly simulate the changes in the mean pressure field between seasons. Similarly, the standard deviation of the model mean varied between the seasons in phase with the NCEP standard deviation. Over Australia, the models gave similar variance to the NCEP simulation, but some differences emerged in the Southern Ocean, especially in winter and spring.

The second simulation using the NCEP Reanalysis data is the unforced NCEP simulation. This simulation employs the same downscaling technique as that used for the GCMs: SST only forcing from the host to the 0.5-degree model, and then SST and atmospheric forcing between the 0.5-degree model and 0.1-degree model. This allows us to compare the atmospheric variables in both simulations and thus examine the effects of the SST-only downscaling.

As discussed earlier in this report, global climate models are not forced by observations of current climate. As such they often have biases that cause their simulation of the current climate to differ from the observed current climate. To more accurately represent the current climate, we chose to bias-adjust the SSTs from the GCMs. The decision to bias-adjust SST means that forcing the atmosphere was not appropriate (Katzfey et al 2009). The consequences of this decision are examined below.

In comparing the forced and unforced NCEP simulations, we concentrated on three variables: mean monthly sea level pressure, mean annual rainfall and mean monthly daily maximum temperature (Tmaxscr). The period of comparison is between January 1961 and December 2006.

The annual mean daily maximum screen temperature (Tmaxscr) is very similar for both the forced and unforced NCEP (Figure 5.24). The simulations have very closely matching spatial structure and similar

Downscaling Temperature

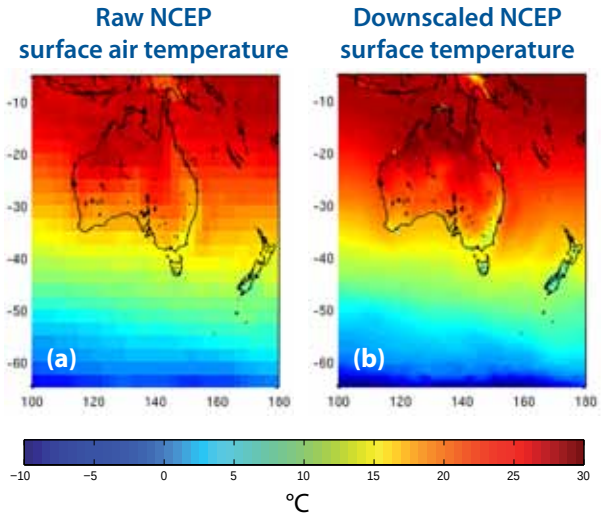

Figure 5.21 Mean surface temperature for the period 1961-1990 from (a) the global NCEP Reanalysis and (b) the 0.5-degree downscaled simulation of NCEP.

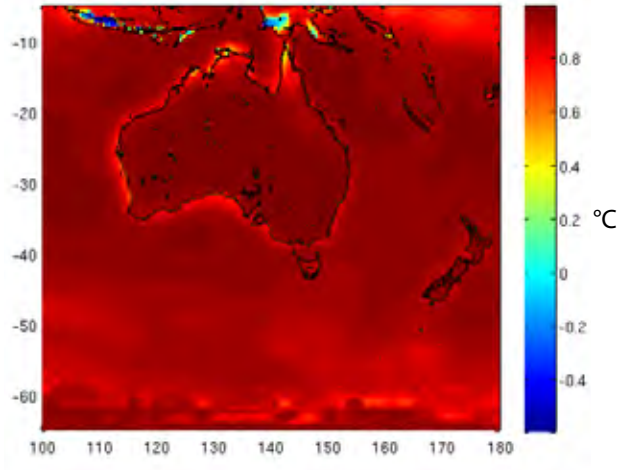

Figure 5.22 Temporal correlation of mean surface temperature over the period 1961-1990 between the global NCEP Reanalysis and the downscaled 0.5-degree simulation of NCEP.

values. There is a slight cold bias of less than 2 °C over Australia in the unforced simulation compared to the forced simulation. The temporal correlation between the two simulations (not shown) is greater than 0.98, reflecting the strong seasonal signal for screen temperature. Given the common SST used to force both simulations this strong similarity for screen temperature validates the approach, even though the temperature over land can evolve independently in the unforced simulation.

The unforced and forced mean monthly mean sea level pressure display a generally similar structure in the south-east Australian region. The unforced mean monthly mean sea level pressure exhibits a stronger meridional gradient than the corresponding forced surface pressure (Figure 5.25). A notable feature of surface pressure in many climate models is the

Seasonal Pressure

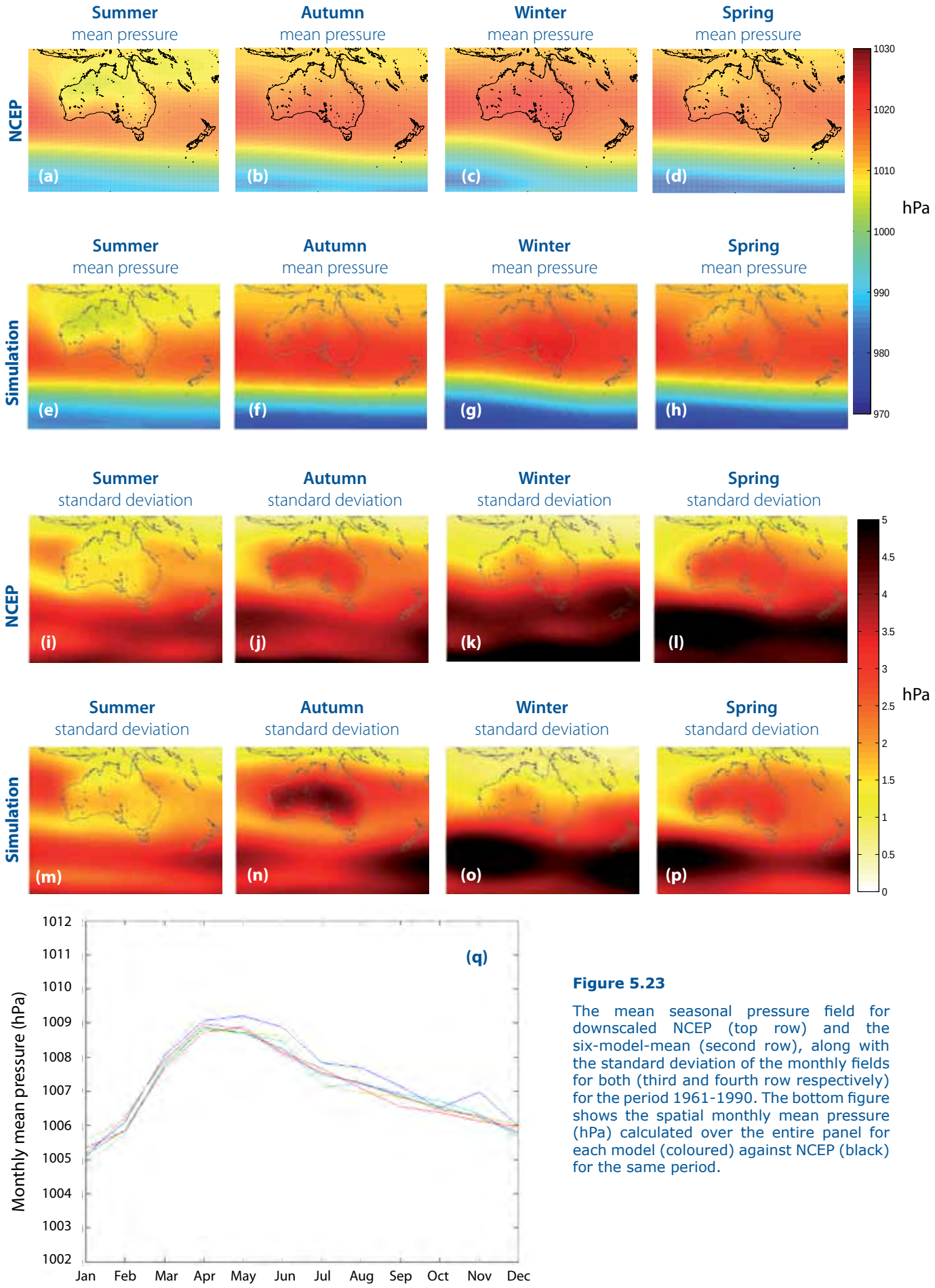

Figure 5.23

The mean seasonal pressure field for downscaled NCEP (top row) and the six-model-mean (second row), along with the standard deviation of the monthly fields for both (third and fourth row respectively) for the period 1961-1990. The bottom figure shows the spatial monthly mean pressure (hPa) calculated over the entire panel for each model (coloured) against NCEP (black) for the same period.

change of curvature of the isobars directly south of Tasmania to a slightly more meridional configuration. The unforced NCEP surface pressure displays less curvature of the isobars in this region than the forced NCEP simulation. The differences between the two versions of NCEP ranges between approximately minus 2 hPa and 2 hPa.

The spatial structure of the unforced NCEP mean annual rainfall resembles the structure of the corresponding forced NCEP rainfall (Figure 5.26). This suggests that the unforced simulation is resolving the main climate features driving rainfall over the region. However, the unforced simulation does have a wet bias south of Tasmania, possibly related to the more zonal flow of the winds.

The simulation forced using NCEP atmospheric fields gives some measure of how well the model can reproduce the observed regional climate. The simulation using only NCEP SSTs (no atmospheric forcing) then gives a measure of how well the downscaled model can reproduce the observed climate without atmospheric forcing. This then gives us a measure of how accurately the downscaling is preserving the atmosphere of the GCM simulations.

It is clear from Figure 5.24, Figure 5.25 and Figure 5.26 that the decision to use only SST to force the GCM downscaling simulations does have an effect on the resulting patterns of rainfall, temperature and mean sea level pressure (and by implication all atmospheric variables) when compared to combining SST and atmospheric forcing. However, GCM rainfall and circulation patterns are not perfect. GCMs are designed to be correct in the long term and at the spatial resolution of hundreds of kilometres (their grid scale). The NCEP Reanalysis, while not perfect, attempts to analyse the atmospheric circulation as accurately as possible within the limitations of the available observational data, the analysis system and the resolution used. By only using SST as forcing, we allow the downscaled model to evolve its own atmospheric circulation independent of the bias or errors that exist in the host GCMs and trust that the downscaled model can produce an atmosphere that is as close to, if not closer, than the observed climate over the region of interest. The bias-adjustment of the SSTs from the GCMs brings the climatology of the SSTs closer to observed climate, and draws the mean atmospheric circulation closer to the observed pressure. The results presented in this section demonstrate that the downscaled model (forced with only SST) can produce a modelled climate close to the observed climate and thus largely validates this approach.

Forced and Unforced NCEP – Temperature

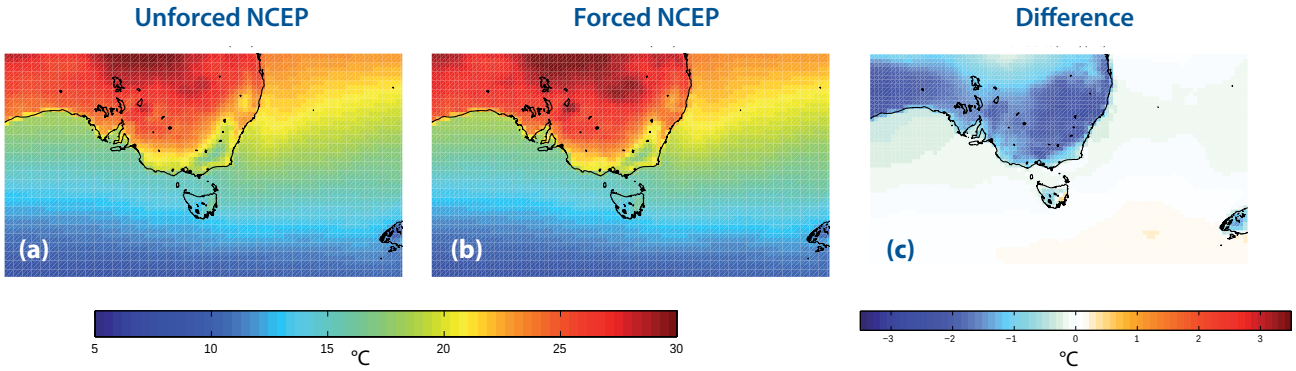

Figure 5.24 The mean daily maximum screen temperature for (a) the unforced NCEP simulation and (b) the forced NCEP simulation and (c) the difference between the unforced and forced simulations, for the time period 1961-2006.

Forced and Unforced NCEP – Pressure

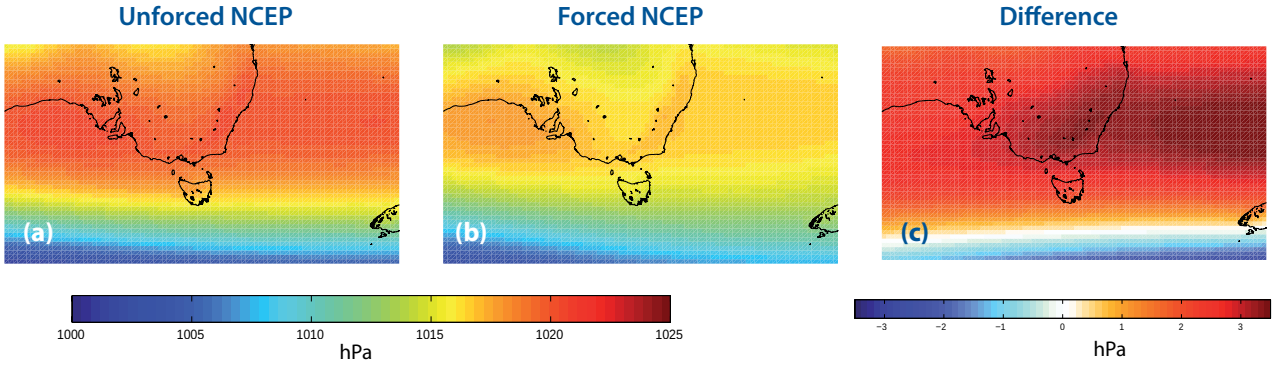

Figure 5.25 The mean surface pressure for (a) the unforced NCEP simulation (b) the forced NCEP simulation and (c) the difference between the two, for the time period 1961-2006.

Forced and Unforced NCEP – Rainfall

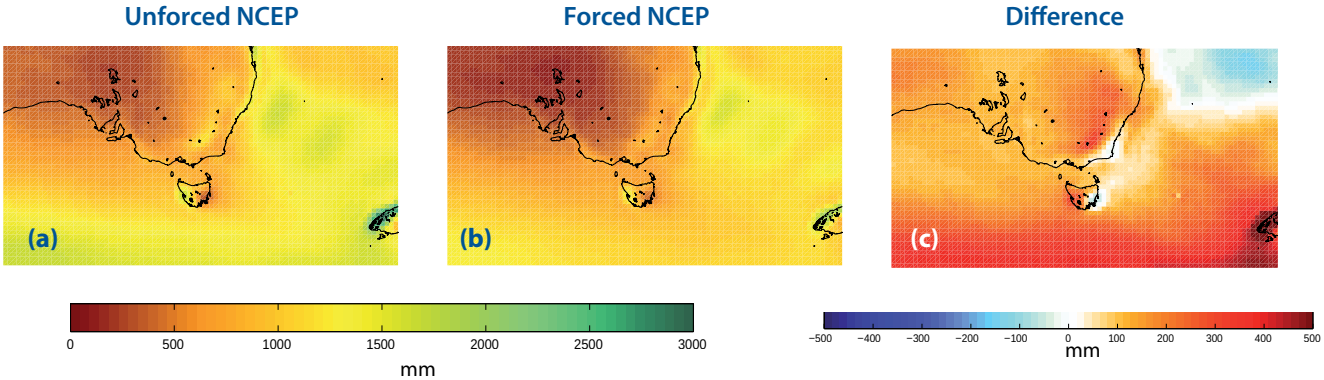

Figure 5.26 The mean annual rainfall for (a) the unforced NCEP simulation (b) the forced NCEP simulation and (c) the difference between the two, for the time period 1961-2006.

Figure 5.24 and Figure 5.26 show that for temperature and rainfall the regions of greatest difference between the forced and unforced NCEP simulations occur over land in the mountainous regions along the east coast of Australia. This rainfall result is not surprising. The forced NCEP simulation is forced so that the broad spatial features of the temperature (and pressure) are similar to the global 2.5-degree NCEP Reanalysis. This constrains the ability of the downscaled model to freely evolve the temperature in regions of complex topography. Over land, the unforced model is free to evolve its own temperature, rainfall and pressure. Thus, it is better able to model the effects of the topography on the rainfall. This result further reinforces the decision to force the downscaled models with only SST from the GCMs (and NCEP in the unforced model run).

We have shown that the unforced NCEP model produces an atmosphere that has similar characteristics and mean pattern to the forced NCEP model. While this is only a preliminary analysis, this analysis demonstrates that the method of forcing the downscaled models with only SST is valid and allows for the creation of an atmospheric circulation that is similar to the observed climate.

The time series for each of temperature, rainfall and pressure are shown in Figure 5.27. This shows that the (spatial) mean temperature for the forced and unforced downscaled NCEP simulations, while not in-phase, are similar in magnitude and variability (standard deviation (unforced) of 0.24 and standard deviation (forced) of 0.26), and display a similar trend over the 46 years shown. Rainfall is consistently too high in the unforced simulation, indicating the presence of a bias. The variability of the unforced rainfall (standard deviation of 35.7) is reduced compared to the forced model (standard deviation of 50.8) and both models show a slight increasing trend. The wet bias in the unforced model is due to the strongly increased rainfall over the Southern Ocean that is seen in the unforced model (Figure 5.26). The mean sea level pressure in the unforced simulation is higher than for the forced simulation over most of the domain (the exception being the southern most area of the domain). This is reflected in the time series where the spatial mean of rainfall in the unforced simulation is higher than for the forced simulation. The variability of the unforced model (standard deviation of 0.555) is just over half that of the forced model (standard deviation of 0.957). Neither model displays a discernible trend over the 46-year period.

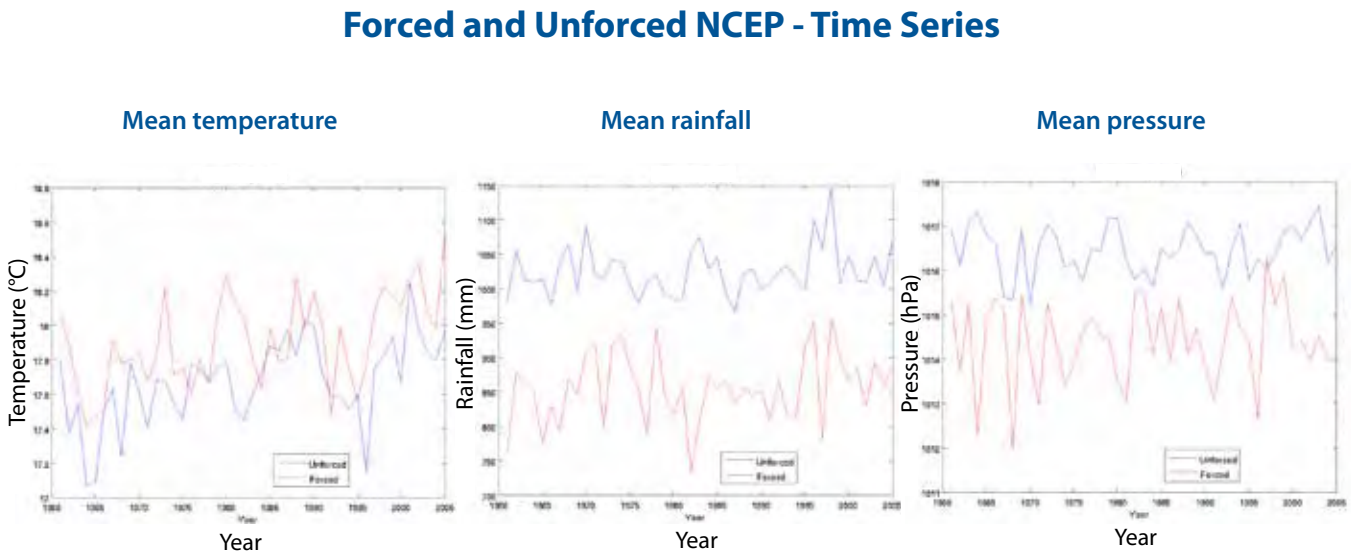

Figure 5.27 Time series (1961-2006) of the annual mean temperature, total rainfall and mean pressure for the 0.5-degree simulations (over the output domain). The unforced NCEP simulation is shown in blue while the forced NCEP simulation is red.

5.6 Downscaling

The principle of the downscaling process is to increase our knowledge of Tasmania's climate by increasing the resolution of the models, while still maintaining consistency with the global climate models that form the basis of the modelling projections to 2100. Accordingly, temperature is better simulated over Tasmania in the 0.1-degree models than in the 0.5-degree models, or in the GCMs, caused by the better representation of topography (Figure 5.28). Similarly, the rainfall is better simulated in the 0.1-degree models, with increased rainfall on the west coast of Tasmania and the corresponding rain shadow in the east (Figure 5.29). We use the GFDL-CM2.1 GCM as an example, since the process and results are similar for all GCMs that were used in the project.

A necessary condition for the downscaling process to be considered effective is that the long-term behaviour of variables across the downscaling region behave in a similar manner to the host GCM. That is, the downscaling process is adding detail to the modelling output, but not changing the overall behaviour or trend seen in the GCM.

The mean temperature of the entire region shown in Figure 5.28 (Tasmania and the immediately surrounding ocean) is 12.99 °C for the GCM, while for the 0.5-degree and 0.1-degree models it is 13.74 °C and 13.48 °C respectively. Over the land surface alone, the mean temperature of the 0.5-degree and 0.1-degree models are close to the value of 10.4 °C calculated with the AWAP data. The downscaling dramatically increases the total rainfall over the Tasmanian region when compared to the GCM, because the GCMs take almost no account of the Tasmanian topography. For the region shown (Tasmania and the immediately surrounding ocean) in Figure 5.29, the mean annual rainfall in the GCM is 746 mm, while it is 1006 mm and 1175 mm for the 0.5-degree and 0.1-degree models, respectively. Note that these rainfall values are calculated over the entire panel and not just over the land surface. Over the land cells in the 0.1-degree model the mean annual rainfall increases to 1385 mm. This compares with the annual mean rainfall calculated from the AWAP data for Tasmania over the same period of 1390 mm. Thus, the downscaling process results in a decreasing difference between the model and observed rainfall. Similar results hold for each of the remaining five GCMs and downscaled models, but are not shown in this report.

5.6.1 Temperature

The downscaled 0.5-degree model used the monthly sea surface temperature from the host GCM as the bottom boundary condition. The 0.5-degree model is in turn used to force the 0.1-degree model. As such, we would expect that on a monthly basis the temperature in the host GCM and the 0.5-degree model shows a strong temporal correlation. The temporal correlation between monthly mean surface

Downscaling Temperature

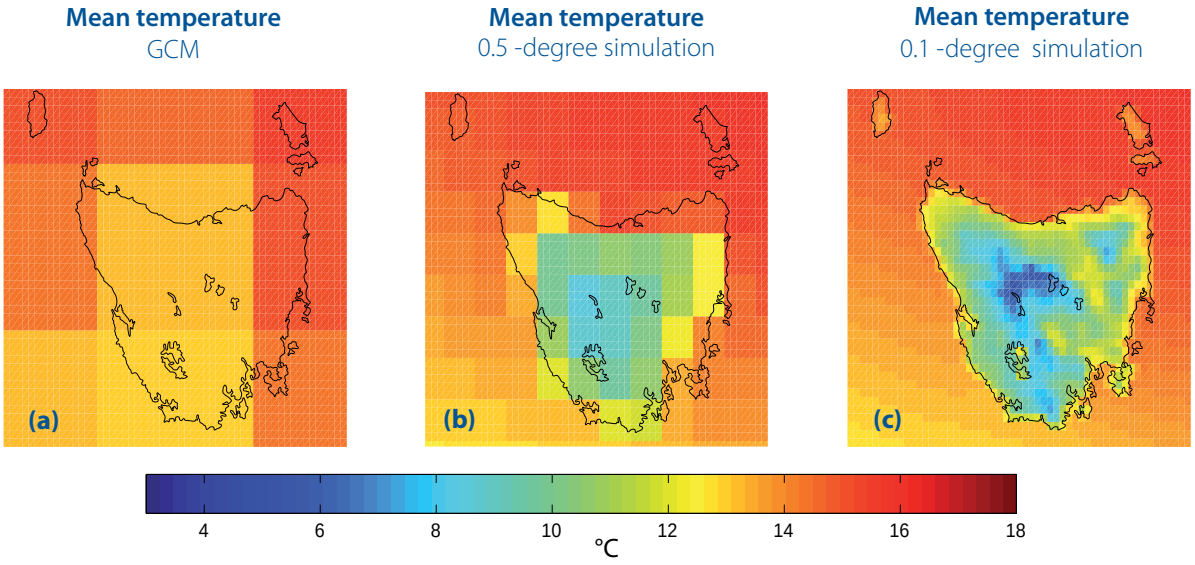

Figure 5.28 Mean temperature for Tasmania for the period 1961-1990 from (a) the GCM GFDL-CM2.1 (b) the 0.5-degree downscaled simulation of the same GCM and (c) the 0.1-degree downscaled simulation of the same GCM.

Downscaling Rainfall

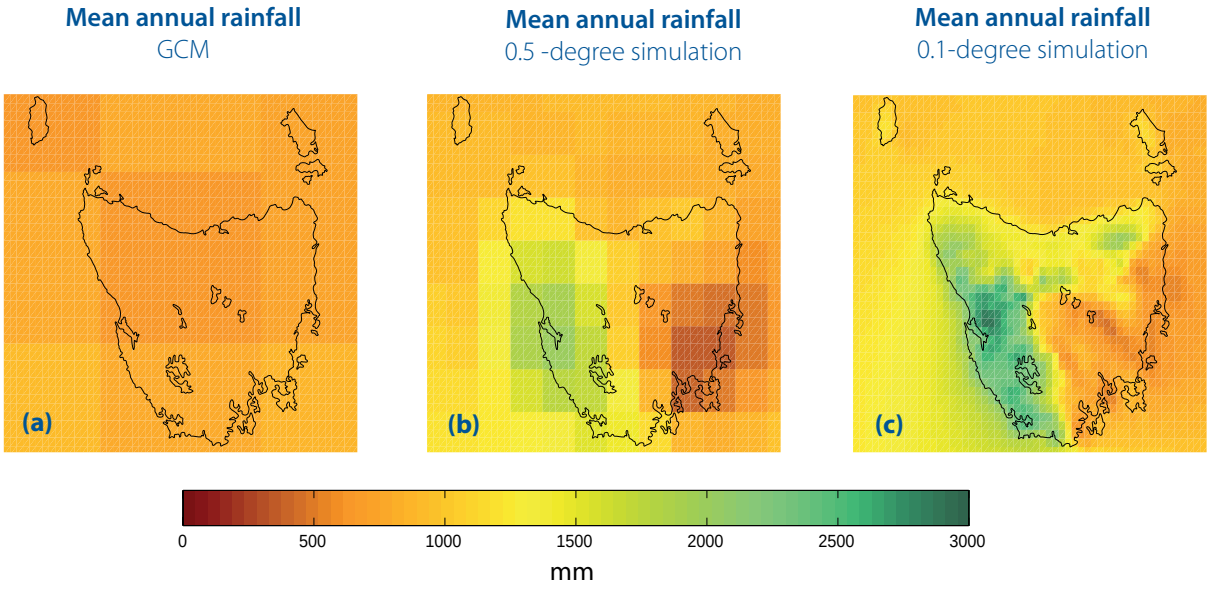

Figure 5.29 Mean annual rainfall for Tasmania for the period 1961-1990 from (a) the GCM GFDL-CM2.1 (b) the 0.5-degree downscaled simulation of the same GCM and (c) the 0.1-degree downscaled simulation of the same GCM.

temperature in the GCM and the 0.1-degree model is similar to that between the GCM and the 0.5-degree model (Figure 5.30), showing that the downscaling process also maintained the general trend of the GCM.

This is further reinforced in Figure 5.30c, which shows the very strong temporal correlation of the monthly mean surface temperature between the 0.5-degree and 0.1-degree models. The spectral nudging between the 0.5-degree and 0.1-degree models is designed to preserve the large-scale weather patterns from the 0.5-degree model into the 0.1-degree model, and thus a strong correlation between the 0.5-degree and 0.1-degree models. The downscaling process also maintained the general trend of the GCM (Figure 5.30a and Figure 5.30b).

5.6.2 Rainfall

Rainfall from the GCM is not used to constrain the 0.5-degree or 0.1-degree simulation in any way. In the downscaled 0.5-degree models, the rainfall is internally generated through such mechanisms as orographic lifting of moist parcels of air, through the passage of frontal systems and though other mechanisms that are observed in a climate system. As such, we do not expect a strong temporal correlation between GCM rainfall and rainfall produced by the downscaling process. As with temperature, the temporal correlation of rainfall between the GCM and the 0.5-degree and 0.1-degree has a plausible pattern (Figure 5.31a and Figure 5.31b). The stronger correlations on the north and west coasts reflect the more seasonal nature of rain in these regions, as compared to the east coast. The 0.1-degree model also generates its own rainfall, however as rain-making systems (fronts, cutoff lows et cetera) are large-scale phenomena, and the atmosphere is forced between the 0.5-degree and 0.1-degree simulations so as to preserve these large-scale features, the rainfall was strongly correlated between the two models (Figure 5.31c).

So far, in this section we have only considered the modelling output on a monthly basis. The sea surface temperature from the GCM modelling output is applied in a monthly time step, and so comparing monthly modelling output to the GCM is appropriate. However, for the downscaling between the 0.5-degree and the 0.1-degree model the atmospheric nudging above 850 hPa is applied continuously. The correlations corresponding to those shown in Figure 5.30c and Figure 5.31c for the daily outputs are similar to the monthly outputs, although the correlation does drop slightly as one would expect. This shows that the downscaling between the 0.5-degree and 0.1-degree models maintained the overall structure of the 0.5-degree model.

The value of the CCAM downscaled simulations over GCMs can be judged by the increase in correlation between the finer-resolution models and the gridded AWAP data. The GFDL-CM2.1 downscaled 0.1-degree model clearly has more skill in simulating the observed spatial patterns in rainfall and temperature over Tasmania than its host GCM (Table 5.1). The GCM shows low correlations of 0.45 for temperature and 0.28 for rainfall, while the 0.5-degree model improves this correlation, and the 0.1-degree model improves on it again. The 0.05-degree model that will be discussed later, further increases this correlation, showing that downscaling achieves the aim of adding local information over Tasmania, thus improving the realism of the simulations of the current climate. An increased ability to simulate and explain the current climate gives us greater confidence that we can accurately project the future climate change over Tasmania. The remaining GCMs and their corresponding downscaled models yield similar correlation statistics.

5.6.3 Pressure

Examining variations in pressure, or characteristics of the pressure field just over the Tasmanian region is not appropriate given the length-scales involved and the small size of the island. When examining pressure fields we only considered the 0.5-degree for a region incorporating Australia, New Zealand, parts of Indonesia and the Southern Ocean (Figure 3.5c).

The 0.5-degree model faithfully reproduced the annual and seasonal mean pressure fields present in the GCM (Figure 5.32). More importantly, it reproduced the changes in the mean pressure field between summer and winter as well as the variance and spatial distribution of mean monthly pressure fields present in the GCM (Figure 5.33), although some differences exist, noticeably in the Southern Ocean, where the resolution of the downscaled model starts to decrease, and in the increased variance in the 0.5-degree downscaled model over continental Australia.

Table 5.1 Spatial correlations between the 0.1-degree AWAP data and GFDL-CM2.1 as the raw GCM and downscaled to 0.5-degree and 0.1-degree for the period 1961-1990.

Model resolution	Mean Monthly Temperature	Mean Monthly Rainfall
GCM	0.45	0.28
0.5°	0.79	0.44
0.1°	0.93	0.63

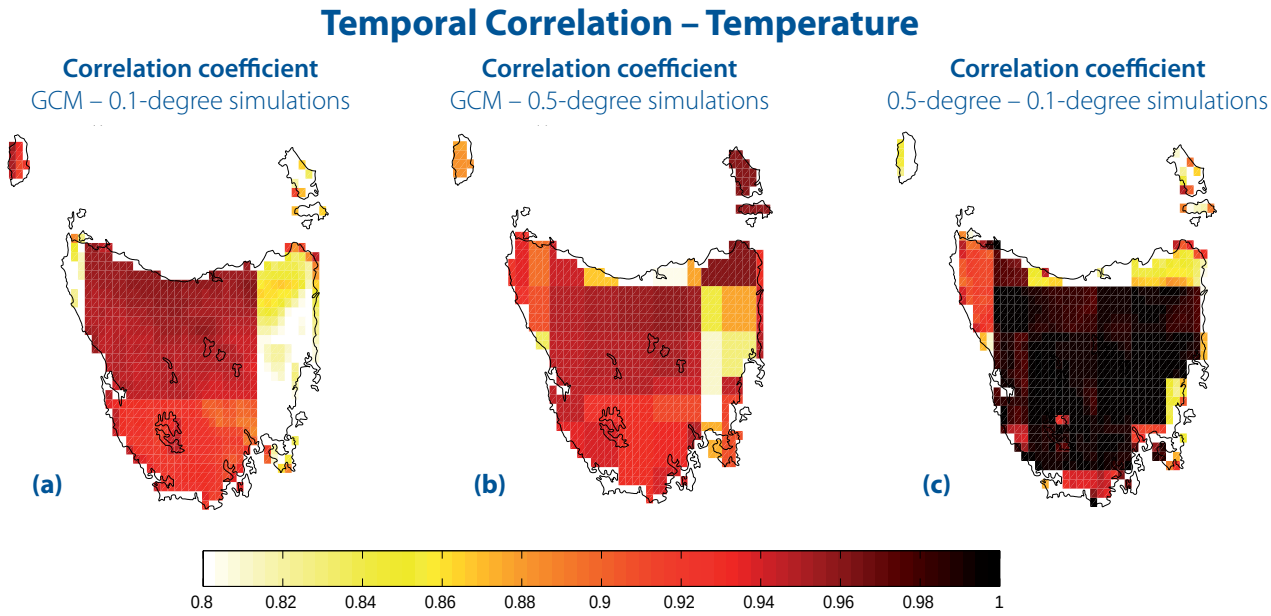

Figure 5.30 Temporal correlation between monthly mean surface temperature in the GCM GFDL-CM2.1 and the downscaled (a) 0.5-degree and (b) 0.1-degree simulations for the period 1961-1990, as well as between the (c) 0.5-degree and 0.1-degree simulations.

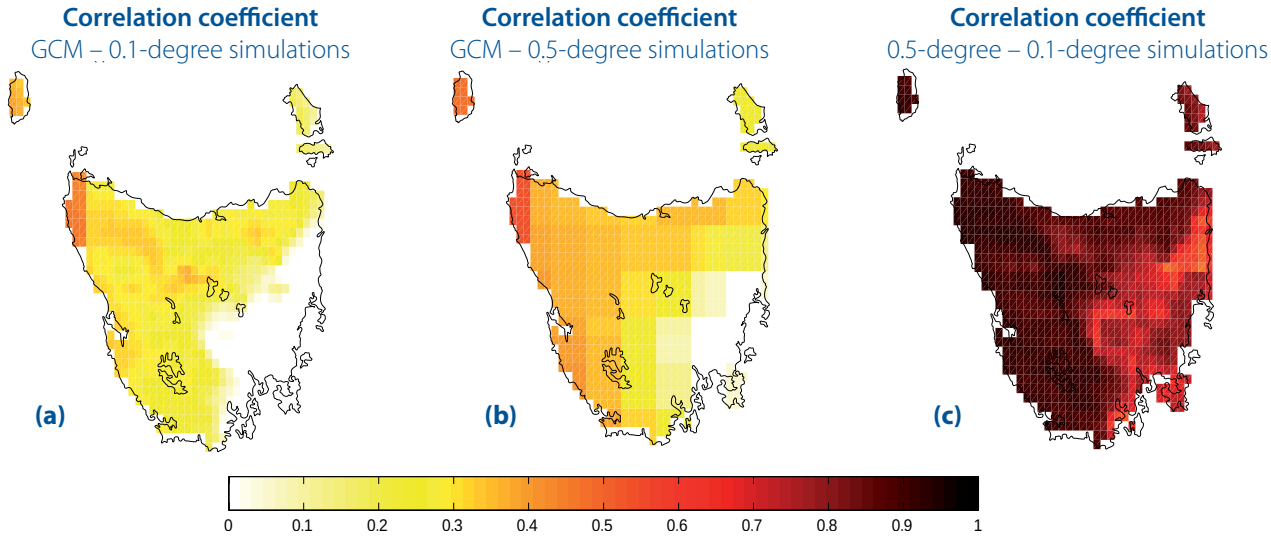

Figure 5.31 Temporal correlation of mean monthly rainfall between the GCM GFDL-CM2.1 and the downscaled (a) 0.5-degree and (b) 0.1-degree simulations for the period 1961-1990, as well as between the (c) 0.5-degree and 0.1-degree simulations.

To this point, our analysis has been confined to the region of the globe where the downscaled simulations are designed to outperform their host GCM. However, since CCAM is a global atmospheric model its performance outside of Tasmania is also of interest. The summer mean sea level pressure from the NCEP Reanalysis, the GCM GFDL-CM2.1 and the 0.5-degree downscaled GFDL-CM2.1 is shown in Figure 5.34. The pressure distribution for both the GCM (b) and the downscaled results (c) are generally very similar to the reanalysis data (a), indicating the GCM can reproduce the current climate, as represented by the NCEP Reanalysis patterns well, even without any direct observational input. The locations and intensities of the major high and low pressure centres, such as the northern Pacific and Atlantic lows, the monsoon low over Indonesia, and the tropical highs over the South Pacific Ocean, Atlantic Ocean and Indian Ocean are all very similar. The main areas of discrepancy are in the polar regions particularly in the northern hemisphere, where there is less observational data to constrain the reanalyses and where impacts of ocean and sea-ice distributions are greatest. In this series of simulations, the downscaled simulation produces a better representation of the pressure field around Tasmania than the GCM (Figure 5.34d and Figure 5.34e). In the GCM, the westerlies are too strong. The strength of these westerlies has a significant impact on the rainfall over Tasmania.

Downscaling Pressure

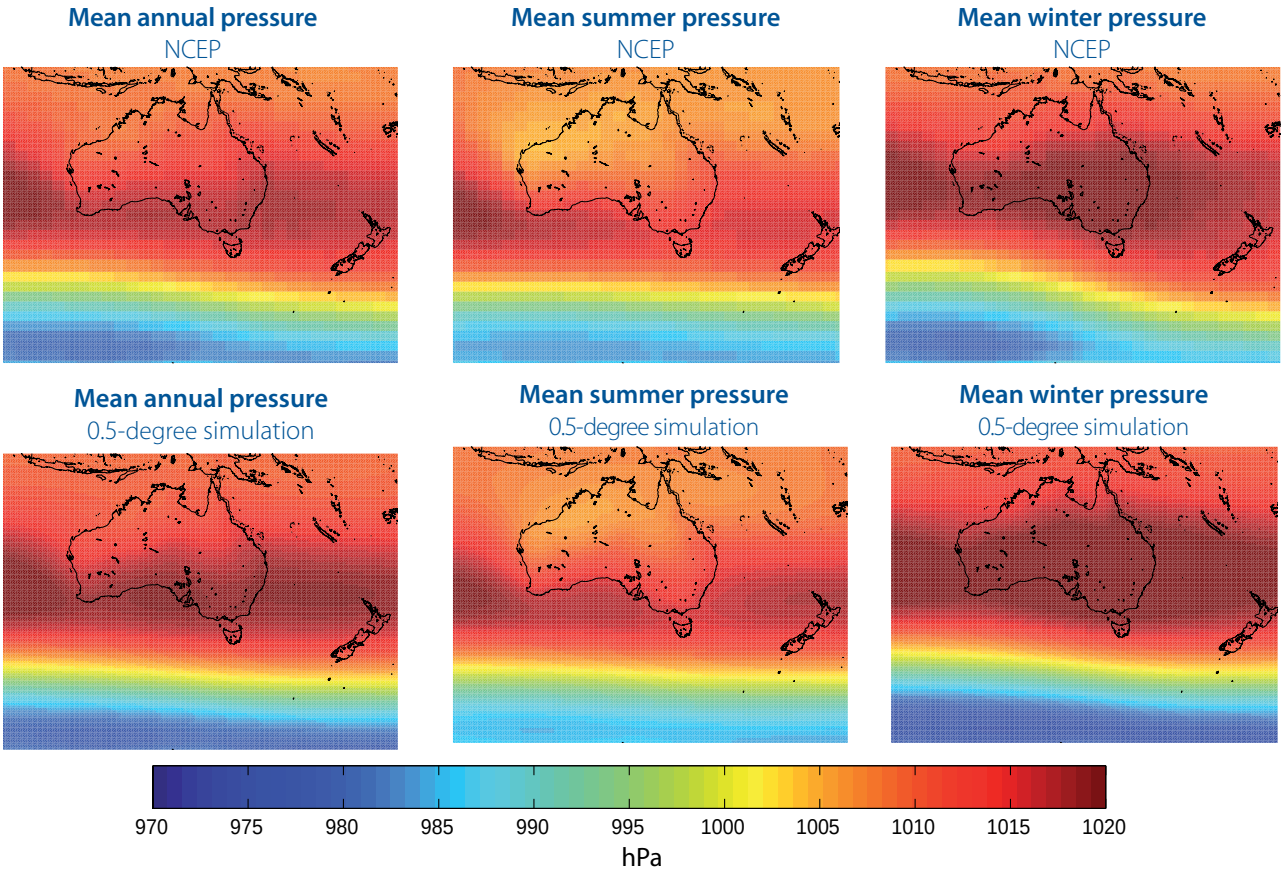

Figure 5.32 Mean pressure fields for the GCM GFDL-CM2.1 (top row) and the corresponding 0.5-degree downscaled simulation (bottom row) for the period 1961-1990. The left column shows the annual pattern, the middle column shows the pattern for the months December to March and the right column the months May to August.

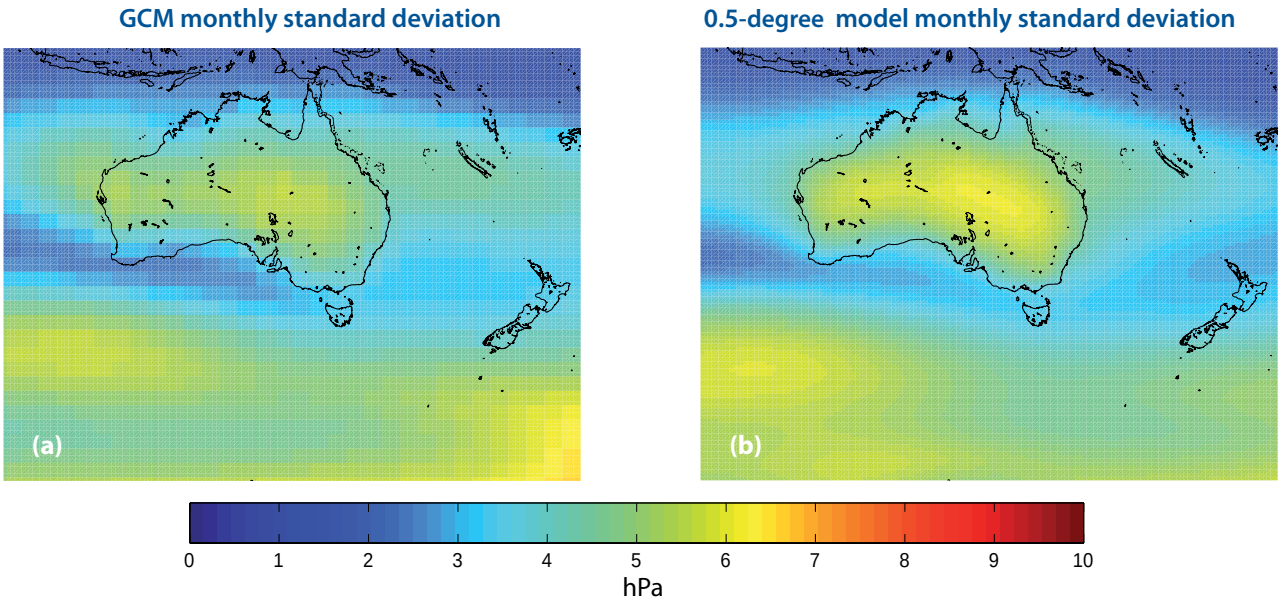

Figure 5.33 Standard deviation in the mean monthly pressure field (hPa) for (a) the GCM GFDL-CM2.1 and (b) the corresponding 0.5-degree downscaled simulation for the period 1961-1990.

Downscaling Pressure

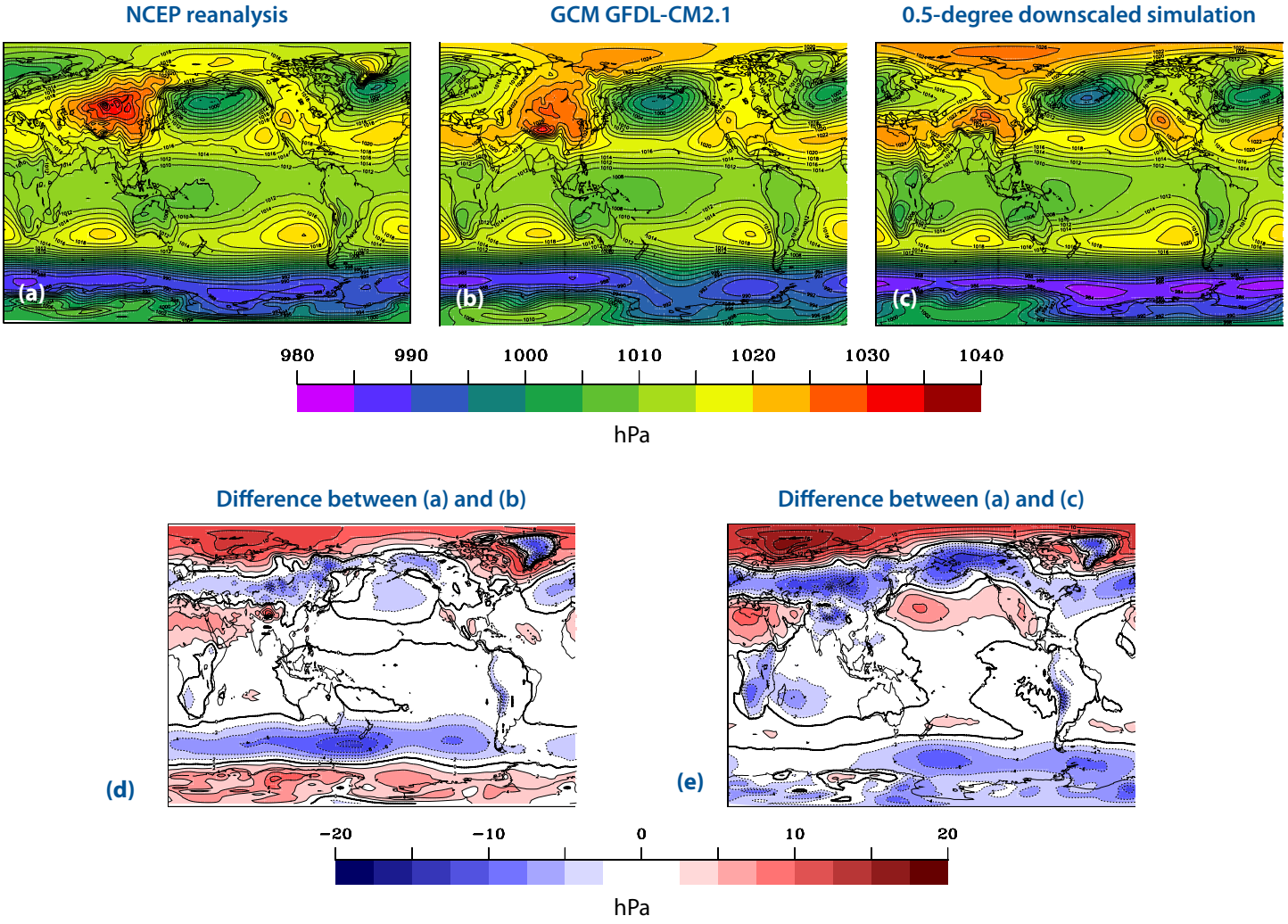

Figure 5.34 Global summer mean-sea-level pressure for (a) NCEP reanalysis, (b) the GCM GFDL-CM2.1 (c) the corresponding 0.5-degree downscaled simulation, (d) difference between NCEP and the GCM GFDL-CM2.1 and (e) difference between NCEP and downscaled simulation. Results shown are for the period 1961-1990.

5.7 Ensemble simulations

Throughout this section, we have shown the capacity of the six-model-mean to simulate Tasmanian climate. Thus far, we have concentrated on the similarities between the six models. Here we examine the degree of variability between the independent 0.1-degree downscaled models.

The six downscaled models considered thus far have been driven by six independent GCMs (all using the A2 SRES emissions scenario). Each of these GCMs has different internal mechanisms driving the model. The different forcing from the GCMs maintains the variability of the GCMs and this variability, reflected particularly in their behaviour of sea surface temperatures (SST) and sea ice, is passed through into CCAM. For the evaluation process, these six models are called the six GCM ensemble. An alternative method for generating variability over the region is to use a single GCM simulation, multiple times, with different initial conditions. In Section 4.2.3, this group of simulations with a single GCM is called the three-member ensemble.

Three independent simulations were undertaken, all using an identically configured version of CSIRO-Mk3.5 for the period 1871-2100. Each simulation started with different, independent initial conditions. Each member of this ensemble was then downscaled through the 0.5-degree model to the 0.1-degree model. This three-member ensemble produces a realistic 30-year climate for Tasmania as illustrated by accurately producing the seasonal difference in Tmin and by the standard deviation of monthly mean Tmin for each season (Figure 5.35). The differences between Figure 5.35 and Figure 5.9 are small, despite this ensemble having half the number of members, all forced from the one GCM.

In each ensemble group, we had three (or six) independent simulations of the Tasmanian climate. The variability between them was assessed by considering each grid cell as follows: for a single variable at each time interval, we calculated the mean value of the variable using the three (or six) simulations of each climate variable. Then the anomalies of each member is computed from this mean. An estimate of the variation of the ensemble was the standard deviation of the set of anomaly values for *every* time interval. For example, the monthly mean maximum temperature (Tmax) of the three-member ensemble for the period 1961-1990, contains 360 mean values (30 years by 12 months) by three (three anomalies from each mean), or 1080 values for each grid point, from which the means and standard deviations were calculated.

For each month in the time series, we calculated the ensemble-mean for Tmax, and then the three (or six) anomalies from this mean. We considered the 1080 (or 2160) Tmax anomaly values as a single set and calculated the standard deviation and mean of this set. The results of this calculation for Tmax for both the six-member ensemble (Figure 5.36a and Figure 5.36b) and the three-member ensemble (Figure 5.36c and Figure 5.36d) show the ensembles produce a very similar mean maximum temperature, but that the six-member ensemble has slightly higher variability across most of the state.

Repeating this calculation for monthly rainfall (Figure 5.37) and monthly maximum meridional (north-south) wind (Figure 5.38) shows that the three-member ensemble has slightly reduced variability in both of these variables compared with the six-model-mean. The variance around the six-model-mean is a measure of the uncertainty of the different GCMs to simulate the climate for the period (1961-1990). This is also a component of the uncertainty in the future climate as well.

Notwithstanding the (unavoidable) difference in ensemble size (six different host GCMs, compared to three initialisations of CSIRO-Mk3.5), this analysis suggests that the differences between downscaled host GCMs is larger than the differences due to internal variability of CSIRO-Mk3.5 (as measured by the spread of the single model three-member ensemble). We have shown that the spread in climate simulations due to model difference is more important than the spread in climate simulations due to model initialisation. That is we have shown that the between-model differences are larger than initialisation differences.

Seasonal Differences in Minimum Temperature

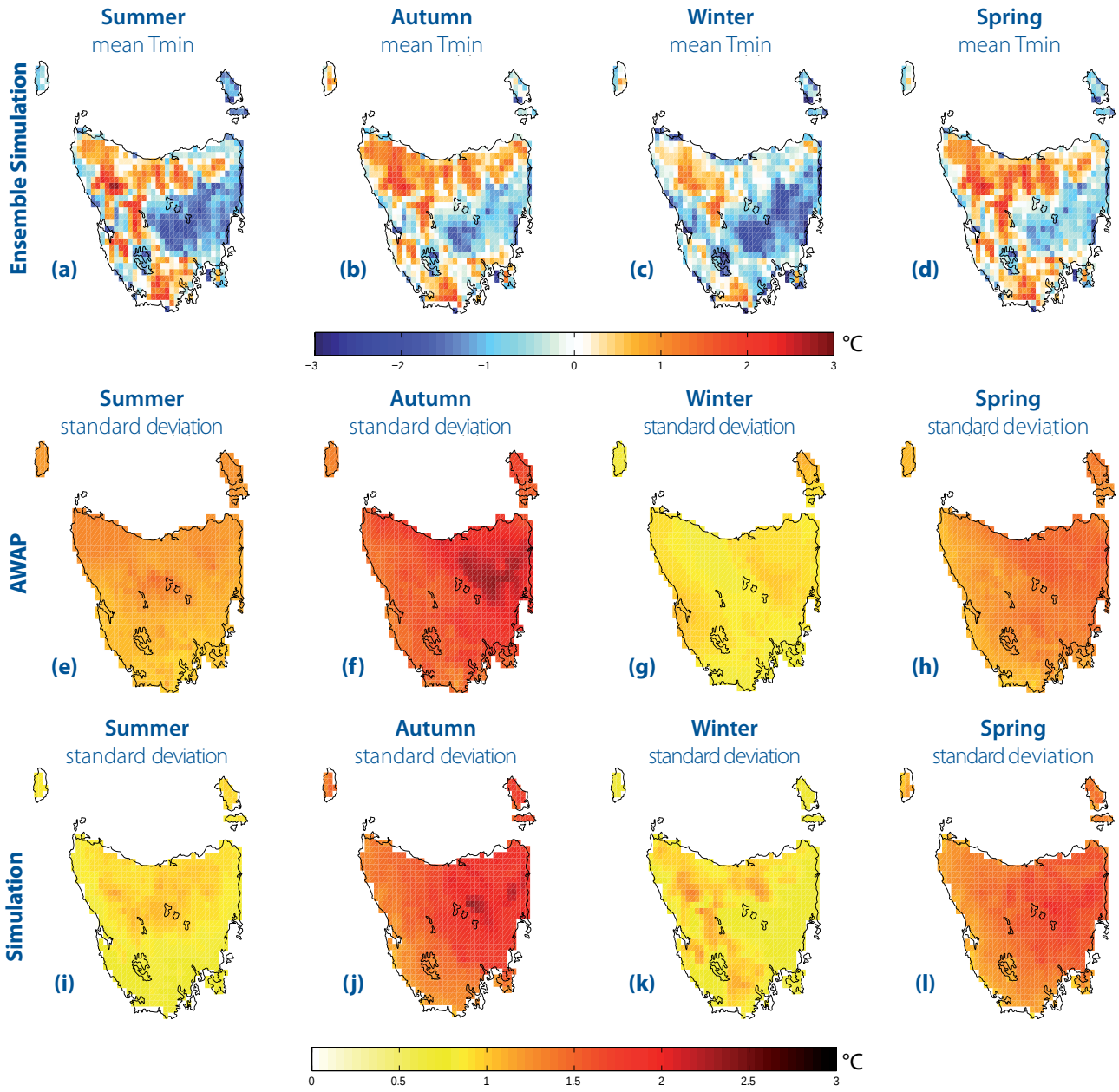

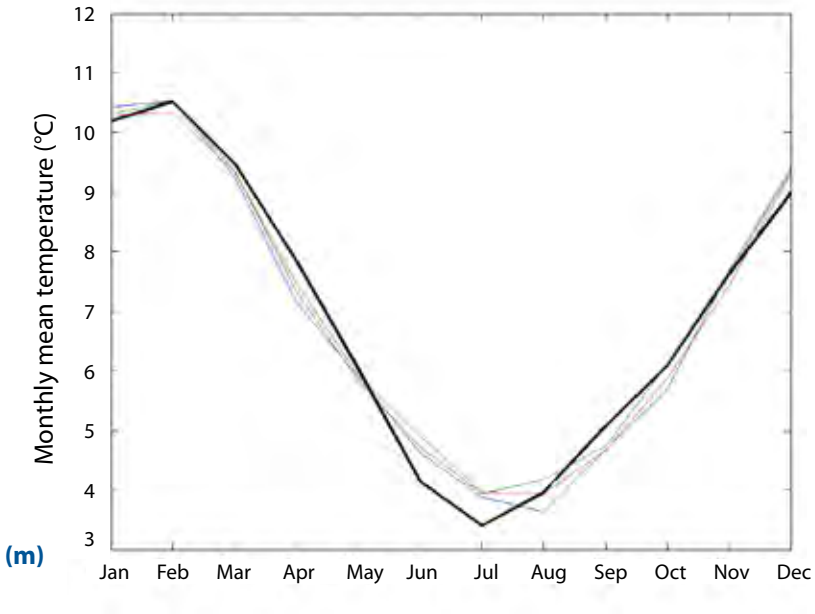

Figure 5.35

Seasonal differences between AWAP and the three-model ensemble-mean for daily minimum temperature for the period 1961-1990. The variances are calculated using the monthly mean for each season. The bottom figure (m) shows the monthly statewide mean daily minimum temperature for each model (coloured) and for AWAP (black line).

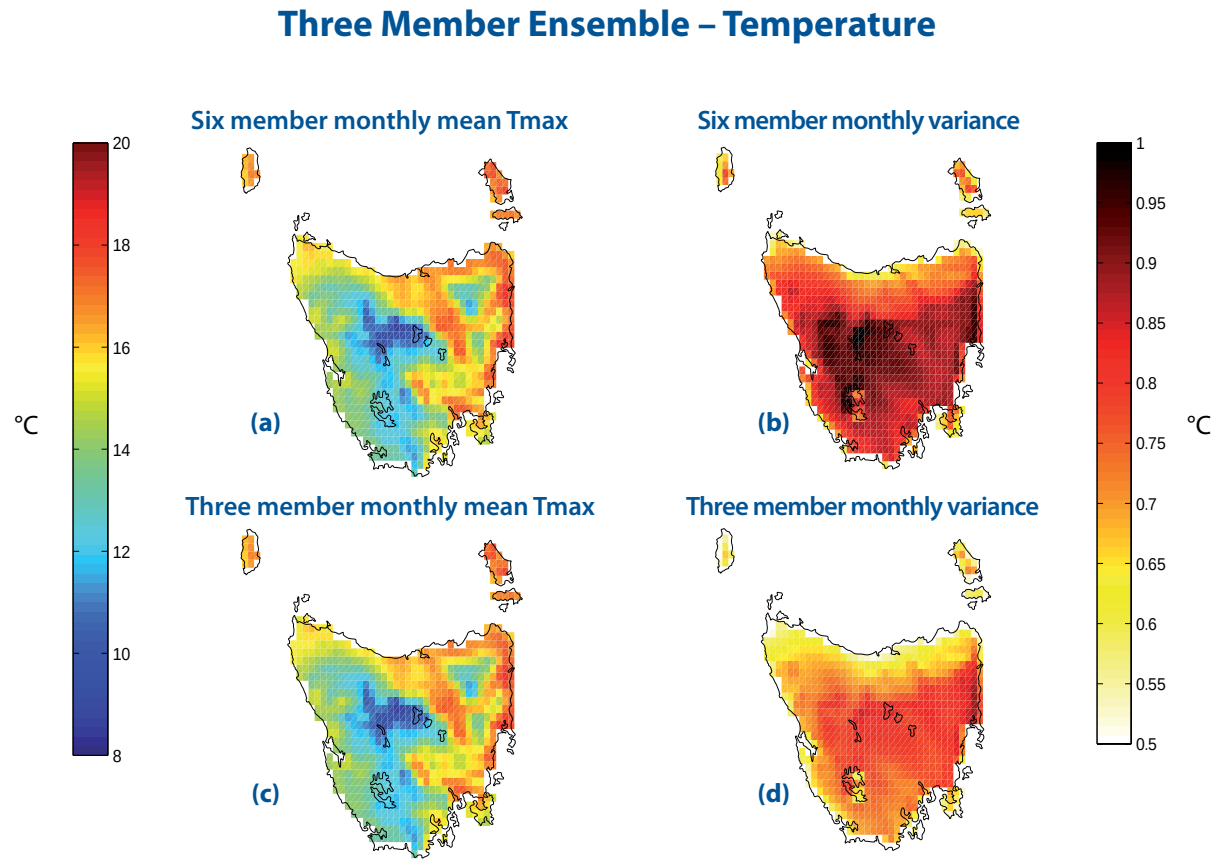

Figure 5.36 Mean (left column) and variability (right column) of mean monthly daily maximum temperature in the six-member ensemble (different GCMs) and three-member ensemble for the period 1961-1990.

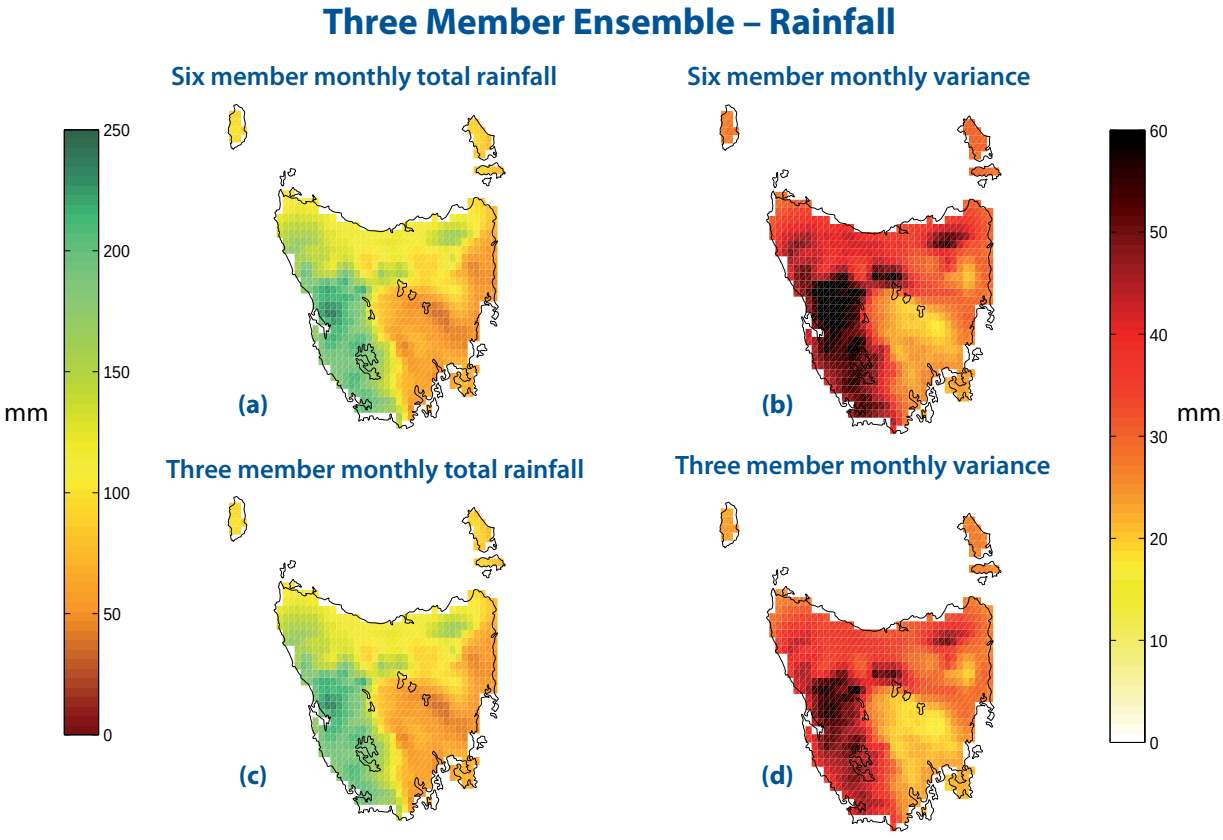

Figure 5.37 Mean and variability of monthly rainfall in the six-member ensemble and three-member ensemble for the period 1961-1990.

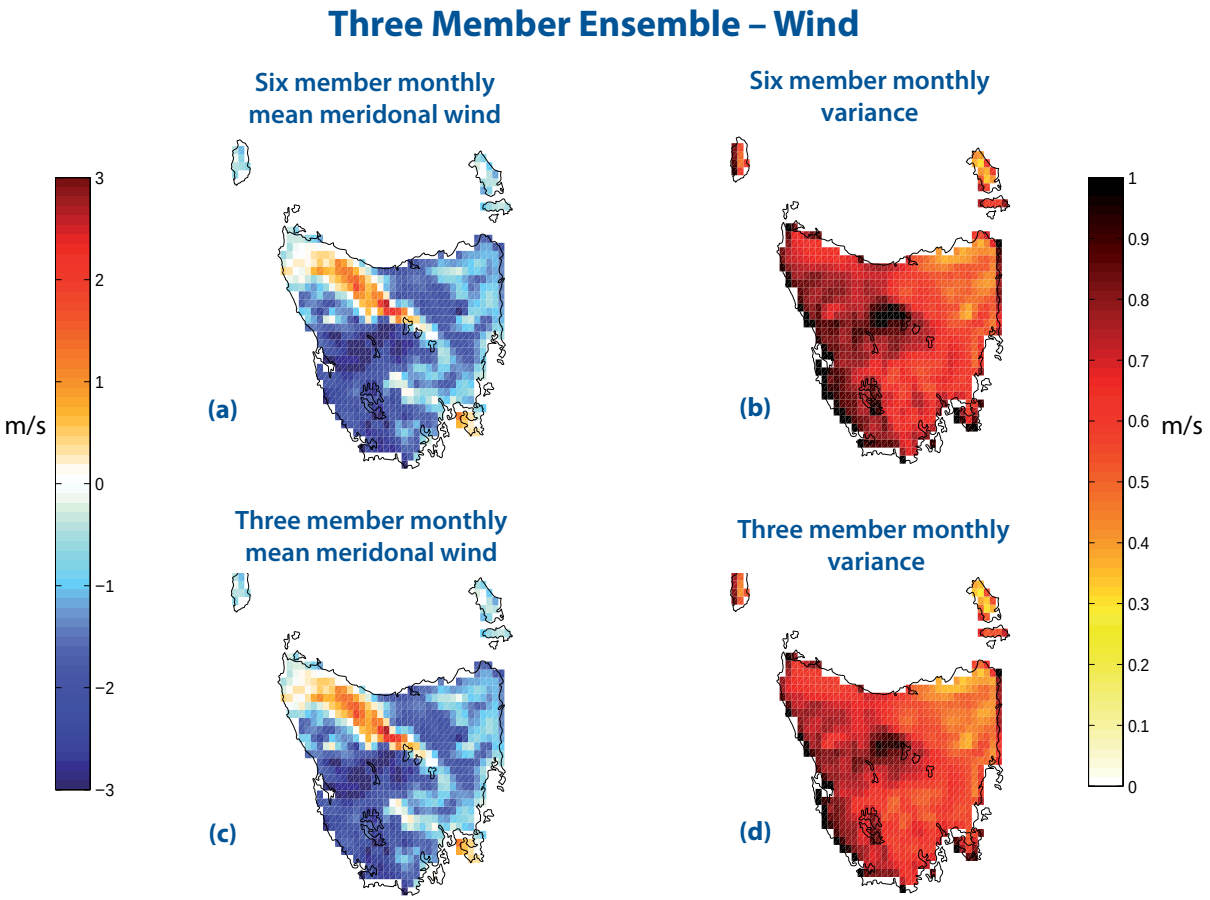

Figure 5.38 Mean and variability of monthly maximum meridional wind in the six-member-ensemble and three-member ensemble for the period 1961-1990.

5.8 High resolution (0.05-degree) simulation

A high-resolution 0.05-degree simulation was undertaken using the CSIRO-Mk3.5, A2 emissions scenario as the host GCM. As explained in Section 3, there were two reasons for undertaking the 0.05-degree simulation:

1. to produce a simulation at the same resolution as the AWAP and SILO gridded data (both are published at 0.05-degree), and

2. to determine if the large bias in rainfall in the northern midlands region was created by topographic effects and therefore reduced by increasing resolution.

The high-resolution 0.05-degree simulation gave an annual rainfall pattern broadly consistent with the 0.1-degree model and with the AWAP data (Figure 5.39). This simulation showed a higher spatial variability that is consistent with the increased resolution. Notably the region inland of the west coast is wetter, as is the Ben Lomond region of the north-east. Both of these regions have steep mountain ranges that are not well resolved in the 0.1-degree model.

Both the 0.1-degree model and the 0.05-degree model were spectrally nudged from the 0.5-degree model using the surface pressure, temperature, atmospheric moisture and wind above 850 hPa.

The exact location of a rainfall event is largely dependent on local orography, particularly in high-resolution models. Figure 5.40 shows the temporal correlation of monthly rainfall between the 0.1-degree and 0.05-degree models. The high correlation in the north and west shows that this area is dominated by seasonal rainfall cycles. However, in the east the correlation is less, possibly demonstrating that orography, or atmospheric convection, is having a significant effect on how and when rainfall occurs in this region.

The difference between the AWAP data and the six-model-mean rainfall on a seasonal and annual basis is displayed in Figure 5.41. The six-model-mean over-estimated rain in the Tamar Valley and northern midlands regions as much as 100% and under-estimated rainfall in other regions by around 50%. Each of the models in the six-model-mean displayed this same pattern of rainfall when compared to the gridded AWAP data (Figure 5.12). These differences in rainfall improved when the 0.05-degree model is compared in the same manner against the AWAP data (Figure 5.41) and with little adverse effects elsewhere across the state. The over-estimate of rainfall in the Tamar Valley/upper midlands region decreased from 100% to 50% in the 0.05-degree model, while in the mountainous regions in the west of the state the rainfall increased by close to 50% along ridgelines that were not resolved in the 0.1-degree model. Rainfall in the Derwent Valley, over-estimated in the 0.1-degree model, is also improved in the 0.05-degree simulation.

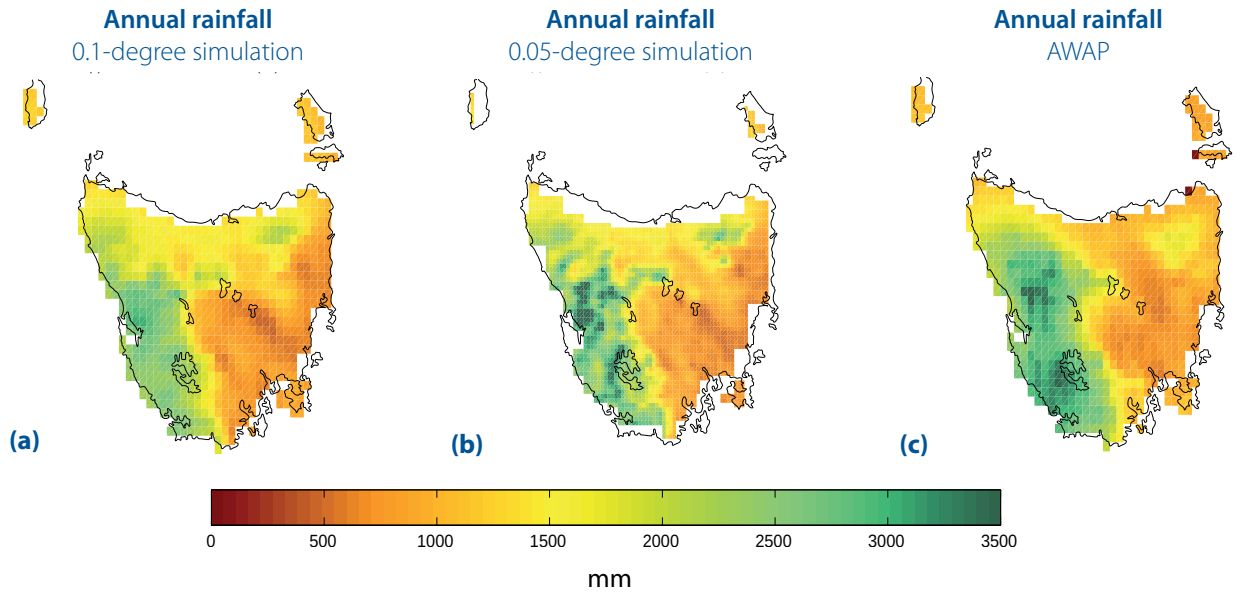

Figure 5.39 Annual rainfall for (a) the 0.1-degree simulation (b) the 0.05-degree simulation and (c) AWAP for the period 1961-1990 (using CSIRO-Mk3.5 as the host GCM).

Screen temperature was also altered by the increase in model resolution. However, the impact of orography is weaker on temperature and was not as affected by the lower resolution of the 0.1-degree model topography of Tasmania. The mean annual maximum temperature for the 0.05-degree model was very similar to the 0.1-degree model (Figure 5.42), and both were similar to the AWAP data (spatial correlation for both models is above 0.95). The 0.05-degree simulation shows more spatial variability, consistent with the increased variability in orography of the higher resolution model. The temporal correlation between the two resolutions was exceptionally high, close to 0.99 across the state. Unlike rainfall, the changes in percentage difference between the AWAP data and the two models is relatively small and appear to coincide with the changes in orography (figures not shown).

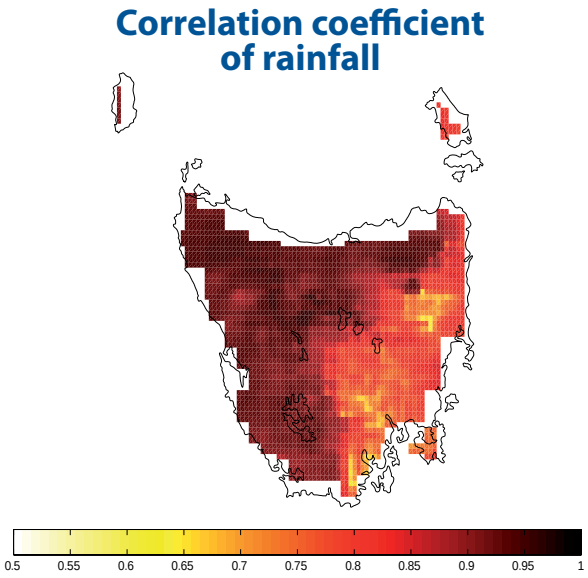

Figure 5.40 Temporal correlation of monthly rainfall between the 0.1-degree and 0.05-degree simulations for the period 1961-1990.

In summary, the increase in resolution has affected the distribution of rainfall across the state and improved the simulation when compared with rainfall calculated from the AWAP data. It does not have as large effect on the daily maximum temperature, except for regions where the increased resolution resulted in noticeable changes in altitude. This is consistent with our argument that differences between the six-model-mean and the AWAP data are largely due to the lower resolution topography in the downscaling of Tasmania. It is clear that in the Tasmanian region increased resolution of the topography yields even better simulations of rainfall and temperature.

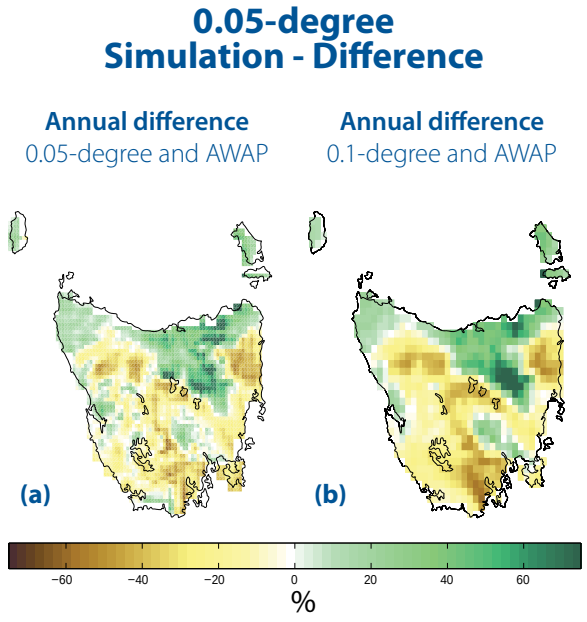

Figure 5.41 The annual percentage difference in total rainfall between AWAP and (a) the 0.05-degree simulation (b) the 0.1-degree simulation for the period 1961-1990.

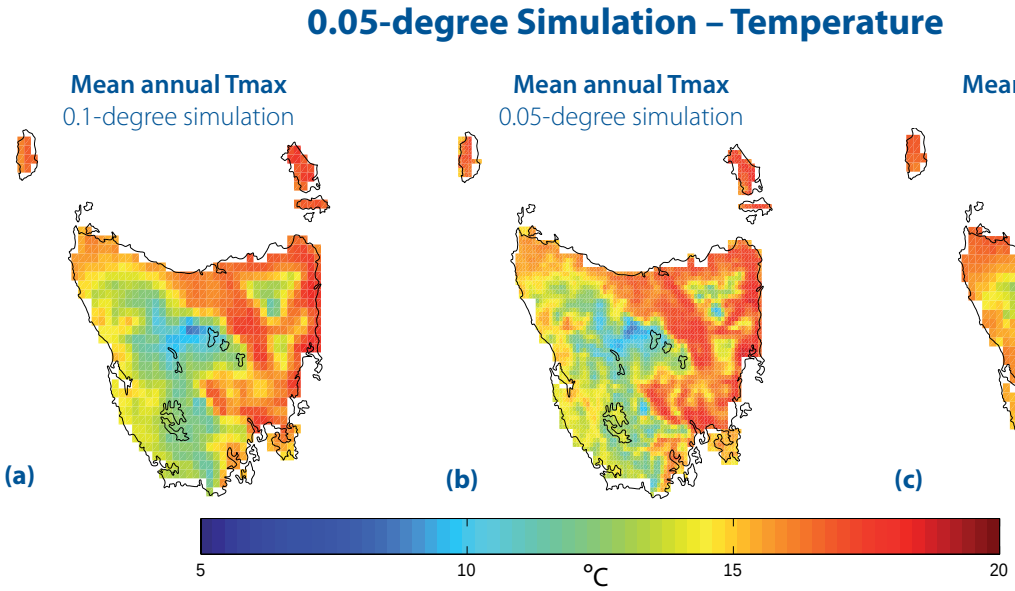

Figure 5.42 Mean maximum daily temperature (°C) for (a) the 0.1-degree model (b) the 0.05-degree model and (c) AWAP, for the period 1961-1990 (using CSIRO-Mk3.5).

6 Bias-adjustment

In the previous section, we demonstrated the skill of the Climate Futures for Tasmania simulations at reproducing the current climate. While the simulations displayed a high level of skill in most variables, at most locations, when compared to the AWAP data, there were some systematic biases. For reporting trends in the climate, and for most applications that require climate modelling output as input, the small biases in the projected climate simulations will not adversely affect the resulting projections. However, some applications exist, particularly in agriculture (Holz et al 2010) and hydrological modelling (Bennett et al 2010), that could result in biased estimates of future change. For example, an agricultural cropping model might 'know' that a certain species of grass will dramatically reduce growth above 28 °C. If our climate simulations have a cold/warm bias in a certain region, so that temperatures are slightly over or under-estimated, then a bias in estimates of the current rate of growth of grass is carried through when reporting on future changes to cropping in this region. For these applications, most dynamical downscaling climate simulations (including our project simulations) need to be bias-adjusted (Boe et al 2007; Wood et al 2004) so that the input for these models correctly simulates the current climate.

Two types of error exist in the Climate Futures for Tasmania climate simulations (and all dynamical models): stochastic (random) error and systematic error. All models have some level of stochastic error (also called noise), two examples of such error in a climate model is a lack of numerical precision in the model and errors in the parameterisation of physical processes in the host GCMs. Our approach of using an ensemble of simulations allows us to make some estimate of the stochastic error. The use of the six-model-mean decreases the effects of these types of errors by averaging over the simulations and thus reducing the error from each host GCM. In contrast, a systematic error (or bias) is a consistent error which can be caused by, for example, the lack of resolution of the spatial grid in accurately simulating a physical process. For example, the 0.1-degree model has grid cells that are roughly 10 km across. Within each grid cell all variables have a single value, thus the orography of the entire 10 km square grid cell is represented by a single height. If the area represented by this cell contains a mountain peak then the model may consistently under-calculate the rain that falls in this cell.

Two methods are commonly used to account for any biases inherent in climate models. The first (and

most common) is to use an historically observed dataset for a given climate variable and add the average change in the variable between the current and future simulated climate. This method is straightforward to apply; for example, we may shift the daily maximum temperature reported in the simulations by a fixed amount, say 2.8 °C, to better match observed records. This ensures that future climate simulations behave in a similar way to the current climate, but bears the signature of climate change. A significant disadvantage of this method is that it restricts the changes that can take place in such things as seasonality, or changes to frequency of extreme weather events. The second method is to use a bias-adjustment process to ensure the current model climate matches the observations over the entire probability distribution, and then apply this adjustment in each quantile of the probability distribution into the future period. This method is more complex, but has the benefit of preserving any changes to the distribution projected by the climate models. We have developed a bias-adjustment process based on the second method.

In most previous studies where climate simulations have been used as input to application models, such as stream flow models, an anomaly of perturbed historical datasets have been used (see for example the Sustainable Yields projects from CSIRO at www.csiro.au/partnerships/SYP.html). The decision by Climate Futures for Tasmania to directly use bias-adjusted simulations is a significant step forward in this area of research. The results of the bias-adjusted fields are reported in the Impacts on Agriculture Technical Report (Holz et al 2010) and the Water and Catchments Technical Report (Bennett et al 2010).

A bias in simulations is a consistent error and can be accounted for if the cause of the bias is understood, or if appropriate observations are available to allow for a comparison with modelling output. We have used a bias-adjustment process to correct for the systematic error in the 30-year climate in five of the key variables in our simulations: daily maximum screen temperature (Tmaxscr), daily minimum screen temperature (Tminscr), total daily rainfall (rnd24), daily total pan evaporation (epan_ave) and daily total solar radiation (daily_rad). These five variables were chosen as they are key observational variables for many of the applications and processes that will be considered in the four technical reports that address water and catchments, general climate impacts, impacts on agriculture and extreme events (Bennett et al 2010; Grose et al 2010; Holz et al 2010; White et al 2010).

Crucially, bias-adjustment can only be applied if reliable observational data is available, such as the AWAP data. Other variables were considered, including wind/pressure and soil moisture, but were excluded due to lack of available, reliable gridded observational data.

A further assumption in the bias-adjustment is that the cause of the biases is constant throughout the adjustment training period, and thus the required adjustments also remain constant. The bias is calculated by determining the offset between the observation and the simulation for each percentile over the training period 1961-2007. This bias is then assumed to be constant and the offset is applied over the entire simulation (for example, out to 2100). As discussed in Section 5, bias can be caused by a number of factors, including errors in modelled large-scale climate drivers or poor resolution of orography. This section also showed that the mean values of the simulations (of the variables that could be compared) were very close to the mean values from the AWAP data. Section 5.8 showed how increasing the model resolution from 0.1-degree to 0.05-degree removed a substantial part of the difference between the AWAP data and the modelling output. These results support the assertion that a large part of the spatial bias seen in the simulations is caused by the limited resolution of topography across the state. Topography does not vary throughout the simulation period (that is, 1961-2100) and thus a significant portion of the bias is constant.

Separate bias-adjusted simulations were created for each of the 0.1-degree simulations. Only output from the 0.1-degree simulations was bias-adjusted, as these simulations compare most closely with the available 0.05-degree AWAP data. The 0.5-degree simulations were not bias-adjusted as these simulations were primarily produced as an intermediate step to allow downscaling to 0.1-degree. In addition, the bias-adjustment was applied only over Tasmania, and did not include the cells over water or mainland Australia.

The bias-adjusted simulations contained the five bias-adjusted variables listed above, as well as a further ten raw (non-bias-adjusted or unadjusted) variables, included because of their relevance to processes that will be considered in the other technical reports. The full list of variables in the bias-adjusted simulations is in Table 6.1.

Table 6.1 The list of variables contained in the bias-adjusted datasets, indicating those that have been adjusted.

Observational variable (units)	Variable name in simulation	Adjusted or Raw
Maximum daily screen temperature (K)	Tmaxscr	Adjusted
Minimum daily screen temperature (K)	Tminscr	Adjusted
Total daily rainfall (mm)	rnd24	Adjusted
Total daily potential evaporation (mm)	epan_ave	Adjusted
Total daily incident solar radiation (MJ/m^2/day)	daily_rad	Adjusted
Low cloud fraction (%)	cll	Raw
Mid-cloud fraction (%)	clm	Raw
Average daily evaporation (mm)	evap	Raw
Maximum daily precipitation rate in a time step (mm/day)	maxrnd	Raw
Mean sea level pressure (hPa)	psl	Raw
Maximum screen relative humidity (%)	rhmaxscr	Raw
Minimum screen relative humidity (%)	rhminscr	Raw
Zonal (east-west) maximum 10 m wind speed (m/s)	u10max	Raw
Meridional (north-south) maximum 10 m wind speed (m/s)	v10max	Raw
Soil moisture as a fraction of mass of top two levels (%)	wbfshall	Raw

6.1 Bias-adjustment method

Several different techniques for implementing bias-adjustment exist. We employed a percentile-binning method based on the work of Panofsky and Brier (1968) to adjust five key variables (Tmaxscr, Tminscr, rnd24, potential evaporation and solar radiation). This process has also been used by Reichle and Koster (2004), Deque (2007), and notably in dynamical downscaling applications by Boe et al (2007) and Wood et al (2004). The percentile-binning method has an advantage over other bias-adjustment methods, as it does not assume that the offset is constant for all values of the variable being adjusted or even that the distribution of the variable being adjusted is normally distributed about a mean.

The bias-adjustment was carried out on a cell-by-cell basis for each of the land grid cells. The AWAP dataset does not have data for water cells and so no comparison (or adjustment) can be made in these regions. An important consideration when bias-adjusting modelling output is that the act of bias-adjusting can alter the physical relationships between different variables (the dynamical balance). Changes in dynamical balance can be caused when variables are adjusted independently of each other, as is the case here.

Temperature often has an approximately normal distribution of values (Figure 6.1) and so a mean/variance method of bias-adjustment may perform satisfactorily. The regions of the distribution where this is likely to break down are the extremes, both hot and cold. In contrast, daily rainfall is not normally distributed (Figure 6.2), with days of no-rain being common. For daily rainfall, a mean/variance method of bias-adjustment would be inappropriate. To maintain consistency in our approach, we used the percentile-binning approach for the bias-adjustment for all of the five climate variables.

Temperature Distribution

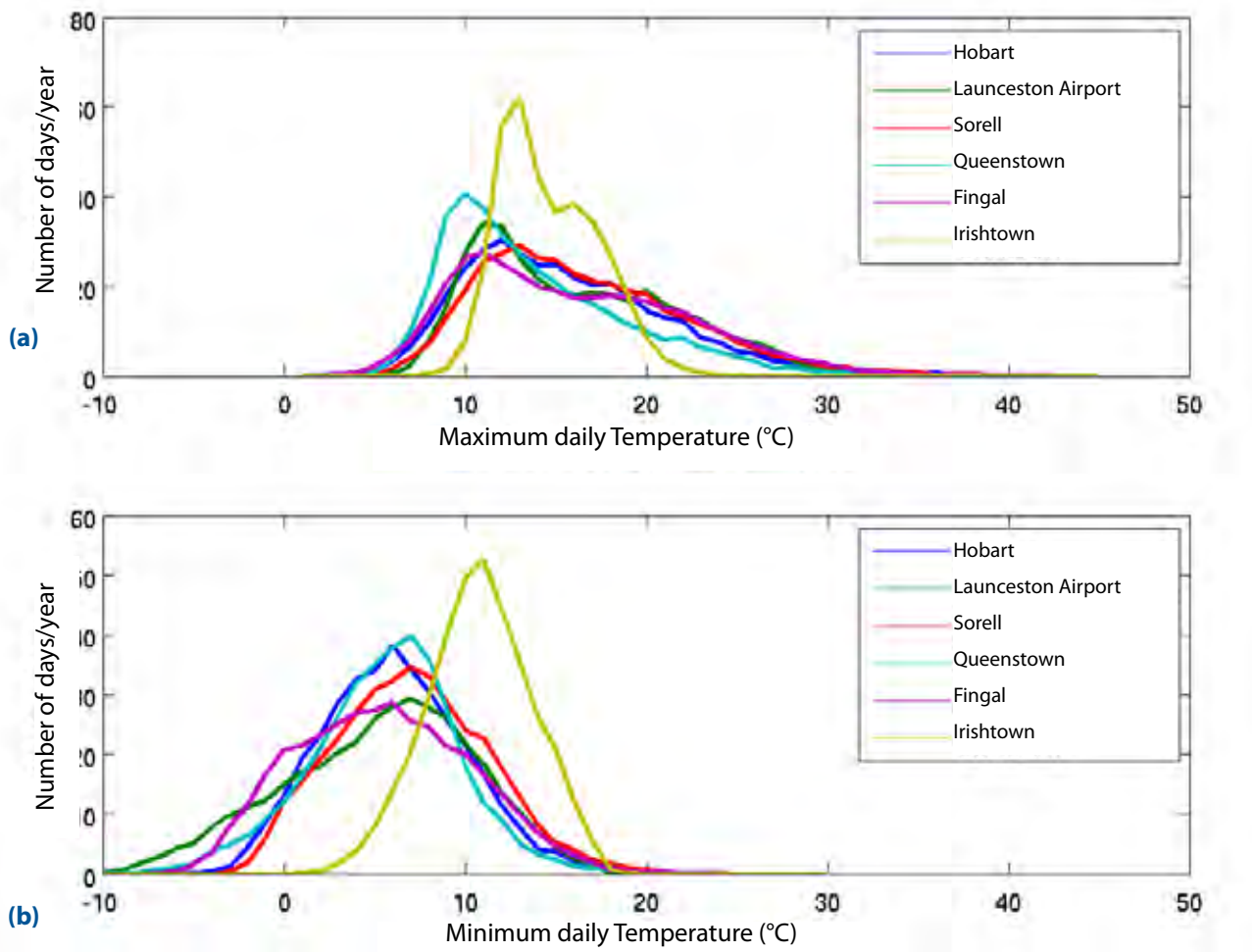

Figure 6.1 Plot of number of days having a given daily (a) maximum or (b) minimum temperature over a 30-year period (1961-1990) for six sites across Tasmania. Note, the approximately normal distribution of the data (using CSIRO-Mk3.5 as the downscaled GCM).

Rainfall Distribution

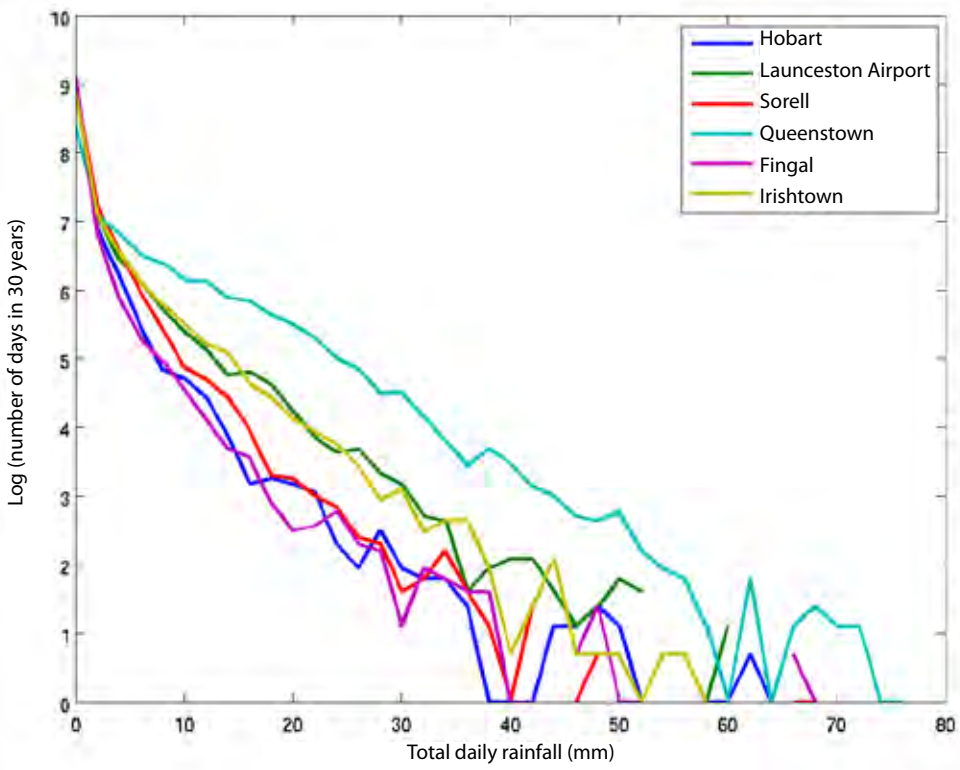

Figure 6.2
Plot of the number of days having a given total daily rainfall over a 30-year period (1961-1990) for six sites across Tasmania. This distribution is certainly not normal, showing something akin to a power law (using CSIRO-Mk3.5 as the downscaled GCM).

The bias-adjustment process can be broken into two stages. The first stage compares the distributions of the modelling output and the AWAP data over the period of time that both datasets exist, and calculates an adjustment factor for each percentile bin. The second stage applies this adjustment factor to each percentile bin over the full 140-year period. Often the highest values of the modelling output are greater than the highest values of the observations. This does not cause problems with this method as every value in the top 1-percentile bin (the 99th-percentile to 100th-percentile bin) is adjusted using the value calculated for this bin.

The overlap between the Climate Futures for Tasmania simulations and the AWAP data is from 01/01/1961 to 31/12/2007; a period of 47 years or 17,155 days. This period forms the overlap period, where we calculate the adjustments made to each percentile bin. For each variable being adjusted both the model and the AWAP data for this period were first detrended using a linear regression to remove effects of any long-term change in the climate (but not to remove the 47-year mean of the modelling output). Each point in the time series was ranked and assigned to a percentile for each simulation. For temperature, the differences between matching bins were stored in a look-up table, while for rainfall the ratios between respective bins were stored. The two different techniques reflect the fact that rainfall has a lower limit of 0 mm and the change in likelihood of a particular quantity of rain scales logarithmically, while temperature has no lower limit, and does not scale logarithmically.

The detrending of the simulations was necessary to ensure that any climate change signal did not affect the percentile rankings. The percentile approach seeks to group together events that were of similar likelihood in their epoch. For example, if there was an increase in mean temperature in the overlap period, then values from later years will be artificially more frequent in the upper percentiles of the Tmax distribution. A 50th-percentile day in the decade 1961-1970 should be grouped with a 50th-percentile day from the decade 1998-2007. It is the relationship between climate drivers, inherent bias and the modelled variable that we are trying to correct, not the exact temperature. Detrending prior to bias-adjustment is even more important in the simulations to 2100, as these have a mean increase in Tmax of approximately 3 °C.

We considered bins with percentile widths of 10 and 5, before deciding on a bin-width of 1-percentile. For the majority of the distribution, the difference between 1-percentile, 5-percentile and 10-percentile bins is small: the magnitude of the adjustments were less than 2 °C. However, at the extremes of the distribution, when the low probability events occur, the difference became marked. When using 10-percentile bins, the final 10% of the distribution undergoes a sizeable change of up to 6 °C (Figure 6.3). If instead we use 5-percentile bins, then only the final 5% of each end of the distribution undergoes this large change (Figure 6.4). Finally, if we use 1-percentile bins, then we can limit the range of the spectrum undergoing adjustments greater than 2 °C to the final 1% (Figure 6.5).

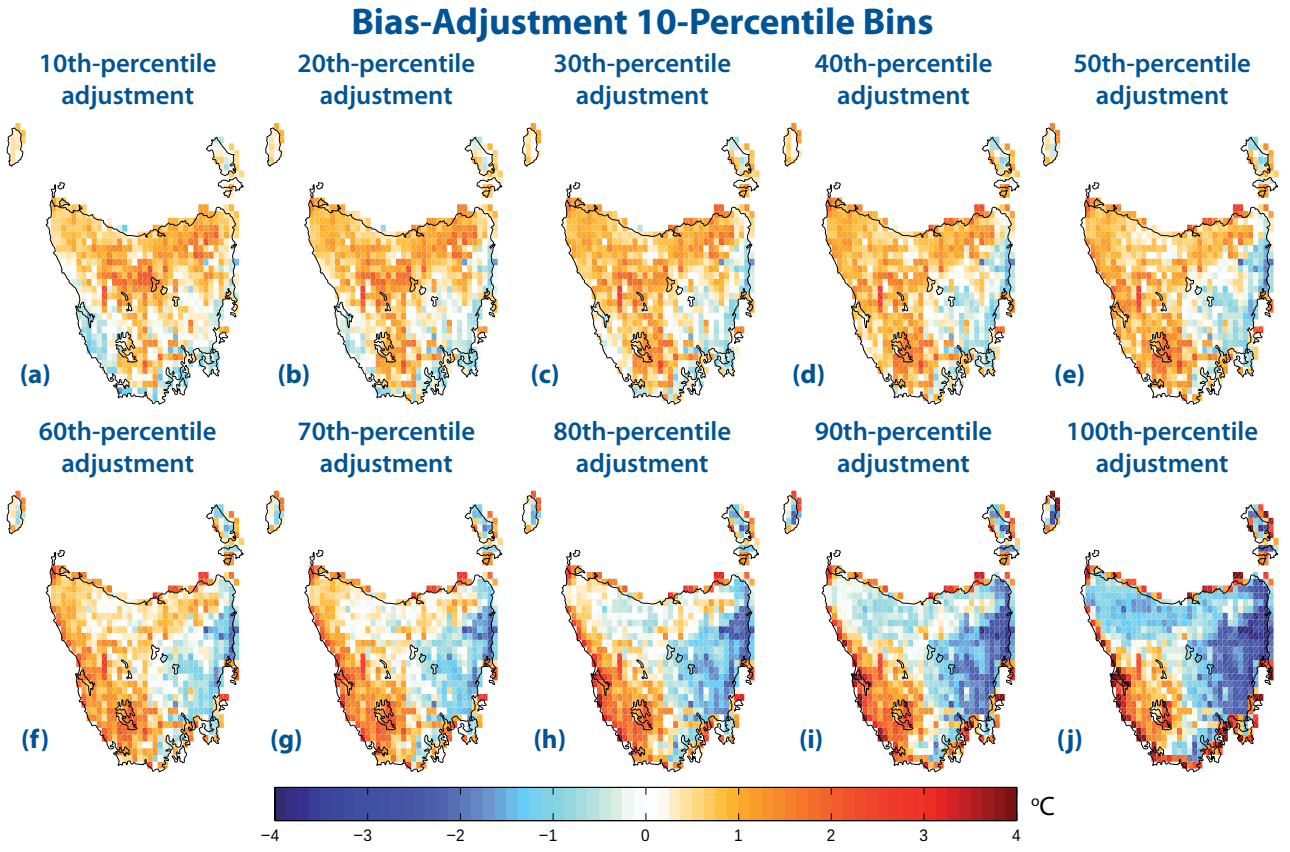

Figure 6.3 The bias-adjustments applied to daily maximum screen temperature for each of the 10-percentile bins for CSIRO-Mk3.5, A2 emissions scenario.

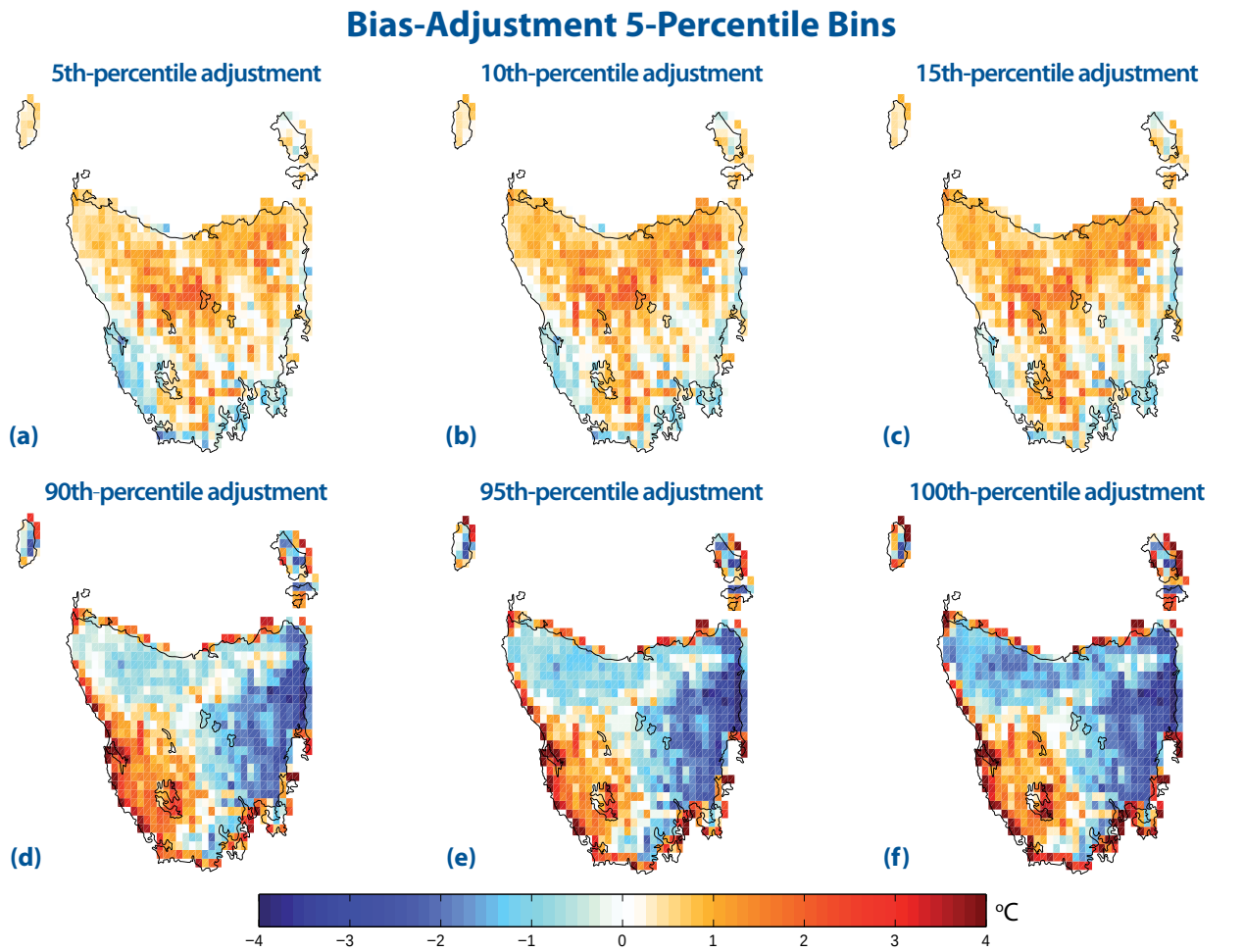

Figure 6.4 The bias-adjustments applied to Tmaxscr for the lowest three (a), (b), (c) and highest three (d), (e) and (f) 5-percentile bins for CSIRO-Mk3.5, A2 emissions scenario.

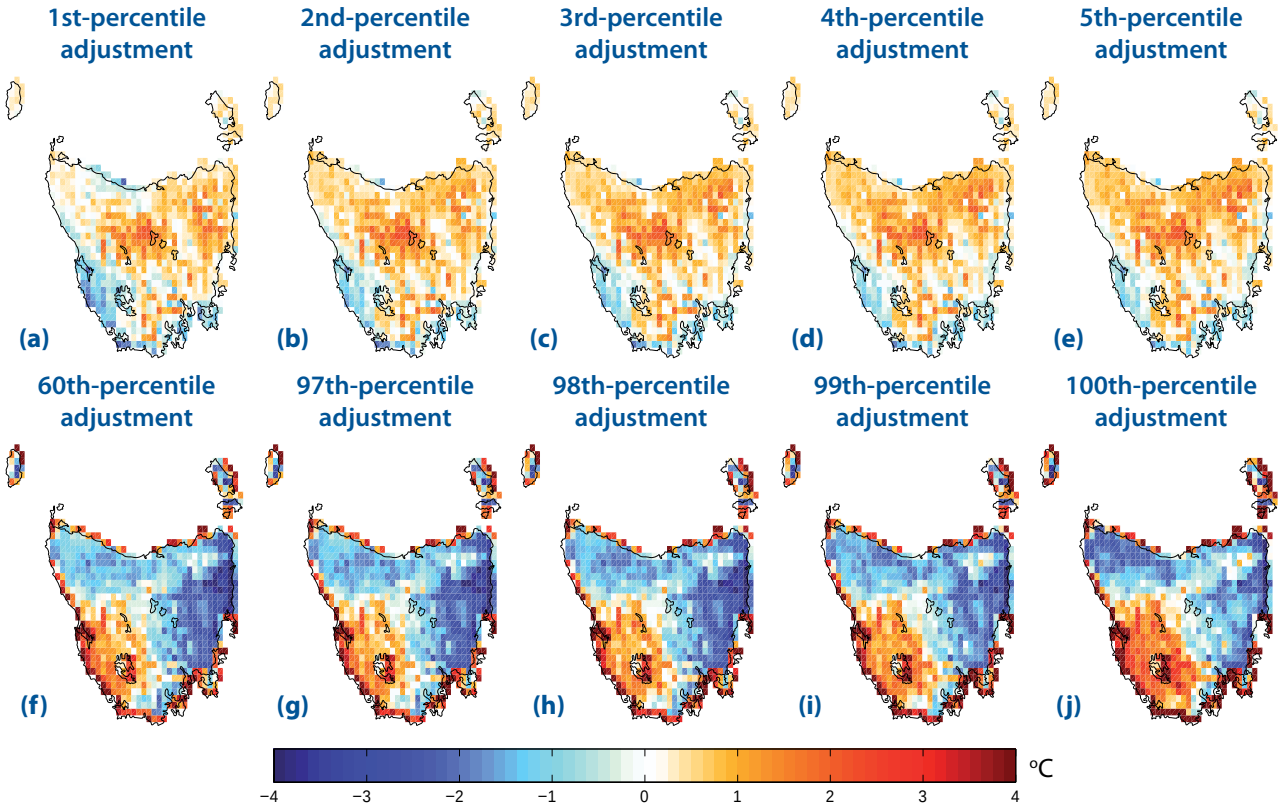

Figure 6.5 The bias-adjustments applied to Tmaxscr for the lowest five (a) - (e) and highest five (f) - (j) 1-percentile bins for CSIRO-Mk3.5, A2 emissions scenario.

Given the importance of extreme events to the project and climate change studies in general, it was important to get the tail of the distributions as accurate as possible. Adjusting the top and bottom 10% of each distribution as one group by up to 6 °C was too coarse to accurately model the extreme events in each variable, and thus in order to do a better estimate of the extremes of each distribution we used 1-percentile bins for the adjustment process. In order to simplify calculations we use 1-percentile bins for the entire distribution. For the majority of the range, the choice of bin size makes little difference, but at the tails of the distribution, the 1-percentile bins behave quite differently from the 5-percentile and 10-percentile bins, justifying our choice of bin size (Figure 6.6). Choosing a bin size of smaller than 1% leads to problems with over-correcting the simulations and having insufficient points in each bin to accurately calculate the adjustment.

Once the bias-adjustment for each percentile bin was calculated from the reference period it was then applied to the full 140-year dataset. Note that having calculated the adjustment using the 47 years of the AWAP data and the first 47 years of the simulation, the 140 years (including the 47-year overlap period) was treated as a single dataset. The adjustments were applied to the simulation using percentiles based on the distribution from the entire 140-year period. The result of this decision is that the modelling output from the first 47 years is not constrained to be exactly like the AWAP data and include the underlying trends on the projections during the overlap period. This allows comparisons in the reference period between the AWAP data and the simulations to provide a check on the effectiveness of the adjustment process.

The adjustments were applied to the time series in the simulations by assigning each modelled daily value to its percentile and then adding (or multiplying for rainfall) the adjustment according to the 47-year overlap period. For temperature, we expect a strong trend in the simulations, and thus it is necessary to remove this trend (the climate change signal) before calculating the percentiles in order to prevent an unrealistic proportion of the high percentile days occurring later in the modelling period. This was done by calculating a 30-year running mean for each of the 140 years of modelling output in the time series, and removing this value from each one-year block of modelling output. For simplicity, we applied the same detrending process to the rainfall. This was done by calculating a 30-year running mean for each of the 140 years of modelling output in the time series. Each day was ranked and the appropriate percentile assigned using this de-trended time series, however the corresponding adjustment was carried out on the original time series (with the trend included).

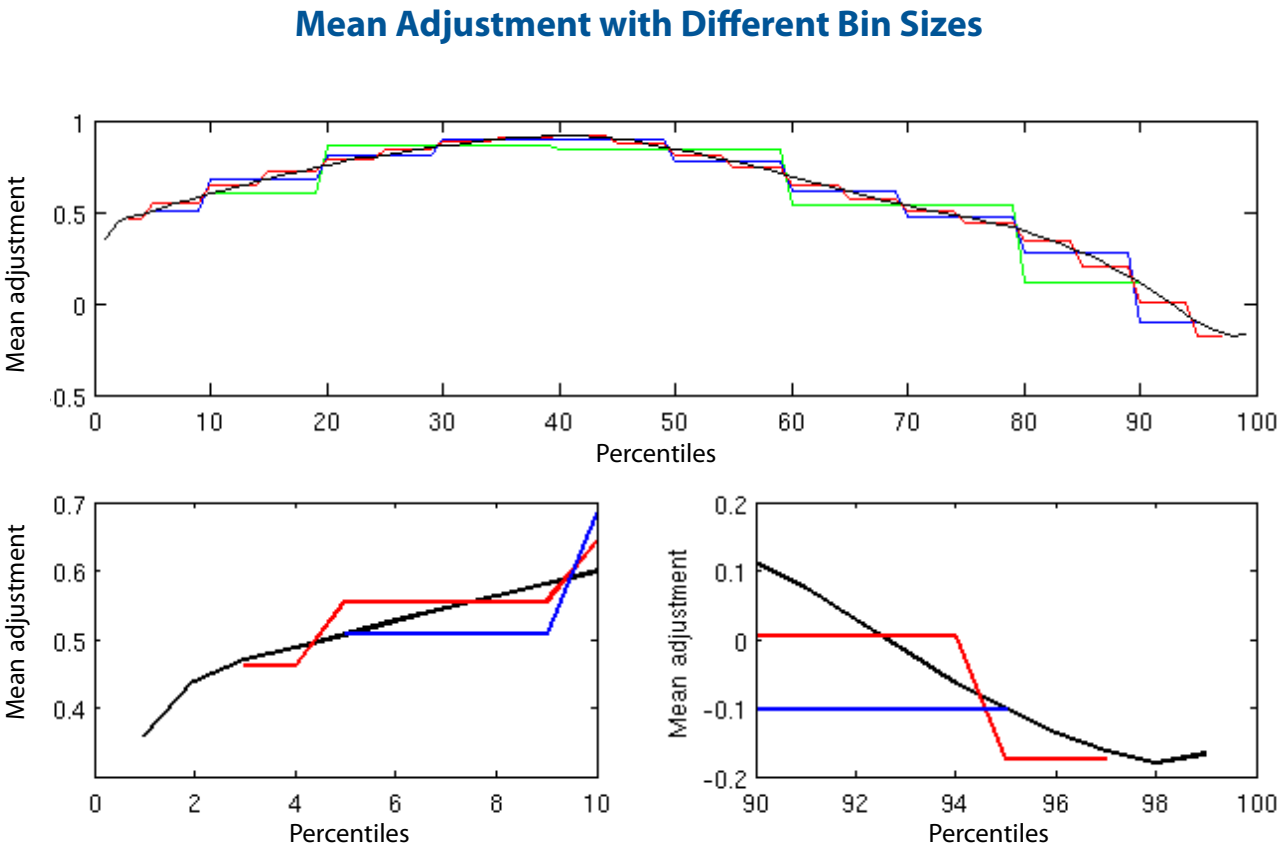

Figure 6.6 The statewide mean bias-adjustment of daily maximum screen temperature for the downscaled CSIRO-Mk3.5 simulation (A2 emissions scenario) when using 1-percentile (black), 5-percentile (red), 10th-percentile (blue) and 20th-percentile (green) bins.

The final stage of the process was to choose whether to apply the adjustment annually, seasonally, monthly or to some other time period. If we calculate the adjustment annually, then we include all 47 by 365 days of output in the overlap period, and 140 by 365 days of modelling output in the full period. With this method, summer days are far more likely to occur at the top of the distribution than winter days, and autumn and spring days are likely to occur in the middle of the distribution. This method was unsatisfactory as it resulted in a process where unusually hot winter days were treated similarly to cold or average summer days. Maximum temperature of above 20 °C on a winter day may not be driven by the same climate drivers as a summer day of the same maximum temperature, and thus should not be adjusted the same way. Further, autumn and spring days almost all fell in the middle of the distribution.

Alternatively we could choose to calculate the adjustment on a monthly, or even weekly basis. For either of these options, the problems described above should not be an issue, but other problems arise. Firstly, there are far fewer days available for calculating the adjustments. For the adjustment process to be effective, we needed the full range of possible values of each variable to occur in the calculation period. This would certainly be an issue if using a weekly adjustment period. The second issue is the number of boundaries between adjustment periods. When using monthly adjustment periods there are twelve boundaries each year (when the calculated adjustments change from one period to another). The more adjustment boundaries the greater the likelihood of having artificial discontinuities occurring in the simulation time series.

Adjusting seasonally solves these problems and becomes a safe middle ground between annual and monthly time periods. Using the current seasons should ensure that days of similar temperature (or rainfall, radiation et cetera) are driven by the same processes. A limitation of seasonal adjustment is that it assumes that the different behaviour of the climate in the different seasons is constant in a changed climate. Changes in the timing and frequency of events (particularly rainfall) are a key component of the project and this may be affected by the adjustments on a seasonal basis. With seasonal adjustment periods we also limit the number of boundaries to only four per year, and ensure that we have at least 47 by 90 days to use in the estimating of the adjustments for each season.

As seasonality, and importantly change in seasonality, is a key component of the project, it is desirable to resolve the seasons and their corresponding bias-adjustment. We investigated the effects of bias-adjustment on a seasonal, monthly and annual basis. This investigation confirmed that seasonal adjustments gave good results in terms of the issues described above.

Applying the adjustments on a seasonal basis involves running the adjustment process four times for each simulation and thus considers 47 summers, 47 autumns et cetera from the 1961-2007 overlap period. Applying the adjustments on any interval less than annual results in a discontinuity between the seasons, that is a day where 50 mm of rain fell in late February (the end of summer) will be treated differently from a day with the same rain in early March. This situation is unavoidable and the problem potentially increases with increasing number of sub-annual divisions. By choosing seasonal adjustments, we have struck a balance between the number of boundaries and accuracy of the adjustments. Adjusting on a monthly basis is also possible, but this would have resulted in far fewer values to provide a robust estimate of the correction function and three times more boundaries to potentially cause subtle discontinuities in the adjusted simulations.

The process as outlined above uses the entire observational period to calculate the adjustments. This maximised the overlap period for calculating the adjustments, however it does not leave any observational data that has not been used in the adjustment process for checking the similarity between the adjusted simulation and observational data. In order to give confidence in the bias-adjustment process, we ran the bias-adjustment process once using the years 1971-2007 as the overlap period, holding back the period 1961-1970. We then compared the bias-adjusted modelling output to the AWAP data for the 'held-back' decade. The results of this analysis can be seen in Section 6.2, specifically Figure 6.15 and Figure 6.16. Further validation of the bias-adjustment process is included in the Water and Catchments Technical Report (Bennett et al 2010).

6.2 Bias-adjustment sample results

The results presented in this subsection illustrate the bias-adjustment process just described. As the bias-adjustment process operates in the same manner on each model, we have chosen to demonstrate the results for each variable from a single model (but change the model displayed with each variable). Further validation of the bias-adjustment of the project modelling output can be seen in the Impacts on Agricultural Technical Report (Holz et al 2010) and the Water and Catchments Technical Report (Bennett et al 2010). It is important to note that we are not seeking to validate the concept of bias-adjustment in this report. We are demonstrating a method to correct small errors and bias in the simulation that can be corrected (when compared to gridded observations) and apply this correction for the entire simulation from 1961 to 2100. We also demonstrate that the bias-adjustment process presented in this report does correct deficiencies in the model (against the gridded observations).

The bias-adjustment process changes the histogram

of rainfall for the recent past, where the AWAP data is available for comparison, and in the future (see Figure 6.7). On the west coast, at Strahan, the 0.1-degree downscaled model of GFDL-CM2.1 over-estimated the rainfall compared to the AWAP data (Figure 6.7a), and at Hobart (in the south-east) the model under-estimated it (Figure 6.7c). The bias-adjustment process correctly changed the distributions to match more closely the AWAP data. For the period from 2070 to 2099, the shape of the histogram changed for both sites, but the change seen to the adjusted simulations is consistent with that from the recent past. This gives us confidence that the bias-adjusted simulations for the future period more accurately model the likely future rainfall, that is, the bias-adjustment process remains valid into the future. All of the subsequent figures featuring rainfall are produced using the downscaled 0.1-degree model with the GFDL-CM2.1, A2 emissions scenario GCM as host.

The capacity of the bias-adjustment process to correct the spatial pattern of the model to match more closely the AWAP data for rainfall is demonstrated in Figure 6.8 through to Figure 6.12, and summarised in Table 6.2. For each of the four seasons, as well as annually, the bias-adjustment process removed the observed seasonal biases in rainfall of up to 50% in some areas. The spatial correlation between the model and the AWAP data increases from between 0.8 and 0.87 for unadjusted modelling output, to 0.99 when using bias-adjusted modelling output. Recall that the 47 years of modelling output in the overlap period between the simulation and the AWAP data were adjusted as part of the 140-year adjustment process and thus are not constrained to behave exactly like the AWAP data. This is different to adjusting the 47 years of modelling output using only the 47-year period. In this case, the adjusted simulation is forced to look exactly like the AWAP data. By treating the initial 47 years as part of the 140-year whole, we can compare the 47-year period to the AWAP data to check the effectiveness of the adjustment process.

The very strong temporal correlation that exists between the unadjusted and adjusted simulations on a daily basis, both in the recent past and period 2070-2099 (Figure 6.13), shows that the bias-adjustment process is having a consistent effect. This indicates that the bias-adjustment process is not significantly changing the daily values or variance at each cell, that is the hot days remain hot, the cold days remain cold, et cetera. Anything less than a high correlation between the unadjusted and adjusted simulations would be a cause for concern.

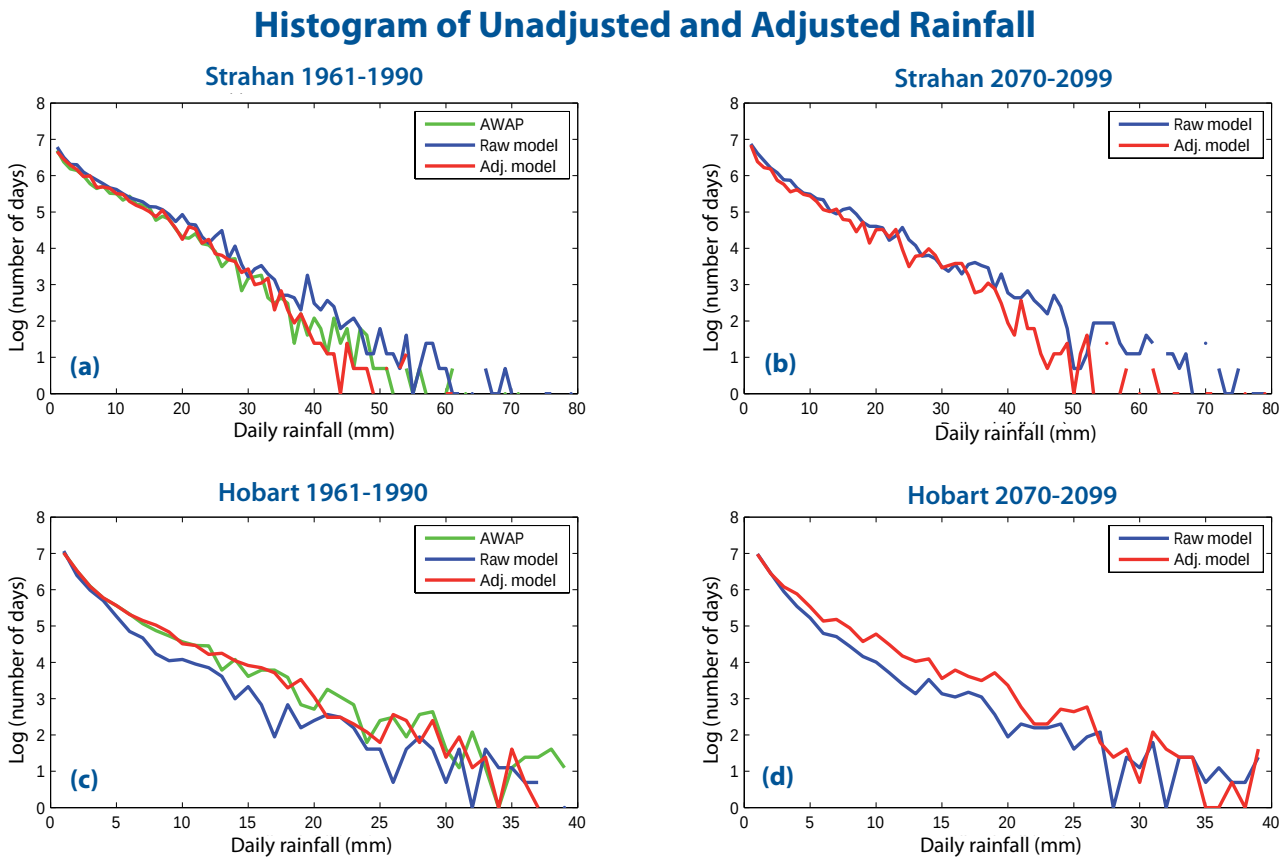

Figure 6.7 Histogram of daily rainfall for Strahan for (a) the recent past (1961-1990) and (b) the end of the century (2070-2099), and Hobart for the same periods (c) and (d). The figures show the values for AWAP data (green line) as well as unadjusted (blue line) and bias-adjusted (red line) simulations for the recent past, and unadjusted and bias-adjusted simulations for the future. The modelling output is for the downscaled GCM GFDL-CM2.1, A2 scenario simulation.

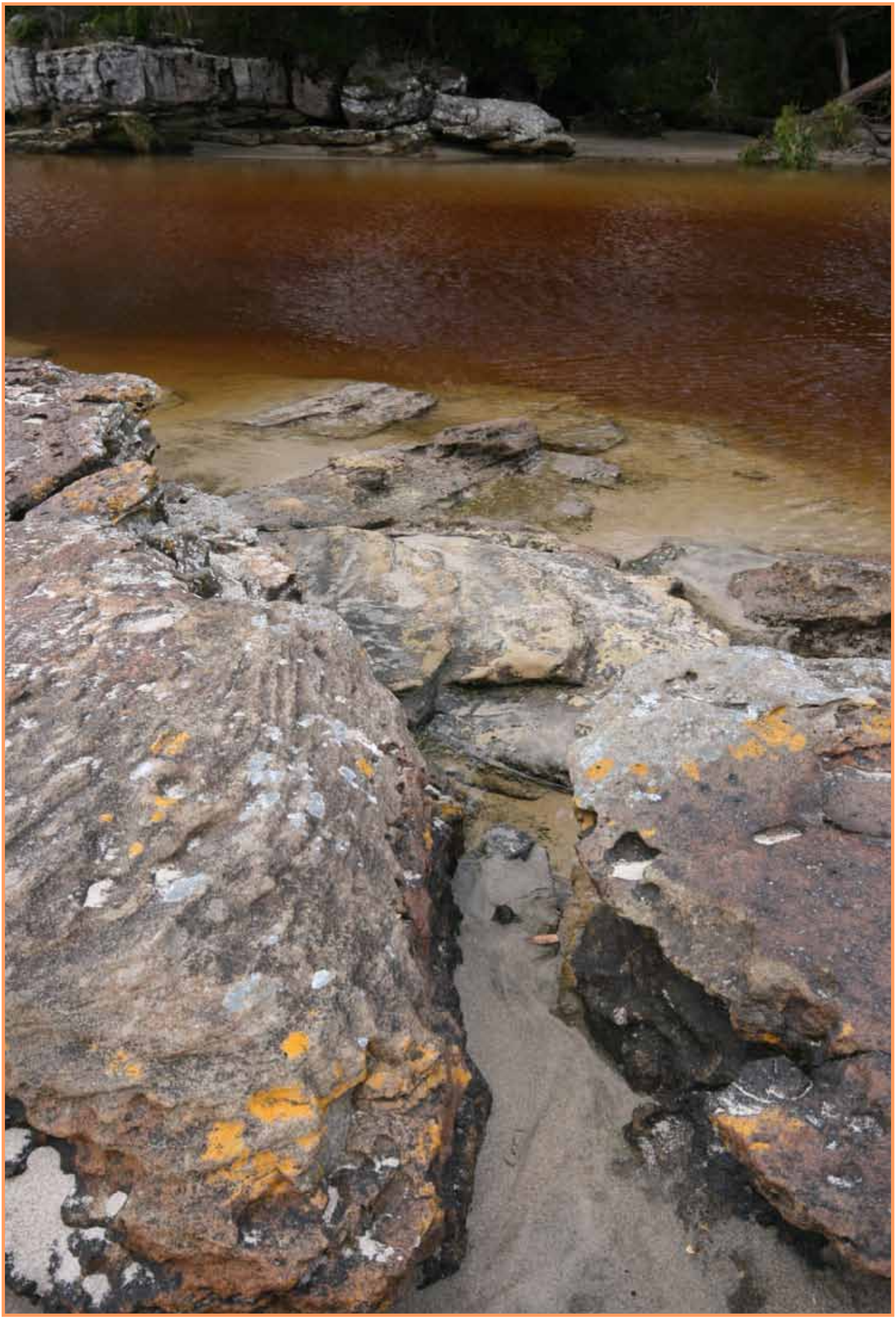

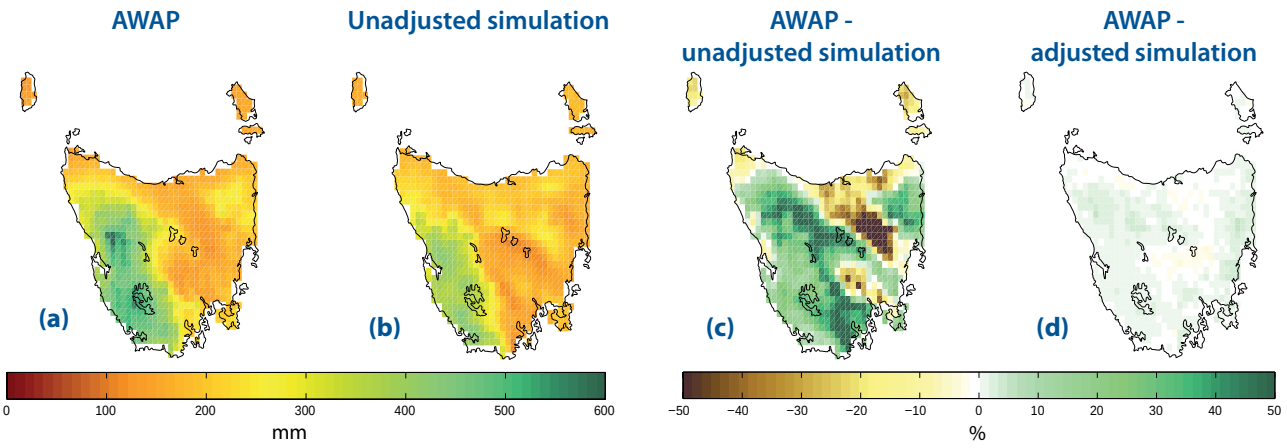

Figure 6.8 The result of the bias-adjustment process for rainfall (mm) for summer for the reference period (1961-2007); (a) AWAP summer rainfall (b) unadjusted summer rainfall for the downscaled GFDL-CM2.1 (A2 emissions scenario) simulation (c) percentage difference between AWAP and the unadjusted simulation for summer rainfall and (d) percentage difference between AWAP and the adjusted simulation for summer rainfall.

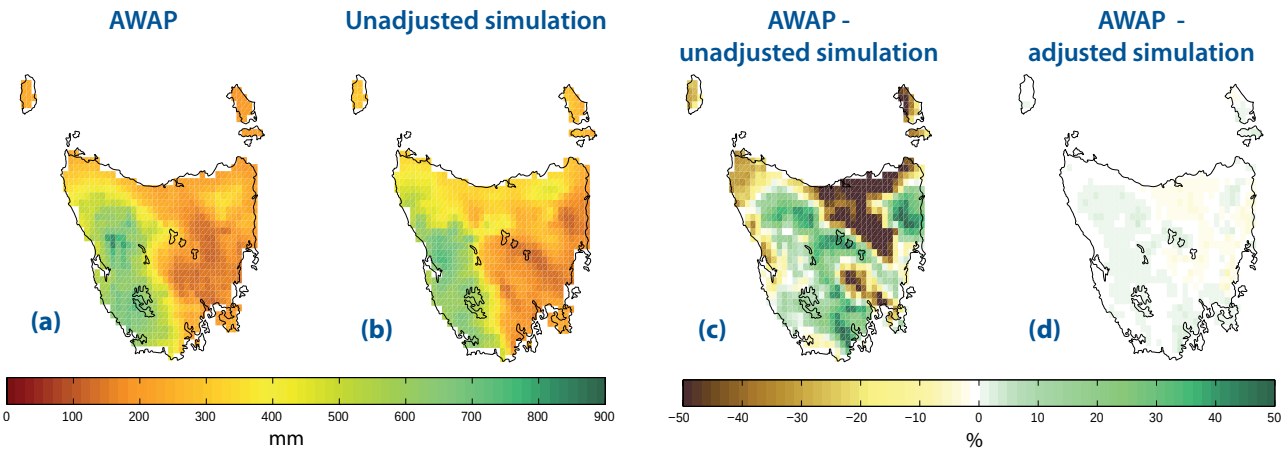

Figure 6.9 The result of the bias-adjustment process for rainfall for autumn for the reference period (1961-2007): (a) AWAP autumn rainfall (b) unadjusted autumn rainfall for the downscaled GFDL-CM2.1 (A2 emissions scenario) simulation (c) percentage difference between AWAP and the unadjusted simulation for autumn rainfall and (d) percentage difference between AWAP and the adjusted simulation for autumn rainfall.

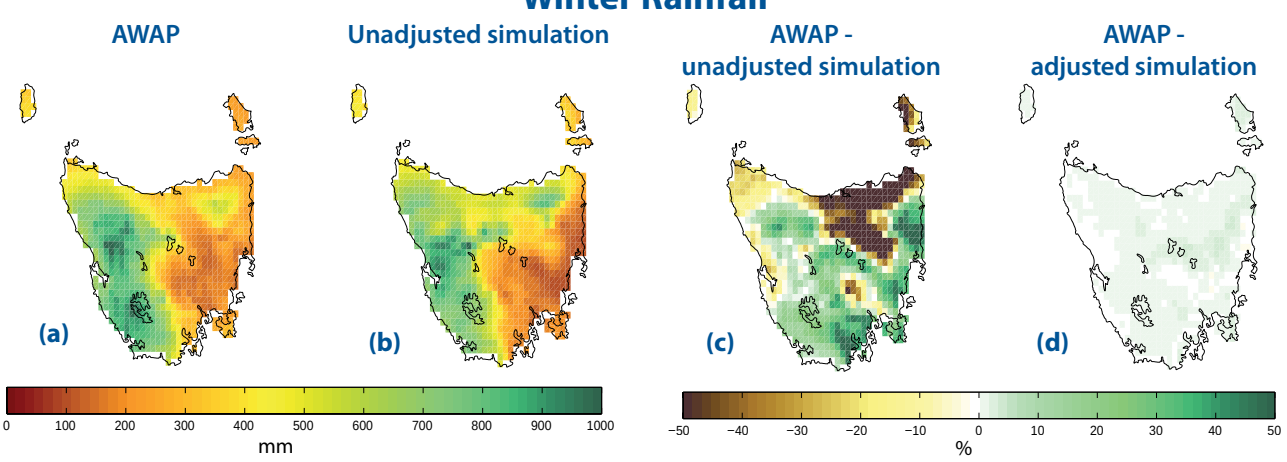

Figure 6.10 The result of the bias-adjustment process for rainfall for winter for the reference period (1961-2007): (a) AWAP winter rainfall (b) unadjusted winter rainfall for the downscaled GFDL-CM2.1 (A2 emissions scenario) simulation (c) percentage difference between AWAP and the unadjusted simulation for winter rainfall and (d) percentage difference between AWAP and the adjusted simulation for winter rainfall.

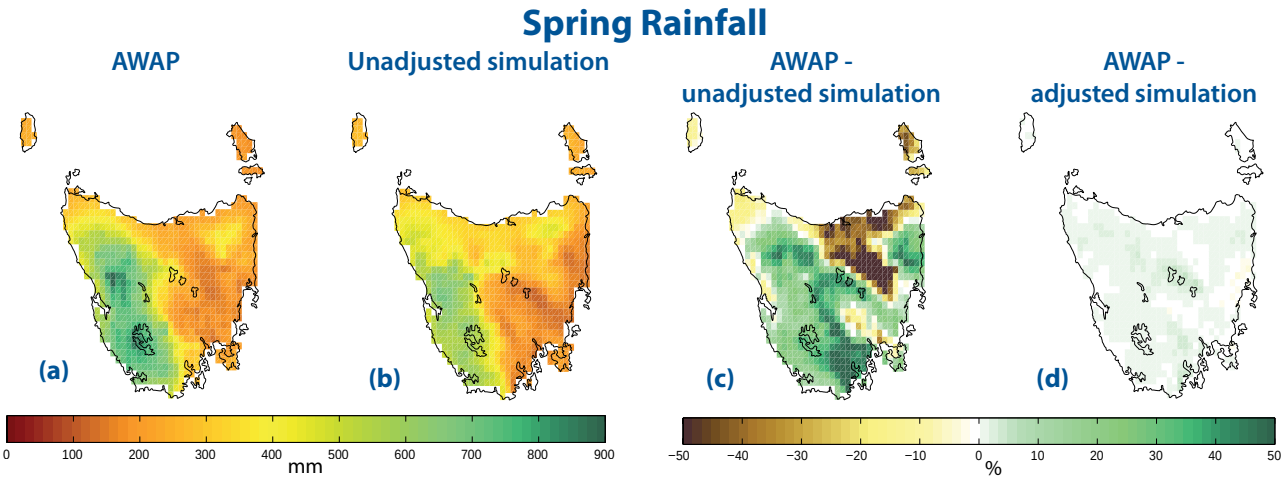

Figure 6.11 The result of the biasadjustment process for rainfall (mm) for spring for the reference period (1961-2007): (a) AWAP spring rainfall (b) unadjusted spring rainfall for the downscaled GFDL-CM2.1 (A2 emissions scenario) simulation (c) percentage difference between AWAP and the unadjusted simulation for spring rainfall and (d) percentage difference between AWAP and the adjusted simulation for spring rainfall.

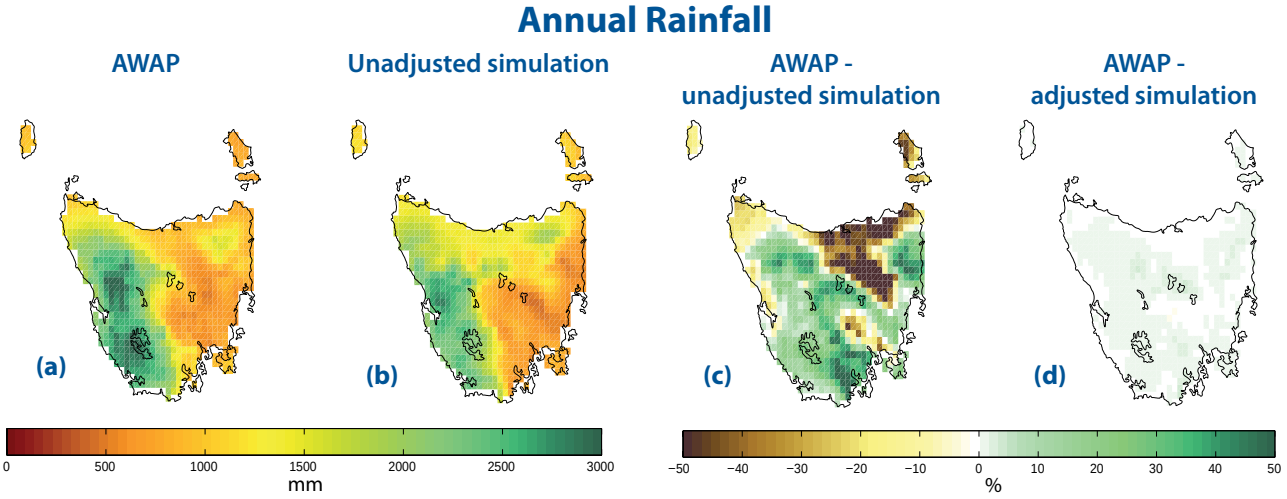

Figure 6.12 The result of the biasadjustment process for annual rainfall (mm) for the reference period (1961-2007); (a) AWAP annual rainfall (b) unadjusted annual rainfall for the downscaled GFDL-CM2.1 (A2 emissions scenario) simulation (c) percentage difference between AWAP and the unadjusted simulation for annual rainfall and (d) percentage difference between AWAP and the adjusted simulation for annual rainfall.

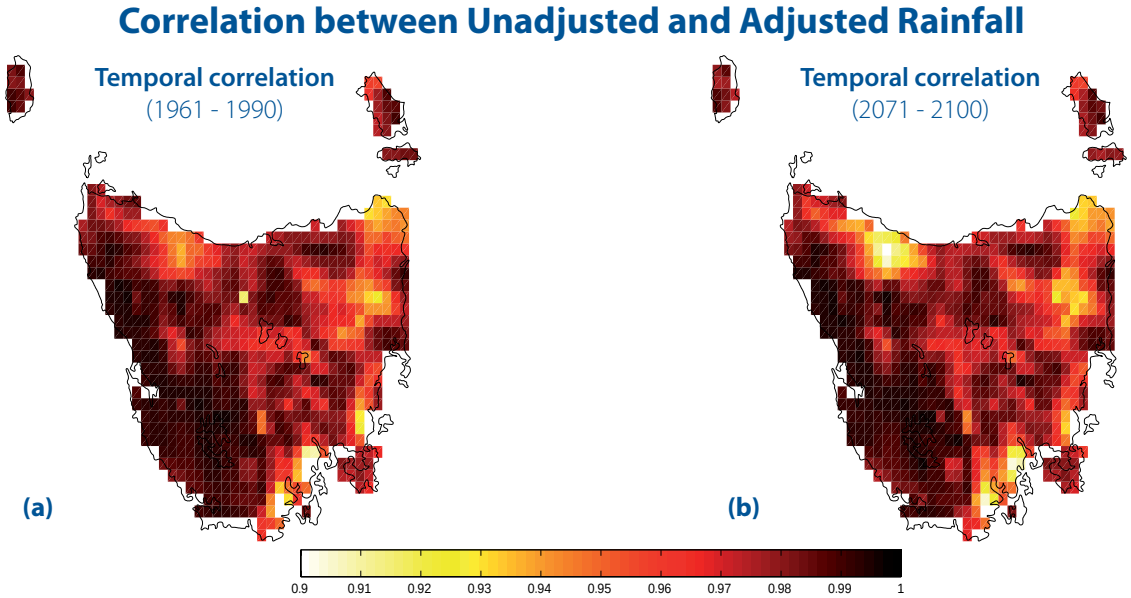

Figure 6.13 The cellwise temporal correlation (calculated on a daily basis) of rainfall between the unadjusted and adjusted simulations for the (a) recent past (1961-1990) and (b) future period (2071-2100). This figure shows the result for the downscaled GCM GFDL-CM2.1, A2 emissions scenario.

Table 6.2 Spatial correlations for rainfall between the AWAP data, the raw simulation and the bias-adjusted simulation. The simulation used is the 0.1-degree downscaled GFDL-CM2.1, A2 emissions scenario.

	AWAP – raw model	AWAP – adjusted model
Summer	0.801	0.998
Autumn	0.871	0.998
Winter	0.872	0.999
Spring	0.857	0.999
Annual	0.862	0.999

In the interests of brevity, we only include the annual results for the remaining bias-adjusted variables. The unadjusted modelling output for daily maximum temperature (Tmax) is more closely correlated to the AWAP data than is the simulated rainfall. When using the 0.1-degree downscaled GFDL-CM2.0, A2 emissions scenario simulation, the spatial correlation between the unadjusted model Tmax and the AWAP data is 0.944. Nonetheless, the adjusted simulations are still significantly better (Figure 6.14). The spatial correlation between the AWAP data and the adjusted six-model-mean output is 0.999.

For the rainfall and daily maximum screen temperature presented so far, we have relied on using the 47-year overlap period to check the effectiveness of the adjustment process. An alternative approach is to calculate the adjustment using only a part of the period where observations exist, and hold back the remaining years where observations exist to evaluate the process. We used the shorter period 1971-2007 to calculate the adjustment, applied it over the entire 140 year simulation and then examined the different values of Tmax (from the AWAP data, unadjusted and adjusted simulations) for the 'held-back' period between 1961 and 1970 period. The figure corresponding to Figure 6.14 was virtually identical (and is not included in this report). As expected, the temporal correlation between the unadjusted and adjusted simulation when calculated on a monthly basis is close to 1.0 over the entire state (Figure 6.15a). Just as importantly, the correlation between the adjusted simulation and the AWAP data is slightly higher than that between the unadjusted simulation and the AWAP data (Figure 6.15b and Figure 6.15c) and Figure 6.16, which shows the difference between Figure 6.15a and Figure 6.15c.

These results demonstrate that the bias-adjustment process works. When a decade in the overlap period (1961 to 2007) is not used in the adjustment calculations, the adjustments applied to the omitted decade remove the bias from the unadjusted model (not shown). Not only that but the adjustment process increases the temporal correlation between the AWAP data and the adjusted dataset, while maintaining a very high correlation between the unadjusted and adjusted simulations.

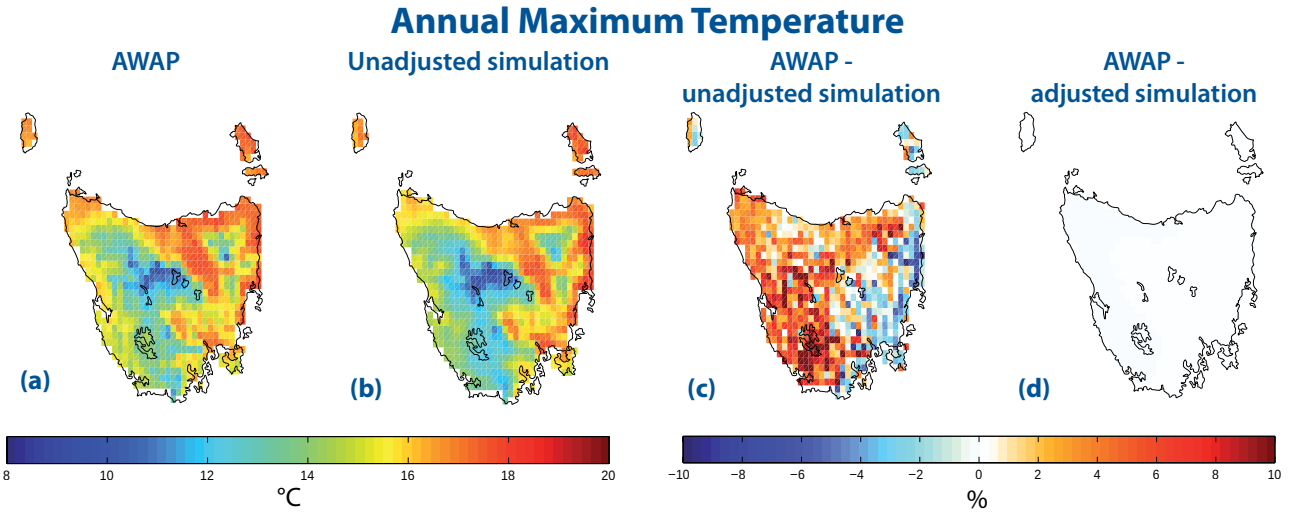

Figure 6.14 Effects of the bias-adjustment process for mean daily maximum screen temperature for the reference period 1961-2007; (a) the AWAP temperature (b) unadjusted temperature for the downscaled GFDL-CM2.0 (A2 emissions scenario) simulation (c) the percentage difference between the unadjusted simulation and the AWAP data and (d) percentage difference between AWAP and the adjusted simulation.

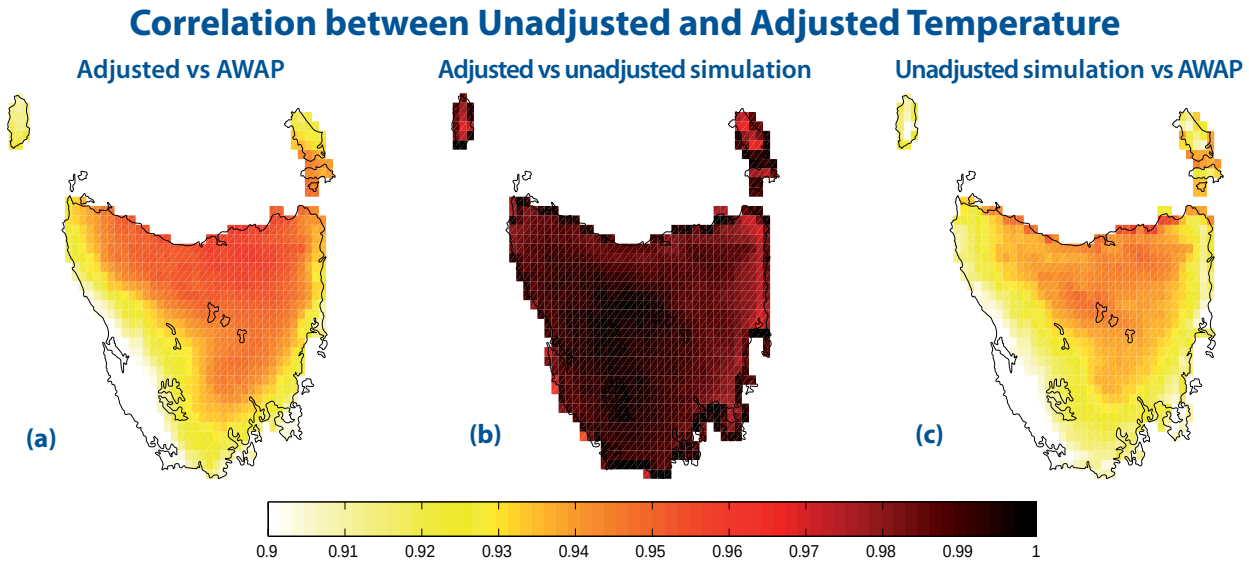

Figure 6.15 The temporal correlation of daily maximum temperature, calculated on a monthly basis, for the period 1961-1970 when this period was held-back from the adjustment calculation process. Correlation between (a) between the adjusted simulation and the AWAP data (b) the adjusted and unadjusted simulations and (c) between the AWAP data and the unadjusted simulation. This figure shows the result for the downscaled GCM GFDL-CM2.0, A2 emissions scenario.

The magnitude of the biases in minimum daily temperature is similar to that for maximum daily temperature. However, a significant warm bias existed in the central east region of Tasmania for daily minimum temperature (Tmin) in the 0.1-degree downscaled ECHAM5/MPI-OM, A2 emissions scenario simulation (Figure 6.17). Once again, the adjustment process removed this bias from the simulation (Figure 6.17d). The spatial correlations for Tmin for the downscaled ECHAM5/MPI-OM are: AWAP data versus unadjusted simulation, 0.903; AWAP data versus adjusted simulation, 0.999; and adjusted simulation versus unadjusted simulation, 0.904.

The bias-adjustment process for solar radiation and potential evaporation was identical to that carried out for rainfall (see Figure 6.18 for solar radiation and 6.19 for potential evaporation). A simpler method of bias-adjustment using monthly mean values of each variable was considered, but rejected because it was not as effective at correcting the bias while maintaining the character of low frequency events.

The major distinction between the AWAP data solar radiation and the unadjusted modelling output is that the simulations under-estimated the radiation in the west and over-estimated it in the east. Figure 6.18 shows the pattern for the downscaled ECHAM5/MPI-OM simulation for the A2 emissions scenario, but the pattern is consistent across all models. Incident solar radiation is related to cloud cover and thus the model seems to be over-estimating the cloud cover in the west of the state and under-estimating it in the east. Figure 6.12 showed that the unadjusted model slightly under-estimated the rainfall in the west of the state, and was mixed in the east. Rainfall and cloud cover are correlated, so an under-estimation of rainfall in the west and over-estimation of cloud

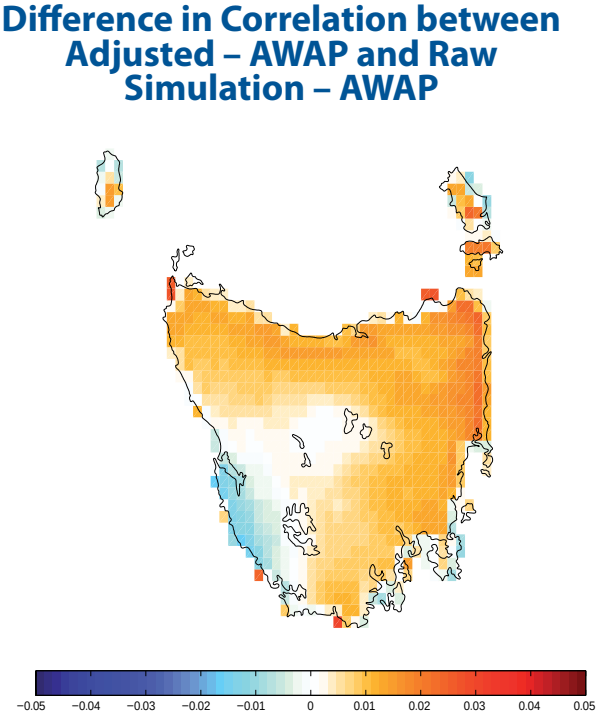

Figure 6.16 The difference between Figure 6.15a and Figure 6.15c.

cover is not necessarily consistent. The unadjusted model is dynamically consistent and this leads us to question the quality of the AWAP data in representing solar radiation. In spite of these questions, the AWAP data still provides one of the best datasets for solar radiation in Tasmania, and thus the bias-adjustment has been carried out using the AWAP data. Furthermore, we have reduced the spatial difference between the model and the AWAP data to near negligible levels (Figure 6.18d). In fact, the spatial correlation is 0.999, whereas the correlation between the unadjusted model and the AWAP data is 0.889.

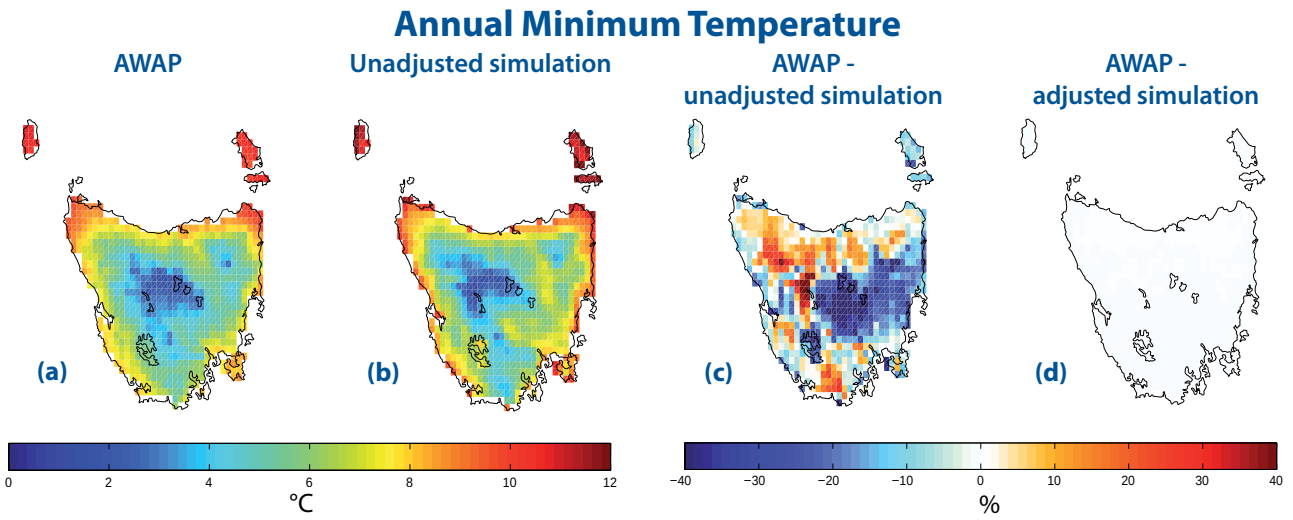

Figure 6.17 Effects of the bias-adjustment process for mean daily minimum screen temperature for the reference period 1961-2007; (a) the AWAP temperature (b) unadjusted temperature for the downscaled ECHAM5/MPI-OM (A2 emissions scenario) simulation (c) the percentage difference between the unadjusted simulation and the AWAP data and (d) percentage difference between AWAP and the adjusted simulation.

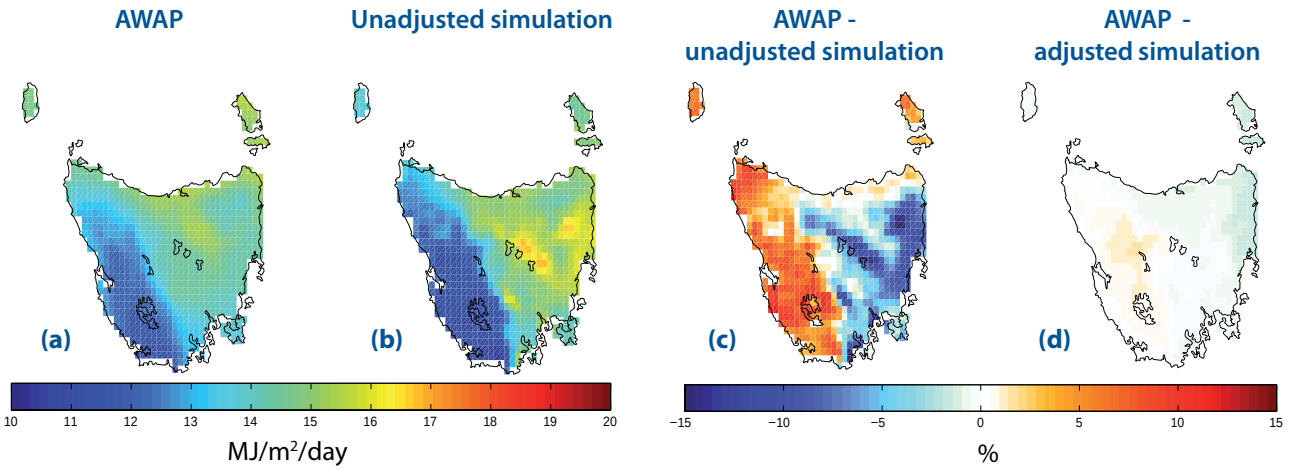

Figure 6.18 The bias-adjustment process applied to annual solar radiation; (a) the mean annual incident solar radiation from AWAP for the reference period 1961-2007, (b) the same for the unadjusted simulation, (c) the difference between AWAP and the unadjusted simulation and (d) the difference between AWAP and the adjusted simulation. This figure shows the result for the downscaled GCM ECHAM5/MPI-OM, A2 emissions scenario.

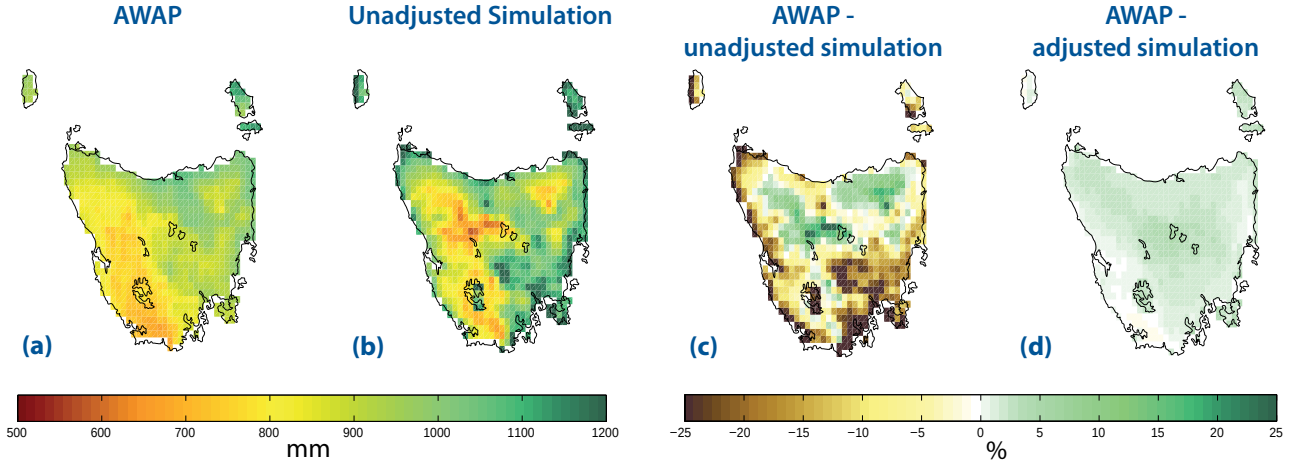

Figure 6.19 The bias-adjustment process applied to potential evaporation (mm); (a) the total annual evaporation from AWAP for the reference period 1961-2007, (b) the same for the unadjusted simulation, (c) the difference between AWAP and the unadjusted simulation and (d) the difference between AWAP and the adjusted simulation. This figure shows the result for the downscaled GCM MIROC3.2(med res), A2 emissions scenario.

As with solar radiation, the potential evaporation from the models appears to be more finely detailed over the state, showing greater variation due to topography than is present in the AWAP data (Figure 6.19 compares potential evaporation for the downscaled MIROC3.2(medres) simulations for the A2 emissions scenario and the AWAP data). The unadjusted simulation is within 20% of the AWAP data, but the adjusted simulation aligns almost exactly (Figure 6.19d) with the AWAP data. Note that like solar radiation there is a strong east-west delineation in the AWAP data, with the east displaying higher annual solar radiation than the west. This pattern is reproduced to a lesser extent in the unadjusted simulations.

We have outlined the method used for the bias-adjustment process in the project and results that start to demonstrate the effectiveness and validity of the method developed. We have demonstrated that the adjustment process can effectively match the simulations to the AWAP data on a seasonal and annual basis for the reference period 1961-2007, while improving the temporal correlation between the simulations and AWAP data on a monthly basis. These results demonstrate that the adjustment ties the current climate (1961-2007) to observations (the AWAP data) and projected climate simulations to realistic values. We have also shown that the adjustment process does not strongly affect the daily variability of the modelling output through the very high correlation between the unadjusted and adjusted simulations. In order to fully validate our method, we need to use the bias-adjusted simulations in applications such as biophysical and hydrological models, and show that the adjusted simulations not only give realistic results but also more robust results than can be obtained when using the unadjusted simulations. This validation process was carried out in the analysis for the water and catchments, and impacts on agriculture technical reports (Bennett et al 2010; Holz et al 2010). These reports include further discussion on the bias-adjustment method, and how it relates to their specific areas.

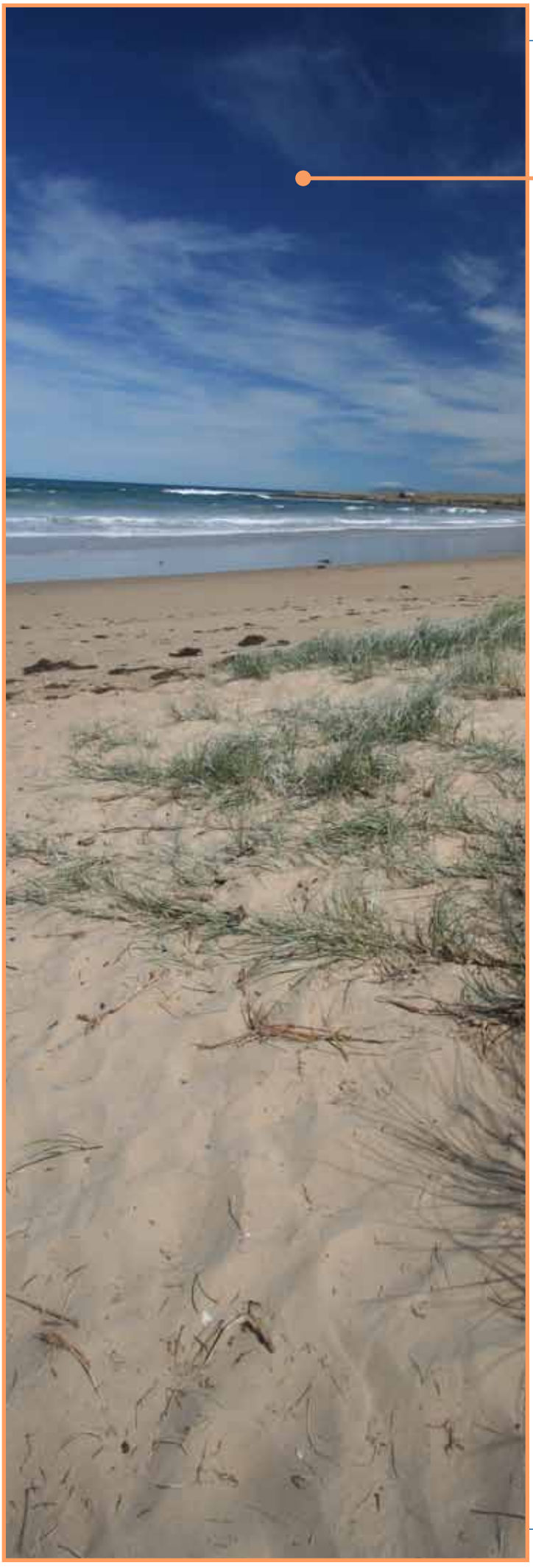

7 Synthesis

Climate Futures for Tasmania has undertaken an extensive climate modelling program in order to deliver high quality projections of Tasmanian climate to 2100. The end products include 17 simulations of the climate of Tasmania at a resolution of 0.1-degree (about 10 km) or better. These simulations were all downscaled from global climate models of the kind used in the IPCC Fourth Assessment Report (IPCC 2007). The simulations contain more than 140 variables recorded every six hours, and provide estimates of the Tasmanian climate for both the recent past (1961-2007) and the future (2010-2100). For some variables, such as temperature and rainfall, modelling output is available every three hours. The suite of simulations took approximately 1300 days of continuous computer time on a 0.82 teraflop machine and required in excess of 75 Terabytes of storage.

To achieve a final resolution of 0.1-degree (about 10 km) we undertook a two-stage dynamical downscaling process using CSIRO's Conformal Cubic Atmospheric Model (CCAM). The two-stage process used sea surface temperature from six global climate models (each with two IPCC emissions scenarios) to create intermediate resolution (0.5-degree, or 60 km) simulations over Australia. These intermediate-resolution simulations were then used as input for the high-resolution simulations over Tasmania.

Downscaling six GCMs for two emissions scenarios allowed for a more robust estimate of the climate change signature by examining the ensemble mean of key variables (such as temperature and rainfall) as well as an estimate of the uncertainty in these estimates through the spread of the models. We used six GCMs to produce fine-scale climate projections over Tasmania. These six GCMs (ECHAM5/MPI-OM, GFDL-CM2.0, GFDL-CM2.1, MIROC3.2(medres), CSIRO-Mk3.5 and UKMO-HadCM3) were chosen for their capacity to simulate present day climate means and variability of south-east Australia using a range of metrics.

The future global emissions profile is unknown. In order to provide projections for a range of likely futures, we chose to downscale each GCM using two SRES emissions scenarios, one high (A2) and one low (B1). This decision not only allowed us to report on the spread of each key variable under two different climate futures, but provided increased confidence in the results (where the two emissions scenarios agree) and a better estimate of the variability and sensitivity of those results.

The climate models are not perfect. They do not (and cannot) capture every aspect of the climate of Tasmania. However, climate models can reproduce many aspects of climate, and as such are a vital tool for assessing potential changes in the future climate. Section 5 discussed the high level of skill that the downscaled models have in reproducing the recent climate of Tasmania across a range of climate variables. For the period 1961-1990 the six-model-mean statewide daily maximum temperature calculated from the Climate Futures for Tasmania simulations is within 0.1 °C of the Bureau of Meteorology observed value of 10.4 °C, while the annual total rainfall of 1385 mm is very close to the observed value of 1390 mm. Furthermore, temperature has a spatial correlation of 0.93 with gridded observations over the state, while for rainfall the correlation is 0.63.

This skill of capturing the climate of the recent past gives us confidence that the models are able to provide realistic projections of the Tasmanian climate to 2100. The ability to accurately simulate present climate is a preferable, but not wholly sufficient, condition for a good projection of climate change.

Global and regional climate models provide the best estimates for assessing potential changes to our climate over the coming century. However, climate models cannot provide all the information that is needed regarding climate change. In many situations, conceptual models, such as agricultural or hydrological models, are essential to model changes to specific operational information (such as changes to crop yields or river flows). All climate models contain biases. For reporting climate trends, these biases may not affect the output. However, conceptual models often contain non-linearities that mean the climate simulations used as input into these models must be aligned with current climate. In order to use the Climate Futures for Tasmania simulations as input into conceptual models we created bias-adjusted simulations for each downscaled simulation using the AWAP data as a gridded observational dataset. The Impacts on Agriculture Technical Technical Report (Holz et al 2010) and Water and Catchments Technical Report (Bennett et al 2010) give examples of these models.

The bias-adjustment process was applied to five variables: daily maximum temperature, daily minimum temperature, daily rainfall, mean solar radiation and daily evaporation. The bias-adjusted variables have been modified on a cell-by-cell basis using a percentile-binning technique so that the shape of the probability distribution function of the modelling output from the recent past matches the current climate in terms of absolute value and seasonal range. For both temperature and rainfall, the spatial correlation of the bias-adjusted simulations was above 0.99.

References

Anderson CJ, Arritt RW, Takle ES, Pan Z, Gutowski WJ, da Silva R, Caya D, Christensen JH, Lüthi D, Gaertner MA, Giorgi F, Grell G, Hong S-Y, Jones C, Juang H-MH, Katzfey JJ, Lapenta W, Laprise R, Liston G, McGregor JL, Pielke RA, Prego JA, Roads JO & Taylor J 2003, 'Hydrologic processes in regional climate model simulations of the central United States flood of June-July', *Journal of Hydrometeorology*, vol. 4, pp. 584-598.

Allen RG, Pereira LS, Raes D, Smith M 1998, 'Crop evapotranspiration: guidelines for computing cropwater requirements', FAO Irrigation and Drainage Paper 56, Food and Agriculture Organization of the United Nations, Rome.

Bennett JC, Ling FLN, Graham B, Grose MR, Corney SP, White CJ, Holz GK, Post DA, Gaynor SM & Bindoff NL 2010, *Climate Futures for Tasmania: water and catchments technical report*, Antarctic Climate and Ecosystems Cooperative Research Centre, Hobart, Tasmania.

Boe J, Terray L, Habets F & Martin E 2007, 'Statistical and dynamical downscaling of the Seine basin climate for hydro-meteorological studies', *International Journal of Climatology*, vol. 27, pp. 1643-1655.

Charles SP, Bari MA, Kitsios A & Bates BC 2007, 'Effect of GCM bias on downscaled precipitation and runoff projections for the Serpentine catchment, Western Australia', *International Journal of Climatology*, vol. 27, pp. 1673-1690.

CSIRO 2009, *Climate change projections and impacts on runoff for Tasmania*, Report two of seven to the Australian Government from the CSIRO Tasmania Sustainable Yields Project, CSIRO Water for a Healthy Country Flagship, CSIRO (Australia). www.csiro.au/partnerships/TasSY.html

Cubasch U, Storch Hv, J.Waszkewitz & Zorita E 1996, 'Estimates of climate change on southern Europe derived from dynamical climate model output', *Climate Research*, vol. 7, pp. 129-149.

Denis B, Laprise R & Caya D 2003, 'Sensitivity of a regional climate model to the resolution of the lateral boundary conditions', *Climate Dynamics*, vol. 20, pp. 107-126.

Denis B, Laprise R, Caya D & Cote J 2002, 'Downscaling ability of one-way nested regional climate models: the Big-Brother Experiment', *Climate Dynamics*, vol. 18, pp. 627-646.

Deque M 2007, 'Frequency of precipitation and temperature extremes over France in an athropogenic scenario: model results and statistical correction according to observed values', *Global and Planetary Change*, vol. 57, pp. 16-26.

Engelbrecht FA, McGregor JL & Engelbrecht CJ 2009, 'Dynamics of the Conformal-Cubic Atmospheric Model projected climate-change signal over southern Africa', *International Journal of Climatology*, vol. 29, pp. 1013-1033.

Fawcett R, Trewin B & Barnes-Keoghan I 2010, *Network-derived inhomogeneity in monthly rainfall analyses over western Tasmania*. IOP Conference Series: Earth and Environmental Science, vol. 11, p. 012006, 10.1088/1755-1315/11/1/012006 10.1088/1755-1315/11/1/012006.

Fox-Rabinovitz M, Côté J, Dugas B, Déqué M & McGregor JL 2006, 'Variable resolution general circulation models: Stretched-grid model inter-comparison project (SGMIP)', *Journal of Geophysical Research*, vol. 111, pp. D16104-D16124.

Fox-Rabinovitz M, Côté J, Dugas B, Déqué M, McGregor JL & Belochitski A 2008, 'Stretched-Grid Model Inter-comparison Project: decadal regional climate simulations with enhanced variable and uniform-resolution GCMs', *Meteor. Atmos. Phys.*, vol. 100, pp. 159-178.

Fu C, Wang S, Xiong Z, Gutowski WJ, Lee D-K, McGregor JL, Sato Y, Kato H, Kim J-W & Suh M-S 2005, 'Regional Climate Model Inter-comparison Project for Asia', *Bull. Amer. Meteor. Soc.,*, vol. 86, pp. 257-269.

Georgelin M, Bougeault P, Black T, Brzovic N, Buzzi A, Calvo J, Casse V, Desgagne M, El-Khatib R, Geleyn J-F, Holt T, Hong S-Y, Kato T, Katzfey JJ, Kurihara K, Lacroix B, Lalaurette F, Lemaitre Y, Mailhot J, Majewski D, Malguzzi P, Masson V, McGregor JL, Minguzzi E, Paccagnella T & Wilson C 2000, 'The second COMPARE exercise: A model inter-comparison using a case of a typical mesoscale orographic flow, the PYREX IOP3', *Quarterly Journal of the Royal Meteorological Society*, vol. 126, pp. 991-1029.

Gordon HB, O'Farrell SP, Collier CG, Dix MR, Rotstayn LD, Kowalczyk EA, Hirst AC & Watterson IG 2010, *The CSIRO Mk3.5 Climate Model*, CAWCR Technical Report, The Centre for Australian Weather and Climate Research, Melbourne.

Grose MR, Barnes-Keoghan I, Corney SP, White CJ, Holz GK, Bennett JC, Gaynor SM & Bindoff NL 2010, *Climate Futures for Tasmania: general climate impacts technical report*, Antarctic Climate and Ecosystems Cooperative Research Centre, Hobart, Tasmania.

Holz G, Grose MR, Bennett JC, Corney SP, White CJ, Phelan D, Potter K, Kriticos D, Rawnsley R, Parsons D, Lisson S, Gaynor SM & Bindoff NL 2010, *Climate Futures for Tasmania: impacts on agriculture technical report*, Antarctic Climate and Ecosystems Cooperative Research Centre, Hobart, Tasmania.

IPCC 1996, Climate Change 1995: *The Science of Climate Change. Contribution of Working Group I to the Second Assessment Report of the Intergovernmental Panel on Climate Change*, [Houhton J, Meira Filho L, Callander B, Harris N, Kattenberg A & Maskell K (eds)], Cambridge University Press, Cambridge, United Kingdom.

---- 2001, Climate Change 2001: *The Science of Climate Change. Contribution of Working Group I to the Third Assessment Report of the Intergovernmental Panel on Climate Change*, [Houghton J, Ding Y, Griggs D, Noguer M, van der Linden P, Da X, Maskell K & Johnson C (eds)], Cambridge University Press, Cambridge, United Kingdom.

---- 2007, *Climate Change 2007: The Physical Science Basis. Contribution of Working Group I to the Fourth Assessment Report of the Intergovernmental Panel on Climate Change*, [Solomon S, Qin D, Manning M, Chen Z, Marquis M, Averyt KB, Tignor M & Miller HL (eds)], Cambridge University Press, Cambridge, United Kingdom and New York, NY, USA.

Jeffrey SJ, Carter JO, Moodie KM & Beswick AR 2001, 'Using spatial interpolation to construct a comprehensive archive of Australian climate data', *Environmental Modelling and Software*, vol. 16, pp. 309-330.

Jones DA, Wang W & Fawcett R 2009, 'High-quality spatial climate data-sets for Australia', *Australian Meteorological and Oceanographic Journal*, vol. 58, pp. 233-248.

Joubert AM, Katzfey JJ, McGregor JL & Nguyen KC 1999, 'Simulating midsummer climate over southern over southern Africa using a nested regional climate model', *J. Geophys. Res.*, vol. 104, pp. 19015-19025.

Kalnay E, Kanamitsu M, Kistler R, Collins W, Deaven D, Gandin L, Iredell M, Saha S, White G, Woollen J, Zhu Y, Leetmaa A, Reynolds R, Chelliah M, Ebisuzaki W, Higgins W, Janowiak J, Mo KC, Ropelewski C, Wang J, Jennec R & Joseph D 1996, 'The NCEP/NCAR 40-year reanalysis project', *Bull. Amer. Meteor. Soc.,*, vol. 77, pp. 437-470.

Katzfey JJ, McGregor JL, Nguyen KC & Thatcher M 2009, Dynamical cownscaling techniques: Impacts on regional climate change signals. *Proceedings, World IMACS/MODSIM Congress*, Cairns.

Kowalczyk EA, Garratt JR & Krummel PB 1994, *Implementation of a soil-canopy scheme into the CSIRO GCM - regional aspects of the model response*, vol 32, Research CDA, CSIRO Div. Atmospheric Research Tech. Paper.

Lacis A & Hansen J 1974, 'A parameterisation of the absorption of solar radiation in the Earth's atmosphere', *Journal of Atmospheric Science*, vol. 31, pp. 118-133.

Lal M, McGregor JL & Nguyen KC 2008, 'Very high-resolution climate simulation over Fiji using a global variable-resolution model', *Climate Dynamics*, vol. 30, pp. 293-305.

Leggett J, Pepper WJ & Swart RJ 1992, *Emissions Scenarios for the IPCC: an Update*, Climate Change 1992: The Supplementary Report to The IPCC Scientific Assessment, [Houghton JT, Callander BA & Varney SK (eds)], Cambridge University Press, Cambridge, United Kingdom.

Maximo CC, McAvaney BJ, Pitman AJ & Perkins SE 2008, 'Ranking the AR4 climate models over the Murray-Darling Basin using simulated maximum temperature, minimum temperature and precipitation', *Int J Climatol*, vol. 28, pp. 1097-1110.

McGregor JL 2003, *A new convection scheme using a simple closure*, Current issues in the parameterization of convection, vol 93, Bureau of Meteorology Research Centre, Melbourne.

---- 2005, *CCAM: geometric aspects and dynamical formulation*, Technical Paper 70, CSIRO Atmospheric Research, Melbourne.

McGregor JL & Dix MR 2001, The CSIRO conformal-cubic atmospheric GCM. Proceedings, IUTAM Symposium on Advances in Mathematical Modelling of Atmosphere and Ocean Dynamics.

---- 2008, 'An updated description of the Conformal-Cubic Atmospheric Model', *High Resolution Simulation of the Atmosphere and Ocean*, [Hamilton K & Ohfuchi W (eds)], Springer, pp. 51-76.

McGregor JL, Gordon HB, Watterson IG, Dix MR & Rotstayn LD 1993, *The CSIRO 9-level atmospheric general circulation model*, CSIRO Atmospheric Research Technical Paper, vol 26, CSIRO Atmospheric Research, Melbourne.

McIntosh PC, Pook MJ & McGregor JL 2005, *Study of future and current climate: a scenario for the Tasmanian region (stages 2 & 3) (CSIRO)*, A report for Hydro Tasmania, CSIRO Marine and Atmospheric Research, Hobart.

Meehl G, Covey AC, Delworth T, Latif M, McAvaney BJ, Mitchell JFB, Stouffer RJ & Taylor KE 2007a, 'The WCRP CMIP3 multi-model dataset: A new era in climate change research', *Bulletin of the American Meteorological Society*, vol. 88, pp. 1383-1394.

Meehl GA, Stocker TF, Collins WD, Friedlingstein P, Gaye AT, Gregory JM, Kitoh A, Knutti R, Murphy JM, Noda A, Raper SCB, Watterson IG, Weaver AJ & Zhao Z-C 2007b, 'Global Climate Projections', *Climate Change 2007: The Physical Science Basis. Contribution of Working Group I to the Fourth Assessment Report of the Intergovernmental Panel on Climate Change*', [Solomon S, Qin D, Manning M, Chen Z, Marquis M, Averyt KB, Tignor M & Miller HL (eds)], Cambridge University Press, Cambridge, United Kingdom and New York, NY, USA.

Min SK, Legutke S, Hense A & Kwon WT 2005, 'Internal variability in a 1000-yr control simulation with the coupled climate model ECHO-G - II. El Nino Southern Oscillation and North Atlantic Oscillation', *Tellus, Series A: Dynamic Meteorology and Oceanography*, vol. 57, pp. 622-640.

Nagata M, Leslie L, Kamahori H, Nomura R, Mino H, Kurihara K, Rogers E, Elsberry R, Basu BK, Buzzi A, Calvo J, Desgagne M, D'Isidoro M, Hong S-Y, Katzfey JJ, Majewski D, Malguzzi P, McGregor JL, Murata A, Nachamkin J, Roch M & Wilson C 2001, 'A mesoscale model inter-comparison: a case of explosive development of a tropical cyclone (COMPARE III)', *J. Meteor. Soc. Japan*, vol. 79, pp. 999-1033.

Nagata M, Leslie L, Kurihara Y, Elsberry R, Yamasaki M, Kamahori H, Abbey Jr. R, Bessho K, Calvo J, Chan J, Clark P, Desgagne M, Hong S-Y, Majewski D, Malguzzi P, McGregor JL, H. Mino, Murata A, Nachamkin J, Roch M & Wilson C 2000, 'Third COMPARE Workshop: A model inter-comparison experiment of tropical cyclone intensity and track prediction 13-15 December 1999', *Bull. Amer. Meteor. Soc.,* vol. 82, pp. 2007-2020.

Nakicenovic N & Swart R (eds) 2000, *Special Report on Emissions Scenarios. A Special Report of Working Group III of the Intergovernmental Panel on Climate Change*, Cambridge University Press, Cambridge, United Kingdom.

Panofsky HA & Brier GW 1968, *Some applications of statistics to meteorology*. The Penn. State University Press, University Park.

Perkins SE & Pitman AJ 2009, 'Do weak AR4 models bias projections of future climate changes over Australia?', *Climatic Change*, vol. 93, pp. 527-558.

Randall DA, Wood RA, Bony S, Colman R, Fichefet T, Fyfe J, Kattsov V, Pitman A, Shukla J, Srinivasan J, Stouffer RJ, Sumi A & Taylor KE 2007, *Climate models and their evaluation*, In *Climate Change 2007: The Physical Science Basis. Contribution of Working Group I to the Fourth Assessment Report of the Intergovernmental Panel on Climate Change*, [Solomon S, Qin D, Manning M, Chen Z, Marquis M, Averyt KB, Tignor M & Miller HL (eds)], Cambridge University Press, Cambridge, United Kingdom.

Raupach MR 2000, 'Equilibrium evaporation and the convective boundary layer', *Boundary-Layer Meteorol.*, vol. 96, pp. 107-141

Raupach MR 2001, 'Combination theory and equilibrium evaporation', *Quart. J. Roy. Meteorol. Soc.*, vol. 127, pp. 1149-1181

Reichle RH & Koster RD 2004, 'Bias reduction in short records of satellite soil moisture', *Geophysical Research Letters*, vol. 31, pp. L19501-L19504.

Reichler T & Kim J 2008, 'How Well Do Coupled Models Simulate Today's Climate?', *Bull. Amer. Met. Soc.*, vol. 89, pp. 303-311.

Renwick JA, Katzfey JJ, McGregor JL & Nguyen KC 1999, 'On regional model simulations of climate change over New Zealand', *Weather and Climate*, vol. 19, pp. 3-14.

Reynolds RW 1988, 'A real-time global sea surface temperature analysis', *Journal of Climate*, vol. 1, pp. 75-86.

Rotstayn LD 1997, 'A physically based scheme for the treatment of stratiform clouds and precipitation in large-scale models', *Quarterly Journal of the Royal Meteorological Society*, vol. 123, pp. 1227-1282.

Rotstayn LD, Collier MA, Dix MR, Feng Y, Gordon HB, O'Farrell SP, Smith IN & Syktus J 2010, 'Improved simulation of Australian climate and ENSO-related rainfall variability in a global climate model with an interactive aerosol treatment', *International Journal of Climatology*, vol. 30, pp. 1067-1088.

Schmidt F 1977, 'Variable fine mesh in spectral global model', *Beitr. Phys. Atmos.*, vol. 50, pp. 211-217.

Schwarzkopf MD & Fels SB 1991, 'The simplified exchange method revisited: An accurate, rapid method for computation of infrared cooling rates and fluxes', *Journal of Geophysical Research*, vol. 96, pp. 9075-9096.

Smith IN & Chandler E 2009, 'Refining rainfall projections for the Murray Darling Basin of south-east Australia-the effect of sampling model results based on performance', *Climatic Change*, vol. pp. DOI 10.1007/s10584-10009-19757-10581.

Smith IN & Chiew FHS 2009, Document and assess methods for generating inputs to hydrological models and extend delivery of projections across Victoria, Final report for Project 2.2.5P, South East Australian Climate Initiative.

Suppiah R, Hennessy KJ, Whetton PH, McInnes K, Macadam I, Bathols J, Ricketts J & Page CM 2007, 'Australian climate change projections derived from simulations performed for the IPCC 4th Assessment Report', *Aust. Met. Mag.*, vol. 56, pp. 131-152.

Takle ES, Gutowski WJ, Arritt RW, Pan Z, Anderson CJ, da Silva RR, Caya D, Chen S-C, Giorgi F, Christensen JH, Hong S-Y, Juang H-MH, Katzfey JJ, Lapenta WM, Laprise R, Liston GE, Lopez P, McGregor JL, Pielke RA & Roads JO 1999, 'Project to inter-compare Regional Climate Simulations (PIRCS): description and initial results', *Journal of Geophysical Research*, vol. 104, pp. 19443-19461.

Thatcher M & McGregor JL 2009, 'Using a scale-selective filter for dynamical downscaling with the conformal cubic atmospheric model', *Monthly Weather Review*, vol. 137, pp. 1742-1752.

van der Linden P & Mitchell JFB (eds) 2009, ENSEMBLES: Climate Change and its Impacts: Summary of research and results from the ENSEMBLES project, Met Office Hadley Centre, Exeter.

van Oldenborgh GJ, Balmaseda MA, Ferranti L, Stockdale TN & Anderson DLT 2005, 'Evaluation of atmospheric fields from the ECMWF seasonal forecasts over a 15-year period', *Journal of Climate*, vol. 18, pp. 3250-3269.

Watterson IG 2008, 'Calculation of probability density functions for temperature and precipitation change under global warming', *Journal of Geophysical Research*, vol. 113, pp.

White CJ, Sanabria LA, Grose MR, Corney SP, Bennett JC, Holz GK, McInnes KL, Cechet RP, Gaynor SM & Bindoff NL 2010, *Climate Futures for Tasmania: extreme events technical report*, Antarctic Climate and Ecosystems Cooperative Research Centre, Hobart, Tasmania.

Wood A, Leung LR, Sridhar V & Lettenmaier DP 2004, 'Hydrologic implications of dynamical and statistical approaches to downscaling climate outputs', *Climate Change*, vol. 62, pp. 189-206.

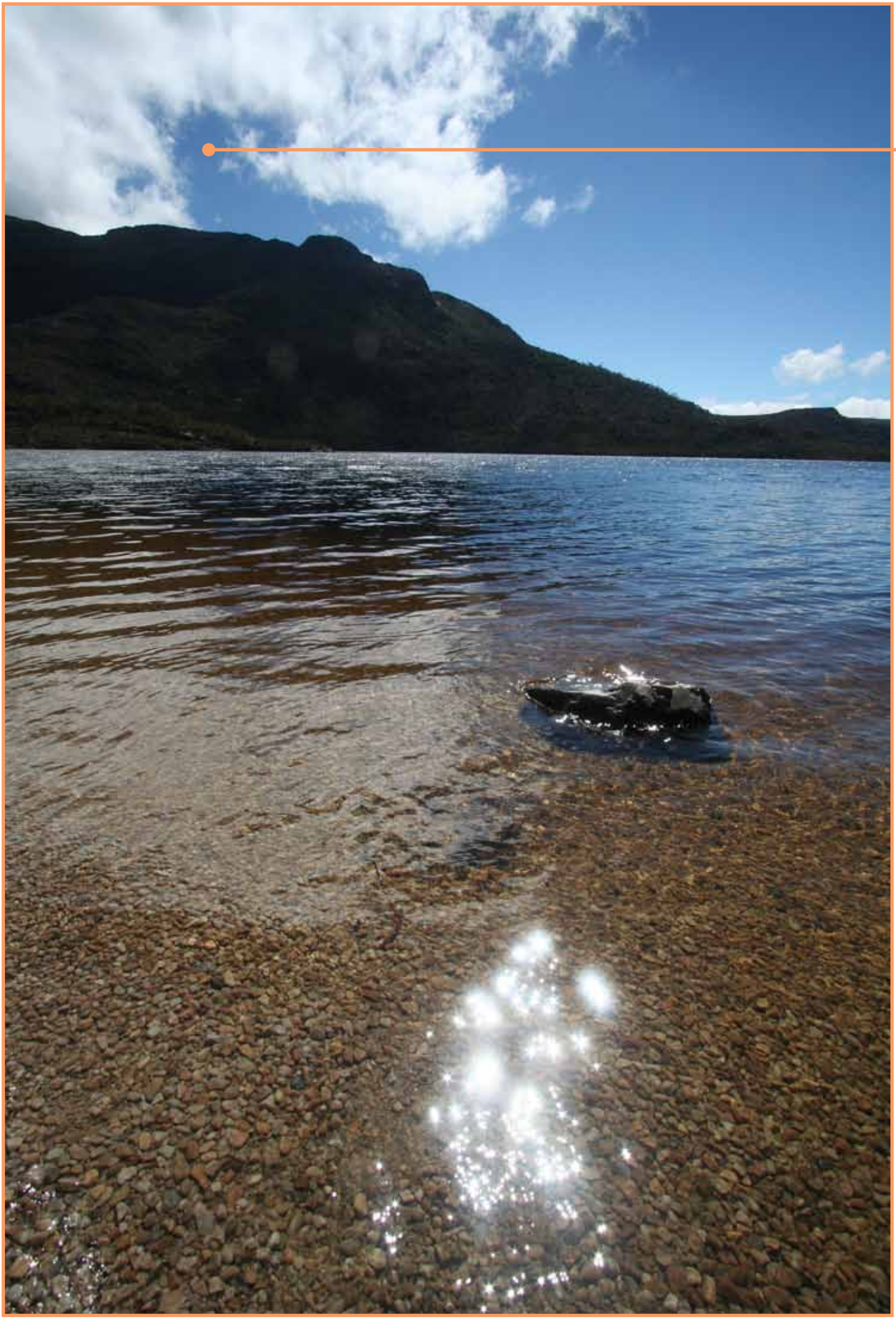

Project Acknowledgements

The Climate Futures for Tasmania project was funded primarily by the State Government of Tasmania, the Australian Government's Commonwealth Environment Research Facilities Program and Natural Disaster Mitigation Program. The project also received additional funding support from Hydro Tasmania.

Scientific leadership and contributions were made from a consortium of organisations including: Antarctic Climate & Ecosystems Cooperative Research Centre, Tasmanian Department of Primary Industries, Parks, Water and Environment, Tasmanian State Emergency Service, Entura (formerly Hydro Tasmania Consulting), Geoscience Australia, Bureau of Meteorology, CSIRO, Tasmanian Partnership for Advanced Computing, Tasmanian Institute of Agricultural Research and the University of Tasmania.

The generation of the Climate Futures for Tasmania climate simulations was commissioned by the Antarctic Climate & Ecosystems Cooperative Research Centre (ACE CRC), as part of its Climate Futures for Tasmania project. The climate simulations are freely available through the Tasmanian Partnership for Advanced Computing digital library at www.tpac.org.au.

Climate Futures for Tasmania is possible with support through funding and research of a consortium of state and national partners.

Climate Futures for Tasmania is possible with support through funding and research of a consortium of state and national partners.

ACE CRC
ANTARCTIC CLIMATE & ECOSYSTEMS CRC

Australian Government
Department of Sustainability, Environment, Water, Population and Communities

Tasmania
Explore the possibilities

Australian Government
Attorney-General's Department

State Emergency Service Tasmania

Australian Government
Bureau of Meteorology

Hydro Tasmania
The power of natural thinking

Australian Government
Geoscience Australia

CSIRO

UTAS

tiar
Tasmanian Institute of Agricultural Research

TPAC